Tracking connections between striatum, and frontal and motor cortices using diffusion tensor imaging and tractography

Kati Penttinen

School of Electrical Engineering

Thesis submitted for examination for the degree of Master of Science in Technology
In Espoo, 4.10.2016

Thesis Advisor and Supervisor:

Professor Synnöve Carlson

Aalto University
School of Electrical
Engineering

Author: Kati Penttinen

Title: Tracking connections between striatum, and frontal and motor cortices using diffusion tensor imaging and tractography

Degree programme: Bioinformation technology

Major: Computational and Cognitive Biosciences **Code:** IL3003

Thesis supervisor and advisor: Professor Synnöve Carlson

Date: 4.10.2016 **Number of pages:** 7+63 **Language:** English

Abstract

The striatum contributes to several motor and executive functions, such as preparation for and execution of movement, and control of goal-directed and habitual behaviour. While the connections between the striatum and cortex have been extensively studied in animals, the routes and locations of the anatomical pathways in humans have been the focus of only a handful of experiments. In this thesis, the anatomical connections between the striatum (the caudate nucleus and putamen), and the frontal areas (the dorsolateral and ventrolateral prefrontal cortex) and the motor areas (the primary motor cortex, premotor cortex, supplementary motor area and presupplementary motor area) were tracked using diffusion tensor imaging (DTI) and tractography. Both the individual tracts and population maps of the connections at the group level were calculated.

The found tracts held the same general shape in the different hemispheres and individuals, but the exact locations of the cortical connections and the routes of the tracts varied. This was especially notable in the tracts between the putamen and premotor cortex. All tracts at the individual level were bilaterally similar with only minor differences. The connections generally held the same shape and robustness when converted to the standard space in the group analysis, with the exception of tracts between the putamen and premotor area in both hemispheres and the tracts between the putamen and primary motor area in the right hemisphere.

This thesis provides further evidence of the cortico-striatal circuits and demonstrates the power of the DTI and tractography in studying neural connections between the striatum and cortex. The routes and the locations of connections with the cortex were identified, and this information can be applied in further studies of the striatal function and connectivity, especially in tandem with TMS.

Keywords striatum, cortico-striatal connections, caudate nucleus, putamen, diffusion tensor imaging, tractography

Tekijä: Kati Penttinen

Työn nimi: Striatumin ja otsalohkon sekä motoristen alueiden välisten yhteyksien jäljittäminen diffuusiotensorikuvauksen ja traktografian keinoin

Koulutusohjelma: Bioinformaatioteknologia

Pääaine: Laskennallinen ja kognitiivinen biotiede **Koodi** IL3003

Työn valvoja ja ohjaaja: Professori Synnöve Carlson

Päivämäärä: 4.10.2016 **Sivumäärä:** 7+63 **Kieli:** Englanti

Tiivistelmä

Striatum osallistuu useisiin motorisiin ja kognitiivisiin prosesseihin, kuten liikkeen valmisteluun ja toteuttamiseen sekä käyttäytymisen hallintaan. Yhteyksiä striatumin ja aivokuoren välillä on tutkittu laajasti eläimillä, mutta anatomiset yhteydet ovat olleet aiheena vain muutamassa tutkimuksessa. Tässä diplomityössä jäljitettiin anatomisia yhteyksiä striatumin (jaettuna häntätumakkeeseen ja aivokuorukkaan) ja otsalohkon (eriteltynä dorsolateraaliseen ja ventrolateraaliseen prefrontaaliaivokuoreen) sekä motoristen alueiden (eriteltynä motoriseen aivokuoreen, premotoriseen aivokuoreen, supplementaariseen motoriseen alueeseen ja presupplementaariseen motoriseen alueeseen) käyttämällä diffuusiotensorikuvausta ja traktografiaa. Yhteydet laskettiin sekä yksittäisille koehenkilöille että koko ryhmälle.

Löydetyt radat pitivät saman yleisen muodon eri aivopuoliskoissa ja koehenkilöillä, mutta tarkka kulkureitti ja yhteyskohtien sijainti aivokuorella vaihtelivat. Erot olivat erityisen suuria radoissa, jotka yhdistivät aivokuorukan ja premotorisen aivokuoren. Yksilötasolla löydetyt radat olivat hyvin samanlaisia molemmissa aivopuoliskoissa. Yhteydet säilyttivät muotonsa ja vahvuutensa, kun ne siirrettiin standardiavaruuteen ryhmäanalyysia varten. Poikkeuksen tähän tekivät yhteydet aivokuorukan ja premotorisen aivokuoren sekä aivokuorukan ja primaarimotorisen aivokuoren välillä oikeassa aivopuoliskossa.

Tämä diplomityö tuotti lisätodisteita kortikostriataalisten piirien olemassa olosta ja osoitti diffuusiotensorikuvauksen ja traktografian vahvuudet tutkittaessa hermoyhteyksiä striatumin ja aivokuoren välillä. Tutkimuksessa löydettiin yhteyksien kulkureitit ja yhtymäkohdat aivokuorelle. Tätä tietoa voidaan hyödyntää myöhemmissä tutkimuksissa etenkin yhdessä TMS-tekniikan kanssa.

Avainsanat striatum, kortikostriataaliset yhteydet, caudate nucleus, putamen, diffuusiotensorikuvaus, traktografia

Preface

First of all, I want to thank my advisor and supervisor Synnöve Carlson for her guidance that was invaluable especially in setting the scope and goal of the thesis. This empowered me to boldly crop off the irrelevant branches and keep the whole project from blowing up on my face, or my mind.

Secondly, thank you, ETK, for listening to me vent in those inevitable moments it did feel like explosions were imminent. The immediate response of memes was and is greatly appreciated.

Thank you all who helped me to get here, those recommending the best program for reference management and those listening to me talk about brains without getting (overtly) glassy eyed, among many others.

It has been a wild ride.

Now, to infinity and beyond!

In Espoo, 4.10.2016

Kati Penttinen

Kati Penttinen

Contents

List of tables

List of figures

Abbreviations

AC	Anterior commissure
ADC	Apparent diffusion coefficient
A-O	Action-outcome
ARD	Automatic relevance determination
DLPFC	Dorsolateral prefrontal cortex
DTI	Diffusion tensor imaging
DWI	Diffusion weighted imaging
EEG	Electroencephalography
FA	Fractional anisotropy
FEF	Frontal eye fields
FSL	FMRIB Software library
fMRI	Functional magnetic resonance imaging
HD	Huntington's disease
lDS	Lateral dorsal striatum (in rats, corresponds to the putamen in primates)
M1	Primary motor cortex
mDS	Medial dorsal striatum (in rats, corresponds to the caudate nucleus in primates)
MRI	Magnetic resonance imaging
PD	Parkinson's disease
PET	Positron emission tomography
PFC	Prefrontal cortex
PMC	Premotor cortex
preSMA	Presupplementary motor area
ROI	Region of interest
rTMS	Repetitive transcranial magnetic stimulation
S1	Somatosensory cortex
SMA	Supplementary motor area
S-R	Stimulus-response
STG	Superior temporal gyrus
TMS	Transcranial magnetic stimulation
VAC	Vertical line through anterior commissure (AC)
VLPFC	Ventrolateral prefrontal cortex
WCST	Wisconsin card sort test

1 Introduction

The purpose of this study was to track anatomical connections between the human striatum and the cortical areas, especially the prefrontal areas, and the areas involved in motor functions. The aim was to provide knowledge about the distribution of the anatomical pathways connecting the cortical sites of interest with the striatum. This information can subsequently be used for brain stimulation or connectivity studies, especially in tandem with transcranial magnetic stimulation (TMS). Diffusion tensor imaging (DTI) was used to collect information about the orientations of underlying neural pathways, and tractography to parse this discrete information together into continuous tracts estimating the routes of the fibre pathways.

Functionality of the striatum has an important impact on behaviour as the structure works in the interface of motor and executive control. The structure is known especially for its contributions to motor functions. Motor functions of the striatum include preparation, planning and execution of movement [1], and timing of self-initiated actions [2], among others. Many of these tasks require cognitive control of and executive decisions about the appropriate behavioural responses. Two types of behavioural control critically depend on the striatum: 1) habitual signal-response behaviour that is the basis of instrumental learning and behaviour and 2) higher order goal-oriented behaviour that depends on associating actions with their likely outcomes and evaluating the rewards (For a review of a series of studies contrasting and comparing these types of behavioural control in rats, see: [3]). Changing behaviour when the pursued goal or the reward value of it changes and switching attention between tasks require contribution of the striatum [4]. Furthermore, the striatum monitors and modulates information in working memory [5]. The striatum employs dopamine as the primary transmitter on affecting the other brain areas and performing its functions. Important sources of information about human striatal functions have been degenerative diseases whose primary deficits involve loss of motor control and various cognitive impairments, such as Parkinson's disease (for a review, see: [6]) and Huntington's disease (for a review of the dysfunctions, see: [7]). Both diseases are characterized by progressive degeneration of dopaminergic connections from the substantia nigra to the striatum.

Different parts of the striatum contribute to different functions. The dorsal striatum consists of two functionally and anatomically separable structures, the caudate nucleus and putamen, although collaboration, co-activation and coordination is common. The caudate nucleus is mainly responsible for executive and cognitive functions, whereas the putamen is the major contributor to motor functions. The ventral striatum, on the other hand, is crucial for the reward system, motivation and addiction [8].

Striatum connects with large parts of the cortex forming discrete, focally overlapping cortico-striatal circuits that project back to the cortex through other basal ganglia nuclei (Organization first postulated by Alexander and colleagues [9] and later replenished to include the focal overlap by Haber [10]). As suggested by the functional division of the striatum, the caudate nucleus is primarily connected with the frontal lobes, especially the prefrontal areas that are critical to high order behavioural control, like planning and problem solving. Similarly, the putamen links especially strongly with areas contributing to motor functions, such as the primary motor cortex, premotor cortex and supplementary motor area. The organization of the neural connections has been studied extensively in animals, but the methods used in animal studies are not transferrable to humans as they induce chemical or physiological changes in the brain.

Diffusion tensor imaging (DTI) and tractography offer a non-invasive method for tracking anatomical connections in living subjects, including humans [11]. Diffusion

tensor imaging is a magnetic resonance imaging technique that detects movement of water molecules, i.e. diffusion, in a voxel (the smallest measurement of volume determining the resolution of imaging, analogous to a pixel in three dimensions). Diffusion is fastest in the direction of the least resistance. White matter in the brain consists mainly of neural axons that are organized in tightly packed and often highly oriented fibre pathways. Therefore, in white matter, water molecule diffusion is fastest in the direction of these pathways, moving along them, and highly restricted in the direction perpendicular to the fibres where consistently organized cell membranes and myelin hinders the movement. In DTI, the speed and direction of the movement are measured in several directions, and modelled within a voxel as a three-dimensional ellipsoid, which is called the diffusion tensor. The principle eigenvector of the diffusion tensor indicates the direction of fastest diffusion, i.e. the primary orientation of the underlying fibre pathway. In white matter voxels, the primary direction is easily distinguishable as highly organized fibres consistently district movement in certain directions. On the other hand, in grey matter, which consists mainly of the cell bodies of the neurons, the fibre barriers are randomly organized which district the movement of water molecules in general but without consistent direction. Therefore, diffusion in grey matter voxels is un-directional, i.e. the water molecules move in all direction with approximately the same speed and volume. This shapes the diffusion tensor as a sphere and makes determining the primary direction impossible. Unfortunately, same obscuration occurs also in voxels that contain more than one fibre pathway that travel in crossing directions. Singular diffusion tensor cannot adequately model complicated diffusion patterns as it describes the average diffusion over the whole voxel. This may lead to problems when the tracts are constructed from the data.

Tractography is the algorithm capable of parsing discrete voxels together into continuous trajectories that illustrate the paths of the neural fibres. The first algorithms were developed at the turn of the millennium by Mori and colleagues [12], Conturo and colleagues [13], and Basser and colleagues [14]. A tractography algorithm works by taking a step, whose length can be fixed to an arbitrary number smaller than the voxel dimensions (for example: [14]) or varied depending on the location within a voxel (for example: [12]), in the direction of the fastest diffusion as depicted by the primary orientation of the diffusion tensor that models the diffusion within the voxel in question. In this new location, the primary orientation is determined again from the diffusion tensor prevalent in the new location before the taking the next step along it. The tracking continues until it arrives to grey matter areas where the primary direction of the diffusion tensor is ambiguous, or oriented in an unfeasible angle to the previous direction, which prevents the constructed tract from taking anatomically unfeasible turns.

Tractography methods are divided into two categories. Deterministic methods create only one tract per starting point thus always producing the same results. Probabilistic methods take into account the uncertainty of determining the orientations of a diffusion tensor by drawing the direction of movement from a distribution of possible orientations instead of directly using the primary orientation of the tensor (For example: [15], [16]). Both methods can reconstruct the major neural pathways fairly accurately ([17], [18] for deterministic methods, [19] for probabilistic methods), but deterministic methods are more vulnerable to data artefacts or other discrepancies, such as ambiguity in the primary orientation of diffusion tensor as caused by crossing fibre pathways in the voxel.

Some studies have already successfully used diffusion tensor imaging and tractography on tracking anatomical connections between the striatum and cortical areas ([20], [21], [22], [23]). Knowing the anatomy of the connections is especially advantageous to

transcranial magnetic stimulation (TMS) studies that aim at examining the functions of the striatum by stimulating cortical areas with which the striatum is anatomically connected. Previous studies have shown that stimulating the dorsal prefrontal cortex or the motor cortex activates dopamine release selectively in the caudate nucleus or the putamen, respectively ([24], [25]). As dopamine is the primary transmitter employed by the striatum, stimulating its release may have effects on the motor or cognitive functions that the striatum contributes to. As functions of the striatum are separable to different anatomical sections, stimulation of different areas of the striatum affects different functions. Furthermore, it is crucial to acquire information of the distribution of the corticostriatal connection in individual level since inter-subject variability in both the brain structure and function is great [26]. Individual knowledge of anatomical connections will allow more precise activation of the subareas of the striatum with TMS.

In this study, I concentrate on the dorsal striatum, namely the caudate and putamen nuclei, as they form the primary part of the structure and are involved in the executive, cognitive, and motor functions the structure most crucially contributes to. Specifically, I separately track connections between the caudate nucleus and two areas in the prefrontal cortex, the dorsal prefrontal cortex (DLPFC) and ventral prefrontal cortex (VLPFC), as well as connections between the putamen and four motor areas, the primary motor cortex (M1), premotor cortex (PMC) and supplementary motor area (SMA), divided into the primary SMA and preSMA based on functional differences between the areas. Previous studies have shown that the caudate nucleus has robust connections with the frontal lobes, especially the prefrontal cortical areas, and that it contributes strongly to executive and cognitive functions ([22], for a review of the cognitive contributions of the caudate nucleus, see: [27]). On the other hand, the putamen seems to be the primary source of motor control of the striatum, and links strongly with areas involved in movement, i.e. the above listed motor cortical regions ([22], [21]).

I have organized this thesis so that the next three Chapters concentrate on the background and theory, Chapter 2 introducing the anatomy and functions of the dorsal striatum, and Chapter 3 concentrating on the available knowledge of the striatal connections. Chapter 4 further explores the techniques relevant to this study that were used to track the connections, the diffusion tensor imaging (DTI) and tractography. Chapter 4 also introduces the transcranial magnetic stimulation (TMS) method for stimulating the cortex and subcortical areas through anatomical connections. Then the focus shifts to experimental and methodological parts, with Chapter 5 specifying the data and the experimental design, Chapter 6 introducing the results and Chapter 7 discussing the findings. In Chapter 7, I also discuss the future aspects and possibilities for further research. In the last Chapter, Chapter 8, I conclude the findings and significance of this study.

2 Striatal anatomy and function

The caudate nucleus and putamen are subcortical structures deep in the brain that contribute to various motor, executive and mnemonic functions. Together they form the dorsal section of a structure called the striatum, which in turn is a part of the basal ganglia. The striatum is best known for its involvement in planning, controlling and executing movements. Additionally, the dorsal striatum contributes to two processes within behavioural control and learning: goal-directed learning which forms contingencies between actions and their likely consequences (action-outcome learning, A-O), and habitual learning that associates a stimulus with a response (stimulus-response learning, S-R). The two systems are separate and often antagonistic controlling behaviour in different situations, but also interact and interconnect profusely. For a review contrasting and comparing the two systems in rats, see: [3].

In this Chapter, I introduce the anatomy of the striatum and the most important functions of the caudate nucleus and putamen to justify why studying them and finding ways to control their activation is important. In the first subchapter, I briefly introduce the anatomy of the striatum. The next two subchapters explore the most important functions of the caudate and putamen, respectively. In the last subchapter, I briefly introduce a few of the most important diseases characterized by striatal dysfunction.

2.1 Anatomy of the striatum

The striatum, also known as the neostriatum or the striate nucleus, is a group of subcortical grey matter structures at the base of the forebrain. It is one of the main components of the basal ganglia, which is a collection of various interconnected nuclei spanning the midbrain, telencephalon and diencephalon in both hemispheres. The basal ganglia integrates information from the cortex, thalamus and brainstem, and is critical for various functions including voluntary movement [28], learning ([29], [30]), memory [31], motivation [32], and emotion [33].

The striatum is typically divided into ventral and dorsal sections. The ventral part consists of the nucleus accumbens and olfactory tubercle. The ventral striatum activates when anticipating pleasurable or painful events (e.g. [34], [35], respectively), forming a crucial part of the reward system. It also contributes to the evaluation of emotion: For example, lesions of the ventral striatum impair recognizing signals of aggression [36].

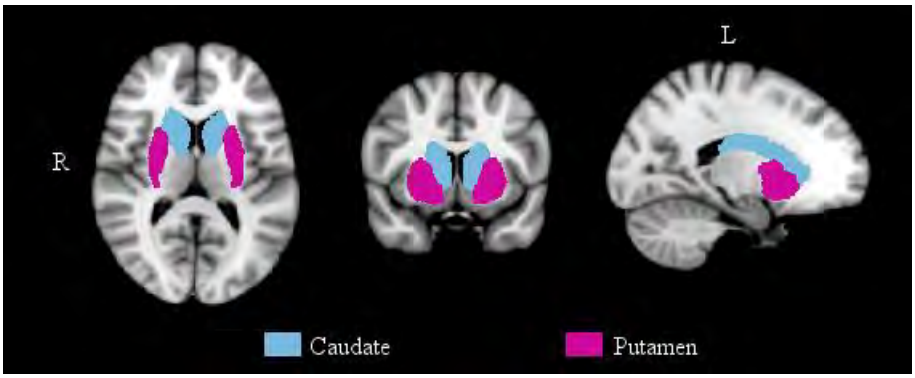

Figure 1: The dorsal striatum consists of two subcortical nuclei deep in the brain: the caudate nucleus (light blue) and the putamen (pink). Here they are depicted in the MNI152 standard brain using the Harvard-Oxford subcortical atlas ([147]–[150]).

The dorsal part of the striatum contains the caudate nucleus and putamen, the two structures that are in the focus of this study. Their locations in the brain are illustrated in Figure 1. These nuclei are anatomically separated from each other by the anterior crus of the internal capsule, which is a large white matter neural fibre bundle connecting the cerebral cortex and spinal cord. The caudate nucleus (light blue in Figure 1) is located medially to this tract. It is bordered by the lateral wall of the lateral ventricle. The putamen (pink in Figure 1) is situated more laterally and posteriorly than the caudate nucleus. Thin grey matter bridges connect the structures over the internal capsule. These connections create the striped appearance that gives the whole group of structures the name, striatum, which is Latin for "striped".

The striatum, especially the dorsal striatum, is the primary input area of the basal ganglia receiving axons from nearly all parts of the cortex, excluding the primary cortices for visual, auditory, and olfactory inputs. The caudate nucleus and putamen connect with the frontal lobes, sensorimotor areas, cerebellum and associative cortices. They are also reciprocally connected with the substantia nigra through the nigrostriatal tract. The majority of the output produced by the basal ganglia travels to the cortex via the substantia nigra or the globus pallidus. The organization of the striatal connections is further explored in Chapter 3.

Both the caudate nucleus and the putamen employ the neural transmitter dopamine to perform their functions as the main connections to and from cortex and other areas of the basal ganglia are either dopaminergic or glutamatergic. Release of striatal dopamine is connected to motor learning, execution of movement, and reward-related processes (For a review of dopaminergic behaviour in humans, see: [37]). In addition, striatal dopamine affects working memory capacity, task accuracy and motor speed [38].

2.2 Functions of the caudate nucleus

The caudate nucleus is heavily involved in goal-directed behaviour. This broad classification includes e.g. switching the response in changing situations, learning contingencies between actions and outcomes, and planning actions to execute. Goal-directed learning (also knowns as action-outcome learning, A-O) requires a flexible mental representation of the pursued goal that can be updated or modified as the circumstances change, and a knowledge of likely consequences, i.e. of the outcome most likely to follow any given action.

The caudate nucleus is involved in learning the contingencies between actions and outcomes. In rats, inactivating the medial dorsal striatum (mDS, which corresponds to the caudate nucleus in primates) either before and after a training period hampers responding to decreasing the desirability of the reward (an experimental method knows as outcome devaluation). This observation indicates that the rats without a fully functioning mDS could not learn the flexible contingency between action and desirable outcome, instead creating a habitual stimulus response contingency that does not allow flexibly re-evaluating the desirability of the reward and ceasing to pursue it ([39], [40]). In monkeys, the caudate nucleus activates during associative learning with a strength that correlates with the rate of learning and peaks when new associations are acquired [41]. In humans, successful action-outcome learning with probabilistic instead of direct associations activates the body and tail of the caudate, and the putamen with higher activity when the associations grow stronger. Activation in the head of the caudate correlates with feedback processing, i.e. with the evaluation of the correctness of the associations and the need to change them. Feedback activity decreases across trials indicating a decreasing need to process feedback as associations between the action and the ex-

pected outcome strengthen [42]. In rule-learning situations where finding correct solutions requires hypothesis testing, activity in the head of the caudate peaks early when solving a novel problem and then rapidly decreases. This suggests a role in the identifying behavioural context and the need for new behaviour [43].

Changing behaviour is a cognitively demanding process. It involves not only the behaviour switch itself, but also evaluating the need for a switch, determining a new appropriate response, and inhibiting ongoing behaviour. Studies with rats have demonstrated that lesions of the mDS impair switching between strategies and create an inability to maintain new behaviour [44]. Additionally, lesions of the mDS disrupt inhibiting an ongoing action in stop-signal tasks [45]. Since a lesion of the nucleus accumbens or the medial prefrontal cortex, areas often connected to the inability to inhibit behaviour in disorders such as attention deficit hyperactivity disorder (ADHD), do not have a similar effect [46], the caudate nucleus seems critical for suppressing ongoing action.

Choice behaviour in rats with lesions of the mDS, especially of the posterior part of it, is inflexible and habitual. For example, Yin and colleagues [47] found that rats with the mDS lesions instilled before a training period could not adjust their learning of the location of a reward to a different situation. The maze the rats had to navigate was revolved 180 degrees so that turning in the opposite direction than in the training situation was required to reach the reward. A control group of rats without the lesions could flexibly adjust their actions to the changed situation and found the reward. This indicates that they had learned the contingency between the action and expected outcome instead of a direct and inflexible response-stimulus association.

Studies with humans have provided more evidence of the role of the caudate nucleus in changing behaviour, especially in set-shifting tasks and with novel actions. Set-shifting, also known as task-switching, refers to the ability to shift attention flexibly between different tasks and sub-goals while bearing in mind the overall goal. The caudate activates selectively when a change of behaviour by implementing a novel action is needed, but not for the change of action itself. This distinction was demonstrated by Monchi and colleagues [4] who experimented with a modulation of the Wisconsin Card Sort Test (WCST). WCST is a commonly used behavioural experimental scenario in which subjects sort cards according to a given rule. The experimenters vary the rule and the way it changes to investigate brain activation patterns and the effects of brain lesions. In this case, the experimenters dissociated 1) the retrieval of the sorting rule, 2) the execution of the shift in behaviour (in a condition in which the rule changed regularly to make evaluating the need for a change in behaviour unnecessary) and 3) the cognitive decision to change the rule to follow. The caudate activated reliably only in the condition where evaluation of the need for a change was required. This stresses the importance of a cognitive evaluation process, not reacting out of habit, for the activation of the caudate. Activation in this evaluation phase of the processing is not specific to modality, as similar caudate activation happens when planning a set-shift with lexical stimuli [48]. The role of the caudate nucleus in planning is further stressed by a finding that the caudate nucleus is the only brain area that activates more when subjects image, i.e. plan, than when they execute novel actions [49].

The relationship between the action and outcome determines the involvement of the caudate and the magnitude of its activation: the more the action influences the outcome, the larger the activation. The contingency, however, does not need to be direct: the caudate activates also in situations where subjects felt that their response determined the outcome, even if not actually true. A perception of contingency is sufficient to activate the caudate. The activation does not depend on the reward or punishment, but on the reinforcement of the link between the action and the outcome. [50]

Additionally, the outcome does not need to be a tangible reward, such as food. An intrinsic, extrinsic, social or even imagined reward activates the caudate nucleus as long as an action-outcome link is present. For example, Tricomi and colleagues [51] examined differences in the activation patterns between an intrinsic (learning itself as a reward) and extrinsic (monetary reward or punishment) motivation in perceptual category learning. Native Japanese speakers learned to distinguish between English L- and R-phonemes with a feedback loop. Experimenters found that the caudate nucleus activated bilaterally in either scenario indicating that with motivated subjects the intrinsic motivation to learn can be as powerful as an outwardly dictated monetary reward.

Effectively executing abovementioned tasks or any kind of goal-directed action requires a utilization of working memory. The caudate nucleus manipulates and modulates information in working memory, but does not participate in maintaining it or in retrieving information from long-term memory. For example, Lewis and colleagues [5] found significant activation in the caudate when manipulation of working memory information was needed. The caudate activates especially when working memory monitoring is self-ordered and intrinsically needed instead of outwardly dictated [52].

In addition to working memory, the caudate nucleus contributes also to long-term memory. The caudate is especially involved in the implicit, procedural memory system, such as learning associations between actions and outcomes, as discussed above. Declarative memory functions depend mainly on the hippocampal system which often functions independently of the procedural memory system. For example, in rule-learning, the hippocampal activity correlates negatively with the learning success which in turn correlates positively with the activation of the caudate nucleus [43]. This finding is in line with the suggestion that the caudate has a critical role in procedural learning whereas the participation of the hippocampal system is not always necessary. Despite this separation, the systems interact and interconnect widely. For example, their interaction can be beneficial in learning situations where both systems can provide solution, such as in motor sequence learning [53]. For an in-depth review of the competition and cooperation between the memory systems, see: [54].

Even though the striatum is strongly connected to motor functions, the caudate nucleus does not seem to be the major contributor as lesions of the caudate only rarely lead to motor disorders [55]. The caudate is involved in the planning of non-routine actions together with the anterior parts of putamen (the areas which form the so-called associative striatum) [56]. The anterior caudate is essential for learning new movement sequences [57]. Contributions of the caudate to motor functions rest on the cognitive or executive parts of the processing, such as selecting a correct action [1], instead of the execution of the action.

2.3 Functions of the putamen

Putamen is the major contributor of the basal ganglia to various motor functions. It is involved in the execution, preparation and planning of movements. It integrates and modulates motor information from all the major motor areas, such as the primary motor cortex, premotor cortex, supplementary motor area and cerebellum. The putamen also partakes in cognitive functions contributing to different types of learning and mnemonic processes, e.g. stimulus-response learning and implicit motor sequence learning. While the caudate nucleus, especially the anterior caudate, seems to be responsible for goal-oriented learning, the stimulus-response learning (S-R) that is essential for forming habits falls under the purview of the putamen.

S-R learning refers to associating a stimulus with a direct behavioural response that leads to a reward. It is the basis of conditioning and habit forming. S-R learning

was long assigned to the striatum as a whole, but lesion studies with rats have indicated that the putamen is selectively responsible for this type of learning. Lesions of the lateral dorsal striatum in rats (lDS, which corresponds to the putamen in primates) impair performance in discrimination tasks that require S-R learning. In contrast, lesions of the medial dorsal striatum (mDS, corresponding to the caudate nucleus in primates), do not have similar effects. ([58], [59])

In contrast to the action-outcome learning and other types of goal-directed learning, an S-R association is not flexible once it is formed. Changing the desirability of the reward or the contingency between a response and an outcome does not affect S-R learning or behaviour controlled by it, as it is, by definition, stimulus-dependant. Thus, behaviour controlled by an S-R association is habitual and often compulsive. Behaviour directed by a goal, on the other hand, can change drastically if the value of the pursued outcome changes. These two types of behavioural control often pull to different directions as habitual, compulsive behaviour control hinders more goal-oriented reacting and vice versa. (For a review of the interactions between the systems especially in rats, see: [3])

The relationship between the S-R and A-O learning has been studied especially in rats. In healthy rats used as controls, repeating an action (e.g. pulling a lever) in a training period leads to a compulsive behaviour in response to the learned stimulus. Repeating the action does not change even if the desirability of the produced reward decreases through overexposure. Learned habitual behaviour persists without regard to the consequences, indicating that an S-R contingency was formed. In contrast, when the lDS is inactivated through chemical lesions, learning and reacting to the changing relationship between the outcome and action improves, i.e. pulling the lever decreases when the associated reward becomes less desirable. This suggests that inactivating the lDS disrupts the development of the normal habit forming S-R contingency thereby leaving the alternative A-O contingency system to control behaviour ([60]). Furthermore, inactivating the lDS does not prevent learning action-outcome contingencies or reacting to changing desirability of the reward acquirable with a certain action, unlike inactivation of the mDS [39]. Yin and colleagues explored the dissociation between the A-O and S-R learning in a series of experiments with rats, all supporting the functional and anatomical separation of the areas corresponding to the caudate nucleus and putamen, respectively. For a review of their work, see: [3].

Like the caudate nucleus, the putamen is involved in working memory processes. The putamen contributes to preventing irrelevant information from claiming working memory capacity. Lesions of the left putamen impair performance in working memory tasks when task-relevant and irrelevant information is presented together [61]. Furthermore, release of dopamine in the putamen correlates positively with motor speed in tasks requiring working memory contribution [38].

Nonetheless, motor functions are what the putamen is best known for. The putamen is a part of a comprehensive network responsible for movement that consists of the motor cortex, premotor cortex, supplementary motor cortex and cerebellum. The putamen is involved in both the preparation for and execution of movements [1], especially when the action is self-initiated. Positron emission tomography (PET) and functional magnetic resonance imaging (fMRI) studies have shown significantly increased activity in the putamen in paced finger tapping tasks when the timing of the taps is self-initiated in comparison to the activation when the tapping is outwardly cue-initiated ([62], [63], respectively). Involvement of the putamen associates especially to self-determining the timing of acting, instead of choosing the appropriate action [2]. Furthermore, the role of the putamen increases when the produced action is new. While the caudate activates in

the cognitive, planning periods of the novel actions, the putamen activates during the execution of the action [4].

Moreover, sequential movement requires contribution of the putamen. The posterior putamen is critical for executing already learned sequences, while damage to the anterior putamen or the caudate nucleus (the areas that form the associative striatum) severely impairs learning new motor sequences [57]. Activity in the posterior putamen increases as the sequence becomes more familiar, while activity in the associative striatum simultaneously decreases [64]. The putamen is also involved in implicit learning of motor sequences, i.e. learning a sequence when it is not explicitly taught or shown, but the performance improves without a conscious contribution as manifested by, for example, shorter reaction times which indicate that learning has occurred ([65], [66]). However, the putamen, or the striatum as a whole, do not appear to be critical for the process, as focal lesions of the area do not impair a patient's ability to implicitly learn motor sequences [67].

2.4 Disorders affecting the striatum

The largest source of knowledge regarding basal ganglia disorders is Parkinson's disease (PD). PD has been studied extensively as it is a fairly common disorder: In Finland there are approximately 14 000 PD patients (Suomen Parkinson-liitto, http://parkinson.fi). The primary characteristic of PD is the dopaminergic neuronal loss in the substantia nigra, which is a structure in the midbrain and a part of basal ganglia. The nigrostriatal tract that connects the dorsal striatum and the substantia nigra, and the mesocortical pathway that links the ventral tegmentum and the medial substantia nigra with the frontal lobe are also affected. As dopamine is the main neurotransmitter employed by the striatum, the structure as a whole is severely compromised in PD. The depletion of dopamine progresses gradually and leads to various impairments in executive and motor functions and, in about 40% of patients, to some form of dementia [68]. The disease affects the putamen more severely than the caudate nucleus in the long run. However, especially in the early stages, PD is characterized by bilateral dopamine depletion in the head of the caudate nuclei.

Motor deficits are the most commonly known symptoms of PD and construct a corner stone of the clinical diagnose. Bradykinesia, rigidity, resting tremors, and loss of postural reflexes are common motor impairments [69]. Motor blocks, such as freezing of gait, occur in approximately a third of patients. Motor blocks refer to an abrupt inability to begin or continue walking, occurring especially in stressful time-constrained situations, or while turning in or entering to narrow areas. Freezing of gate has been hypothesized to reflect an inability to ignore competing, task-irrelevant information when a change in behaviour or an immediate action is needed, similar to attentional set-shifting tasks that the caudate contributes to as discussed in Chapter 2.2. A finding that gate freezing and difficulties in set-shifting tasks correlate in PD patients supports this theory [70]. In the early stages of the disease, the motor symptoms can be treated with L-dopa, a precursor of the neurotransmitter dopamine. L-dopa, unlike dopamine, can cross the blood-brain barrier and increases dopamine levels in the striatum, therefore mitigating the motor deficits. However, the mitigating effect decreases as the disease progresses [71].

PD also impairs goal-directed behaviour. Patients have difficulty to disengage attention from previously relevant information that a change in the situation or goal has now rendered unimportant. This is called perseverance. In addition, PD patients are unable to attend to or learn about information that suddenly becomes relevant to the situation after it was previously declared irrelevant. This is called learned irrelevance. In

contrast, patients with frontal lobe damage demonstrate severe perseverance, but perform normally where PD patients struggle with learned irrelevance [72]. PD patients are often compared to and contrasted with patients with frontal lobe damage, because in the early stages of PD, impairments in executive functions resemble impairments produced by injuries to the frontal lobes. The striatum and the frontal lobes are strongly connected, mainly through dopaminergic tracts, so comparing and contrasting patients with PD and frontal lobe damage may shed light on the how the control of the executive and cognitive functions to which both areas contribute is divided between them and to which functions each area is critical.

Moreover, PD impairs the ability to select appropriate sub-goals, especially when the situation requires temporarily acting in opposition to one's overall goal to achieve it later. This effect has been demonstrated, for example, with the Tower of London test scenario [73]. In an experiment by Owen and colleagues [74], the subjects moved a set of three coloured balls around in "socks" to match a goal arrangement. Long initial thinking time characterized the performance of patients with both mild and severe PD. This refers to the period during which a subject plans a sequence of moves and required sub-goals to achieve the goal. There was no difference in the subsequent thinking or execution times after performing the first move between either of the patient groups (mild or severe PD) or the healthy control group. The accuracy of the solution production was impaired only in severe PD patients.

Another degenerative disease characterized by damage to the striatum is Huntington's disease (HD). In HD, the dopaminergic neurons in the striatum progressively die, starting at the head of the caudate nucleus and continuing in the dorsal-to-ventral direction [75]. The atrophy causes a wide range of cognitive impairments encompassing both visuospatial memory and executive functions as well as disruptions in motor functions. The most characteristic motor deficit in HD is chorea, which means involuntary brief, irregular, and non-repetitive movements that appear to flow from muscle to muscle.

As the HD progresses, deficits in executive functions become more apparent. Patients exhibit severe impairments in flexible problem solving, planning, and ignoring distractions, all of which, as discussed in the previous subchapters, critically depend on the striatum. Similarly to PD, HD patients struggle with perseverance as demonstrated with both the WCST [76] and Tower of London paradigm [77]. HD creates dysfunctions on attention, concentration, visuospatial abilities, mnemonic functions (declarative, procedural and working memory) and processing of emotion, especially recognizing disgust expressed in voice or facial expression. For a review of dysfunctions associated with HD, see: [7].

The striatum has also been connected to spatial neglect. Spatial neglect is a disorder, typically developed following a lesion of or an injury to the parietal cortex, which disrupts or, in severe cases, destroys the ability to respond to stimuli or to subjects located in the contralateral side of the space of the lesion. Neglect is strongly lateralized as it typically develops only after lesions or injury to the right hemisphere. The right superior temporal gyrus (STG) has been identified as the neural correlate of the spatial neglect, but an injury to or a lesion of the right striatum or the right thalamus can also invoke spatial neglect (e.g. [78]–[82]). Especially the putamen and the pulvinar, a subcomponent of the thalamus, have been found to have a central role in the spatial neglect syndrome. An injury to the caudate nucleus can also contribute to the spatial neglect but to lesser degree. [83]

3 Anatomical connections of the striatum

The dorsal striatum is the major input area of the basal ganglia, receiving connections from large parts of the cortex, including but not limited to the associative areas, frontal lobes, motor areas and the cerebellum. The caudate nucleus primarily links with the areas in the frontal lobes, especially with the prefrontal cortex (PFC). The putamen generally links with the sensorimotor regions, such as the primary motor and sensory cortex and the supplementary motor area. This pattern of connectivity reflects the functional division between these two areas, as reviewed previously in Chapter 2.

In this Chapter, I introduce the prevalent theory of the organization of the cortico-striatal connections and some of the most compelling evidence for it. The second subchapter concentrates on the connectivity studies done with human subjects that illuminate the organization of the connections. I review evidence from both anatomical and functional connectivity studies.

3.1 Organization of striatal connections

The cortico-striatal connections are organized within the hemispheres in globally parallel discrete circuits [9] that overlap focally so that functionally related cortical areas connect to the same areas in the ipsilateral striatum ([10], [84]). An influential landmark model was proposed by Alexander and colleagues in 1986 [9]. It states that projections between the striatum and the cortex are organized bilaterally in parallel, discrete circuits each with their own sites of connection in the striatum and cortex that are topographically organized so that projections converge in specific parts of the striatum projecting back to discrete cortical areas through pallidal, nigral or thalamic output structures (see Figure 2). Each loop contributes to different motor or cognitive task, depending on the function of the cortical area in question. The loops separate to 1) a motor circuit connecting the SMA and the putamen, 2) an oculomotor circuit linking the caudate nucleus and the frontal eye fields (FEF) situated at the intersection of the middle frontal gyrus and the precentral gyrus in the frontal lobe, 3) a dorsolateral prefrontal circuit between the dorsolateral prefrontal cortex (DLPFC) and the dorsolateral caudate, 4) a lateral orbitoventral circuit connecting the lateral orbitofrontal cortex and the ventromedial caudate, and 5) an anterior cingulate loop between the anterior cingulate area and the ventral striatum. The organization of the loops is similar in both hemispheres, and the circuits in different hemispheres may connect through the corpus callosum or the anterior commissure (AC), two most significant structures connecting the hemispheres.

In addition to the parallel loop model, several different topographical organization of the connections in striatum have been proposed. The striatum has been divided to three functional zones each receiving input from different cortical regions ([85], [86], [87], [88]). In these divisions, the first zone, the associative striatum consists of the rostral putamen and of a large part of the head of the caudate. It receives inputs from the dorsolateral prefrontal cortex (DLPFC), presupplementary motor area (preSMA), and posterior parietal cortex, thereby loosely corresponding to the dorsolateral prefrontal circuit. The second zone, the sensorimotor striatum, contains the caudal and dorsolateral putamen and the dorsolateral rim of the caudate. It connects with the primary motor area, SMA, and somatosensory cortex (S1), corresponding to the motor loop. The third zone, the limbic striatum, includes the ventral caudate and the putamen. The limbic striatum receives connections from the orbital and medial prefrontal cortex, thereby corresponding to the orbitoventral loop.

A recurring premise of all the models, including the parallel loop model, is that functionally related cortical areas connect to the same striatal areas. Notably, different

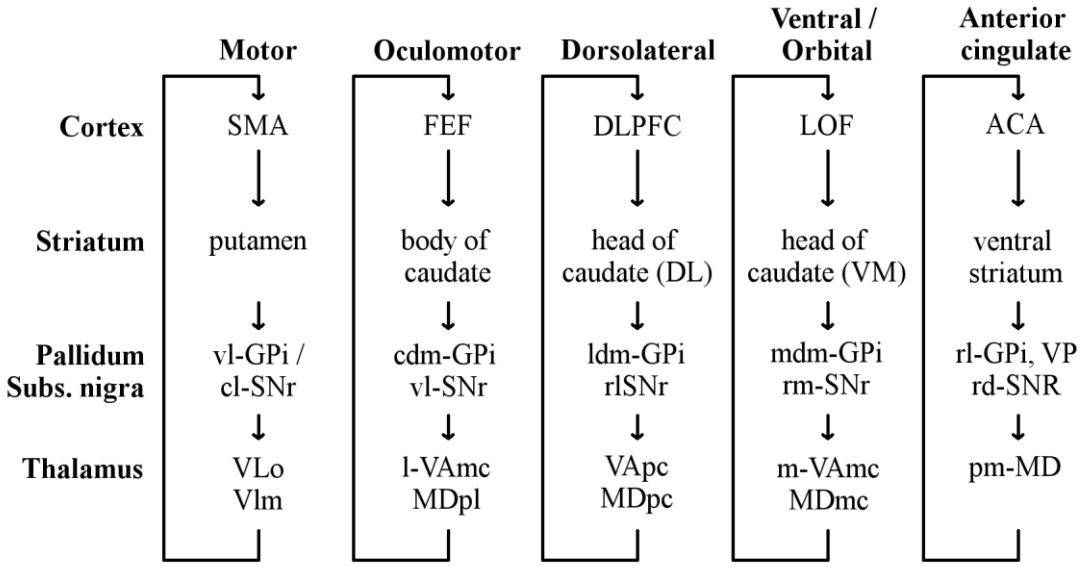

Figure 2: Parallel organization of the cortico-striatal circuits. Different parts of the striatum are connected with distinct parts of the cortex forming circuits that return to the cortical areas through similarly discrete sections of the pallidum, substantia nigra and thalamus. The putamen plays an important part in the motor circuit, while different areas of the caudate nucleus contribute to the oculomotor, dorsolateral and orbitoventral circuits. Adapted from [9].
Abbreviations: SMA – supplementary motor cortex; FEF – frontal eye fields; DLPFC – dorsolateral prefrontal cortex; LOF – lateral orbitofrontal cortex; ACA – anterior cingulate area
DL – dorsolateral; VM – ventromedial
GPi – internal segment of globus pallidus; SNr – substantia nigra pars reticulate; vl – ventrolateral; cl – caudolateral; cdm – caudodorsomedial; ldm – lateral dorsomedial; rl – rostrolateral; mdm – medial dorsomedial; rm – rostromedial; rd – rostrodorsal;
VLo – ventrolateral nucleus of the thalamus pars oralis; Vlm - ventrolateral nucleus of the thalamus pars medialis; VAmc - ventral anterior nucleus of the thalamus pars magnocellularis; MDpl - parvocellular subnucleus of the mediodorsal nucleus of the thalamus; VApc – parvocellular subnucleus of the ventroanterior nucleus of the thalamus; MDpc – parviocellular subnucleus of the mediodorsal nucleus of the thalamus; MDmc – magnocellular subnucleus of the mediodorsal nucleus of the thalamus; pm-MD – posteromedial mediodorsal nucleus of the thalamus.

models are not mutually exclusive but can rather complement and refocus each other. In fact, Alexander and colleagues ([9]) originally prepared their model to be later replenished, stating that they provided only the framework.

The idea of completely separate loops has been complemented with models allowing focal overlap within the loops in both the cortex and the striatum ([10], [84]). The area of the overlap in the cortex has been indicated as the integration area for the reward and control signals arriving from the orbitofrontal cortex and DLPFC, respectively (for a review, see: [8]).

The level of overlap, especially in the striatum, is still controversial. Many theories postulate wide convergence at the cellular level so that axons from several cortical

zones provide information to the same neurons in the striatum. However, cellular level studies have demonstrated that projection within the overlapping zones are sparse, "patchy" patterns of innervation [89], synaptic connections are rare even in projection extending long distances along the striatum, and cortical afferents are rarely shared between adjacent striatal neurons [90]. When convergence of information does happen, the input is likely from nearby cortical neurons instead from areas belonging to the other circuits [91]. Together, all of these findings indicate that information from overlapping input zones is not added together at cellular level within the striatum, suggesting that the information convergence happens in some higher processing level. On the other hand, later studies have identified neurons at the junction of the overlapping zones in the striatum that do react to inputs from different cortical areas. For example, Nambu and colleagues noted convergent inputs from both the M1 and SMA in single cells located at the junction of the input zones from aforementioned cortical areas [92]. However, as both the M1 and SMA are parts of the motor circuit, information convergence between them does not contradict the parallel loop model.

Other animal studies provide support for the parallel loop model, with some caveats for partial overlap. Furthermore, they suggest a further topographical division of the putamen with regards to the connected cortical area. Takada and colleagues examined striatal connections of motor areas, namely the M1 and SMA, in a series of studies ([93], [94]). They found clear segregation between the input zones in the putamen as the M1 projected mainly to the lateral part of the putamen, and the SMA to the more medial areas. However, the areas overlapped partly in the mediolateral central area where, as mentioned earlier, single neurons reacted to both inputs [92]. Similarly, the orbital and medial areas of the PFC in monkeys connect with different, separate parts of the striatum reflecting the functional organization of the PFC [95].

All in all, studies in animals largely support the notion that striatal connections divide into separate cognitive, affective and motor circuits that partly overlap and converge. This strongly suggests functional specialization of different areas of the striatum.

3.2 Striatal connections in humans

Theories of the organization of the striatal connections leaned on interpolations from animal studies and experiments on the functional connectivity for a long time, because methods used in animal studies, namely tracer agents, were not transferrable to humans due long term effects and invasiveness. Anatomical connectivity in humans was explored non-invasively only after the emergence of diffusion tensor imaging (DTI) and tractography. These methods allow tracking of anatomical pathways in living subjects without harmful side-effects. Theory and practicalities behind these methods are discussed further in Chapter 4.

Lehéricy and colleagues [20] provided the first direct evidence of discrete corticostriatal loops in humans in 2004. They demonstrated robust connections between the posterior putamen and the sensorimotor areas in the primary motor cortex, the primary somatosensory cortex and the posterior supplementary motor areas, supporting the existence of the motor loop in humans. A link between the associate compartment of the striatum (the anterior putamen and the caudate nucleus) and PFC, frontal pole, and preSMA supports the idea of the dorsolateral, oculomotor and orbitoventral circuits. Furthermore, the study found highly reproducible connections between the ventral striatum (the limbic compartment) and the orbitomedial frontal cortex, amygdala and hippocampus. Interestingly, connections with the cingulate areas were not found, likely due to limitations of the used techniques.

Several studies of anatomical connectivity support the parallel loop model with some overlap (e.g. [22], [23], [96]). Leh and colleagues [22] demonstrated with DTI that the caudate nucleus is interconnected with the PFC, the inferior and middle temporal gyrus, the frontal eye fields, the cerebellum, and the thalamus. This lends further support for a loop connecting the lateral PFC and the striatum that is always present in theories about the cortico-striatal connections. Additionally, the study found that the putamen interconnects with the primary motor area, primary sensory area, supplementary motor area (SMA), premotor area, the PFC, cerebellum, and thalamus, well in sync with the idea of a sensorimotor circuit. Furthermore, the study also found evidence of further functional division of the striatal projections, suggesting that the dorsal-posterior caudate connects preferably with the DLPFC, whereas the anterior medial caudate interconnects with the ventrolateral PFC. In addition, the study found projections between the dorsal-posterior putamen and the SMA, the medial putamen and the premotor area, as well as the lateral putamen and the primary motor area. Studies concentrating more specifically in a subset of connections have provided further evidence that the putamen interconnects with the M1, SMA and preSMA [21], and the caudate nucleus interconnects with the PFC and thalamus [97].

In addition to the anatomical connectivity, functional connectivity of the striatum in humans have been studied. Functional connectivity refers to a statistical dependency between different brain areas regarding their activation patterns, i.e. the tendency of different brain areas to activate simultaneously. Thus, functional connectivity does not rely on direct anatomical connections nor do an anatomical connection guarantee a functional connection.

A meta-analysis of 126 functional magnetic resonance imaging (fMRI) and positron emission tomography (PET) studies provided evidence that different regions of the striatum have distinct patterns of functional connectivity with the cortical areas [98]. These findings support both the parallel loop model and the division of the striatum to the three sections, the associative, sensorimotor, and limbic zones. The putamen showed a high degree of co-activation with the primary motor areas, as well as the associative areas, such as the posterior parietal lobe. Furthermore, the putamen, especially the left putamen, co-activated with the ipsilateral prefrontal areas, which supports the notion that the putamen also contributes to cognitive and executive processes, instead solely focusing on the motor functions. The co-activation, especially between the putamen and the motor areas, was strongly lateralized to the left hemisphere. This is not surprising as a majority of the human population, and therefore of the subjects the study, are right-handed, leading to the stronger connections within the left hemisphere. In contrast, the caudate nucleus showed strong co-activation with higher level cognitive areas, such as the DLPFC, the rostral anterior cingulate and the inferior frontal gyri. The caudate did not strongly co-activate with the motor areas, supporting the notion that the putamen is primarily responsible for motor functions in the striatum whereas the caudate contributes more strongly to cognitive and executive functions. Functional connectivity has also been studied with so-called resting state connectivity, which has yielded similar results of the organization of the connections between the cortex and the striatum [99].

Striatal connections have also been examined with transcranial magnetic stimulation (TMS). In TMS, a magnetic field, generated by a brief electrical pulse, stimulates cortical neurons either exciting or, via inhibitory synaptic connections, inhibiting their activity. The stimulation affects subcortical structures, such as the striatum, through functional or anatomical connections. The effects can be examined for example with PET or fMRI. The technique is discussed more in length in Chapter 4.3.

TMS studies have demonstrated that stimulation of the motor cortex activates the putamen [100]. Furthermore, stimulation of the motor cortex induces a focal release of dopamine in the putamen without affecting the caudate nucleus [25]. In contrast, similar stimulation of the dorsolateral cortex increases neural activity [101] and dopamine release in the caudate, but not in the putamen [24].

In conclusion, non-invasive experiments in humans on both anatomical and functional connectivity demonstrate that there are strong connections between the striatum and the frontal as well as the motor cortices. The caudate links strongly with the higher order cognitive and executive areas in the frontal lobes, while the putamen connects robustly with the sensorimotor regions. While the putamen also has connections with areas in the frontal lobes that suggest a level of involvement in the executive and cognitive processes, it seems clear that the caudate is the main area of the striatum contributing to such functions, whereas the putamen dominates in the sensorimotor functions.

4 Description of techniques relevant to this study

In this Chapter, I go through the theory behind the techniques that were used in the method section of this study (diffusion tensor imaging and tractography) or that was otherwise relevant (TMS).

The first subchapter covers diffusion tensor imaging (DTI), the method that was used to collect the data. DTI measures the direction and volume of diffusion within the brain tissue and can be used to estimate the orientation of the neural fibre pathways in voxels.

Tractography, the subject of the second subchapter, is an algorithm that uses the DTI data to sparse together continuous trajectories from discrete data points. These trajectories model the routes of the neural pathways revealing anatomical connections between different areas of the brain.

The third subchapter introduces transcranial magnetic stimulation (TMS) that can utilize the connectivity information provided by tractography. TMS induces a brief magnetic field to the surface of the brain which can alternatively excite or inhibit neural activity. The magnetic field activates the cortical areas of at the surface of the brain, but the activation can spread to the subcortical brain areas through anatomical connections. Therefore, knowing the pathways between the brain areas helps to identify target areas for impulses to optimize the spreading of activity.

4.1 Diffusion tensor imaging

Diffusion tensor imaging (DTI) is a specialized application of magnetic resonance imaging (MRI) that is sensitive to diffusion of water molecules. It measures the mean displacement of water molecules in a voxel (a three-dimensional pixel that determines the imaging resolution). It is used, for example, to estimate the direction of neural pathways in white matter areas.

Diffusion means spontaneous movement of molecules that gradually levels concentration differences. Each individual molecule moves randomly through space producing a pathway that is impossible to predict. However, when the number of the molecules is sufficiently large, the averaged squared displacement of a molecule, i.e. the distance from the starting point, becomes directly proportional to the observation time. The constant of this proportionality is called diffusion coefficient. However, the measured overall displacement of the molecules due to diffusion typically differs from the theoretical value of the diffusion coefficient of the molecules in free water. This occurs because the molecules cannot move as freely in all mediums due to natural barriers, such as cell membranes. The observed value of the overall displacement is referred to as apparent diffusion coefficient (ADC). In brain imaging based on magnetic resonance, the observed molecules are invariantly water molecules. The variance in ADC values is caused by the differences in the organization of the medium in which the molecules move, i.e. the cellular level organization of brain tissue.

In an unorganized or free space, diffusion can be described as a surface of a sphere expanding over time (see Figure 3). In such spaces, diffusion is independent of direction and called isotropic. Such is the case in the grey matter areas of the brain. The nuclei of neurons, cell membranes, and dendrites form natural barriers in the grey matter and thus hinder diffusion compared to diffusion in free water, thereby decreasing the ADC value compared to the value of the diffusion coefficient in the free water. As the barriers are not coherently oriented but organized randomly, the mean displacement of water molecules in the grey matter remains un-directional, i.e. the diffusion is equally probable in all directions.

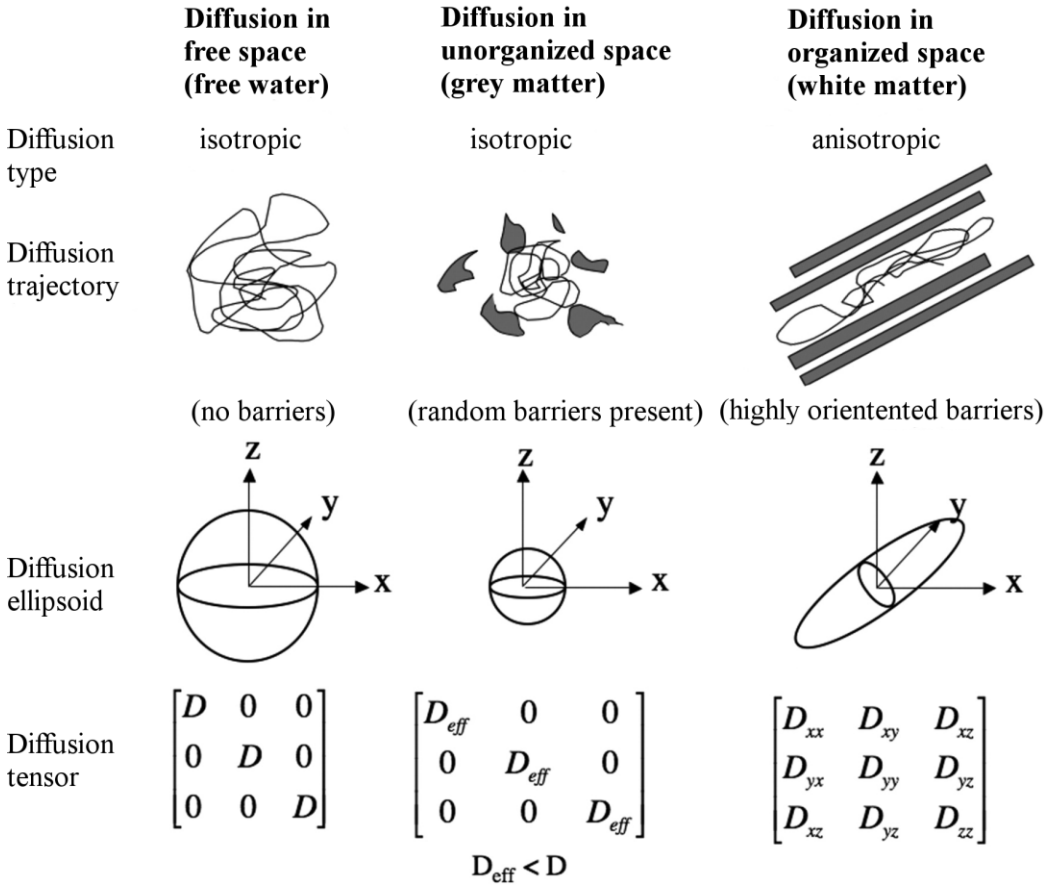

Figure 3: Diffusion in differently organized spaces. In free space, diffusion is isotropic i.e. the displacement of the molecules occurs in all directions with the same probability. The shape of the diffusion ellipsoid approximates a sphere. If barriers are present but randomly organized in the medium, such as is the case in grey matter, the speed of the overall displacement of the water molecules decreases but diffusion remains isotropic as randomly organized barriers do not consistently district the direction of the movement. Therefore, movement in all direction retains equal probability even when the speed and volume of the diffusion are districted. The diffusion coefficient (D) is replaced with an observed diffusion coefficient D_{eff} (corresponds to the apparent diffusion coefficient, ADC) that is smaller than the diffusion coefficient of water molecules in free space. In coherently organized space where the barriers are highly oriented, such as the white matter, diffusion is anisotropic, i.e. directional, as the barriers (most notably intact cell membranes) district the movement of the water molecules consistently in certain directions. The ellipsoid describing the diffusion becomes oblong to indicate the direction of the fastest diffusion, i.e. orientation of the underlying neural fibre pathway. Adapted from: [158].

In white matter, diffusion is typically highly directional. White matter consists of tightly packed bundles of neural axons that connect different grey matter areas. In the neural level, this creates highly oriented barriers that hinder the movement of water molecules. Thus, diffusion is fastest in the direction of the least resistance i.e. the direction along the neural fibres. The directionality is mainly caused by intact cell membranes and further modulated by myelination of axons [102]. Directional diffusion is called anisotropic.

The idea of directional diffusion within a tissue is the basis of diffusion weighted imaging (DWI). Measurements are sensitized to diffusion using two pulsed field gradients with the same duration but opposite directions. The first gradient shifts the phase of a molecules depending on the position of the molecule in question within the direction of the gradient (in the phase coding direction). Intermingled, unsynchronized phases lead to loss of signal as detected by the MRI apparatus. The second gradient is applied in the opposite direction than the first gradient and therefore inverts the phase shifts back to their original states which returns the phase coherence and the original signal. After the two gradients, the loss of phase coherence and therefore the signal is negligible if molecules stay in their original positions allowing the perfect refocusing of the phases. However, during the time between the gradients, diffusion causes molecules to move and change places. This mixes the phases in unpredictable ways, which leads to incomplete refocusing of the phases by the second gradient as it only inverts the phase change caused by the first gradient. Thus, the original phases do not completely refocus

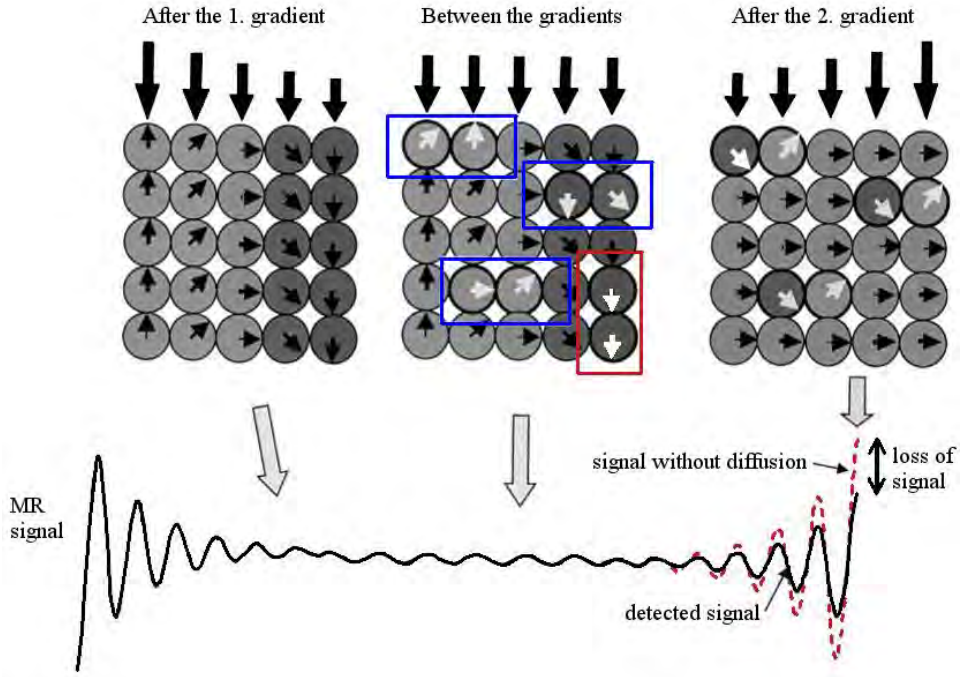

Figure 4: Effect of diffusion on the MR signal. The first gradient shifts the phases of the nuclei so that the phase becomes dependent of the location along the direction of the applied gradient. The resulting un-synchronization of the phases leads to a loss of the detected MR signal. During the time lapse between the gradients, diffusion causes some molecules to randomly change position. Only movement parallel the orientation of the gradient mixes the phases (blue boxes). The second gradient, which has the same duration but the opposite direction than the first gradient, inverts the phase changes caused by the first gradient. If a molecule has retained its original position or moved perpendicular to the direction of the gradient (red box), the second gradient restores its original phase. Phases of the molecules that have moved from their original positions (marked with white arrows) do not return to their original state. The loss of phase coherence causes the detected signal after the gradients to be less than the signal before applying the gradients. MR signal without the decreasing effect of diffusion is shown in dashed red line for reference. Adapted from: [159].

and the signal does not recover fully to the original state. Greater loss of signal indicates higher volume of diffusion, i.e. the faster the movement of the molecules larger the measured ADC value. The phenomenon is illustrated in Figure 4. [103]

The ADC is directionally dependent in areas of high anisotropy (First reported in cat brain by Moseley and colleagues [104], and in human brain by Doran and colleagues [105] and Chenevert and colleagues [106]). Each acquired ADC value represents the volume of diffusion in the direction of the gradient used in the measurement, i.e. the overall movement of water molecules. The weighting gradients can be applied in numerous orientations and thus the measurement of the volume of the diffusion can be collected in several directions. Combining the values produces an overall description of diffusion within a voxel showing both the direction and speed of the diffusion. The mathematical model for this is called a diffusion tensor.

Diffusion tensor describes diffusion as a three-dimensional symmetric matrix. It models the distance of the molecule displacement over a time period between the diffusion-weighted gradients described above as a surface of equal probability. In voxels of isotropic diffusion, the shape of the tensor approaches a sphere as the speed of diffusion is the same in all directions. In voxels where diffusion is anisotropic, the longest axis of the tensor corresponds to the direction of the fastest diffusion and creates an ellipsoidal surface. Eigenvectors of the matrix indicate the principle axes of the tensor, i.e. the orthogonal directions of diffusion within the voxel. An eigenvalue connected to each eigenvector indicate the strength of diffusion in the direction in question so that the largest eigenvector shows the direction of the strongest diffusion.

An unambiguous defining of the diffusion tensor requires diffusion measurements, i.e. the ADC values, in six independent directions and an unweighted measurement for reference. The number of directions used in experiments has rapidly increased as the imaging apparatus has improved. Currently, the diffusion is typically measured in around 30-60 directions to limit the effect of measurement artefacts, such as noise, and to improve the mathematical estimation of the tensor. The diffusion tensor is parsed together from the signal samples using multivariate regression (For detailed description, see: [107]).

A mathematical variable called fractional anisotropy (FA) presents the degree of diffusional directionality within a voxel [108]. Its values vary between zero and one. Larger values indicate greater difference between the eigenvalues of the tensor and therefore more directional diffusion. FA-values are often used to differentiate between areas of white and grey matter.

Unfortunately, a single diffusion tensor cannot adequately model diffusion within a voxel in all cases. The phenomenon is illustrated in Figure 5. A single voxel may contain several fibre pathways as the dimensions of voxels are in different magnitude than the typical diameter of neural fibres or even pathways. A diffusion tensor presents an average over the whole voxel and can therefore mask local differences. This is called partial volume effect. Moreover, simply increasing the resolution may not help as it, in turn, decreases the signal-to-noise ratio in voxels as the amount of tissue creating the signal decreases. This is especially prominent in voxels at the edges of the areas with different tissue types, for example near the ventricles. Even in voxels deep in the white matter, the fibre pathways can travel close enough to each other to fit in the same voxel (Figure 5 A) or cross in their way to different areas (Figure 5 B). Differently oriented pathways in the same voxel force the fitted diffusion tensor in shape of an envelope or a sphere, therefore hiding the actual orientations of the pathways in the voxel and making the tensor indiscernible from a tensor modelling isotropic diffusion.

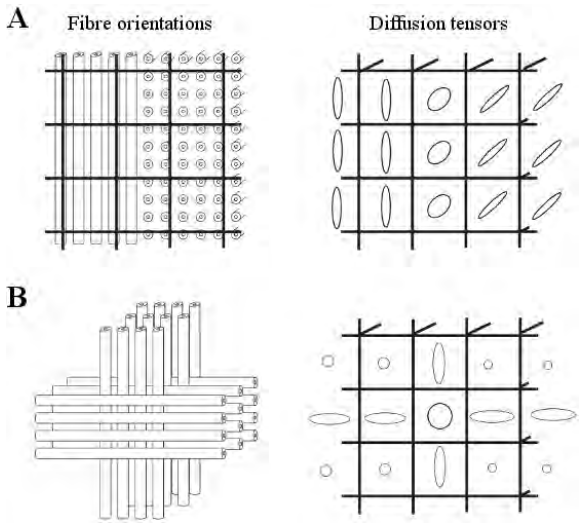

Figure 5: Effect of multiple fibre populations with different orientations in a voxel. A: The adjacent layers of differently oriented fibres cause the diffusion tensor in voxels containing both populations (the middle column) to become round as it estimates the mean diffusion in the voxel. As the fibre population are adjacent but do not cross, increasing the imaging resolution would lead to better estimation of diffusion tensor in this area. B: Crossing fibre bundles cause the diffusion tensor in the middle voxel to become round as it cannot represent the two perpendicular orientations of the fibre pathways simultaneously. The phenomenon cannot be improved with higher resolution as the crossing of fibres is inevitable and singular diffusion tensor cannot model it accurately in any resolution level. Adapted from: [160].

Confusion in the orientation of the diffusion tensor leads to misleading FA-values. An FA-value is an approximation over the whole voxel, so it cannot communicate the reason behind a low value. A voxel in a grey matter and another voxel deep in the white matter which contains crossing neural pathways may have the same FA-value. Thus, separating areas containing different tissue types based solely on the FA-values is not always reliable.

4.2 Tractography

Tractography is a technique for in vivo three-dimensional and continuous tracking of white matter axonal pathways from discrete DTI-data. First tracking methods were introduced around the turn of the millennium by Mori and colleagues [12], Conturo and colleagues [13], and Basser and colleagues [14].

All tracking algorithms assume that in each voxel, the principle eigenvector associated with the largest eigenvalue is parallel to the dominant orientation of the underlying neural fibres. Therefore, the route of the neural pathway can be followed by moving parallel to this orientation to the next point in which the moving direction is adjusted parallel to the orientation of the primary eigenvector in this new location and moving again. Each movement is called a step. The starting point, referred to as the seed point, is usually in a voxel in an area of high anisotropy. This ensures that the tracking starts from an area in which the orientation of the diffusion tensor is unambiguous and, therefore, the tracking does not immediately go awry. Tracking proceeds bi-directionally from the seed point because a diffusion tensor cannot indicate the bearing of the neural

pathway (e.g. whether ascending or descending). The two constructions are combined after the tracking algorithm stops. (For an example algorithm, see: [14])

The step length differs between different algorithms. A tract produced by the simplest solution, moving from one discrete voxel to another, deviates fast from the actual path of the neural fibres, since this strategy only allows moving to one of the neighbouring voxels. Fibre pathways are several times smaller than voxels, so discrete voxel-size blocks do not allow constructing tract that closely follow the actual neural pathways. This principle is illustrated in Figure 6 A. [12]

To compete the deviation problem, either the vector or the tensor field can be made continuous. The former option is utilized in the FACT-algorithm (fibre assignment by continuous tracking) in which it is assumed that the fibre orientation, while uniform within a voxel, at the edges of the voxel changes abruptly to parallel the principle orientation of the diffusion tensor in the next voxel [12]. Thus each step leads to the nearest edge in the direction of the principle eigenvector and therefore, the step length varies. The workings of the algorithm in two dimensions is illustrated in Figure 6 B.

In algorithms using the latter option (e.g. [13], [14]), the continuous tensor field, step length is typically fixed to some arbitrary number smaller than the voxel dimensions. Since information about the orientation of the principle eigenvector is available in any point of the data, thanks to the continuous tensor field, the tracking algorithm can move through any point in the data and thus produce a continuous construction of the neural pathway. This process is dubbed as the evolution of the space curve by Basser and colleagues [14] and it is illustrated in Figure 7.

The tracking continues until it arrives to a point that fails to uphold either of the two termination thresholds. The FA-threshold, which sets the lowest allowed FA-value, seeks to ensure that tracking does not enter grey matter or areas where the orientation of the principle eigenvector is ambiguous. The value is typically set around 0.2 to differentiate between grey and white matter. The second threshold, the angular threshold deter-

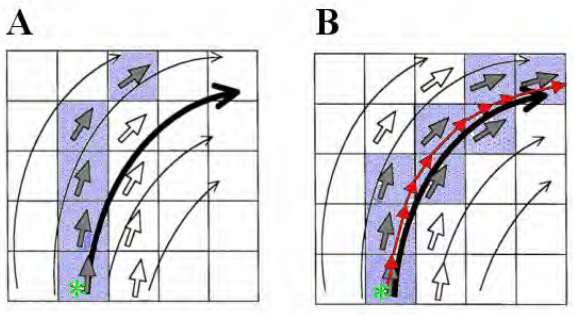

Figure 6: Workings of a tracking algorithm in two dimensions. The black arrows show the pathway of the neural fibres going through the voxels. The large arrow outline in each voxel indicates the orientation of the principle eigenvector, i.e. the constructed approximation of the local direction of neural fibres. Green star indicates the seed point. When tracking moves from one discrete voxel to another, it deviates fast from the real pathway even in short distances (A). Blue shade indicates voxels that tracking stepped through. However, if the vector field is continuous and every step leads to the nearest edge, the construction of streamline, as indicated with red arrows, is much more faithful to the underlying fibre pathway (B). Adapted from [12].

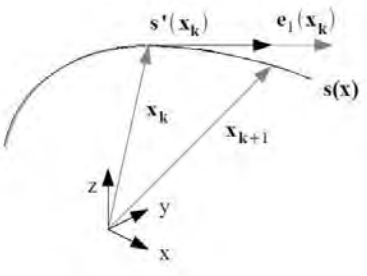

Figure 7: Evolution of the space curve. Space curve s(x) estimates the pathway of the neural fibres. In each point, x_k, the tangent of the curve, $s'(x_k)$, is set parallel to the orientation of the principle eigenvector of the same position, $e_1(x_k)$. This orientation indicates the direction of the next step. The evolution of the space curve is approximated with numerical methods, such as Taylor's series or Runge-Kutta methods. For full details, see: [14].

mines the maximum angle allowed between two consecutive points. The goal is to prevent the constructed tract turning back on itself or making anatomically implausible curves. The allowed angle varies from 20 to 90 degrees depending on the a priori known shape and curvature of the neural pathway under study, used step length, and the voxel dimensions. As of now, there is no general consensus of a universally optimal angular threshold, although some work for the optimization of the threshold has been done [109].

The above-introduced methods are called deterministic tractography methods. They produce one tract per seed point that always travels through the same points in the data. This makes such algorithms vulnerable to distortions in the data caused by noise or other discrepancies (For a review of the problems caused by the noise, see: [110]. For a more general overview covering also other artefacts in the data, see: [111]). Additionally, deterministic algorithms are often blind to branching or crossing fibres as they construct only one of the possible pathways. Deterministic diffusion methods rely on the FA-values and the orientation of the primary eigenvector. As discussed previously in Chapter 4.1, a singular diffusion tensor cannot model complicated diffusion patterns, and as the FA-value is merely an approximation over the whole voxel, it cannot communicate the reason behind a low value. Therefore, voxels containing multiple fibre orientations produce the same FA-value than truly isotropic voxels, hence terminating the tracking algorithm.

Using several seed points for tracking reduces the effect of data uncertainties. Tracking can be launched from multiple points or from specially selected anatomically relevant areas (first utilized in tractography by Conturo and colleagues [13]). Such masks are known as regions of interest (ROI). ROIs can also be used like logical operators to separate the tracts of interest from the data when the tracking algorithm is launched from every available data point and tracts under study are subsequently separated from all constructed pathways with the ROIs. This method is called whole brain tractography. Nowadays, most tractography studies use ROIs or analogous masks to identify the tracts on which the study concentrates. However, utilizing ROIs in a meaningful way requires prior anatomical knowledge and therefore works best when tracking known connections.

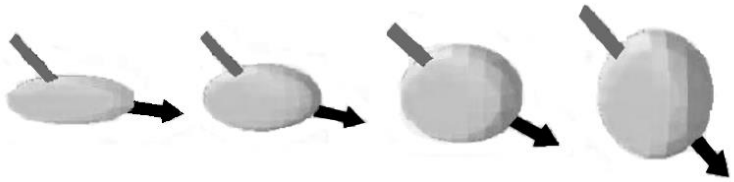

Figure 8: The modulation of the continuing direction (black arrow) by the incoming direction (grey line) to help the tracking algorithm over the voxels with ambiguous principle orientation. If the diffusion tensor is highly anisotropic, the outgoing direction is parallel to the primary orientation of the tensor (left). As isotropy increases (from left to right), the effect of the orientation of the incoming vector increases. In isotropic voxels (right), the outgoing direction in parallel to the incoming direction. In all cases, the incoming direction describes the orientation of the principle eigenvector in the previous position. Adapted from: [161].

The tracking algorithm can also be helped over the problematic voxels by modulating the outgoing (continuing) direction with the incoming (previous) orientation, instead of terminating the tracking when the FA-value sinks below the threshold (Figure 8). This is useful especially in voxels with a low FA-value deep in the white matter through which the neural pathway likely continue. In each point, the diffusion tensor prevalent to said point pushes the orientation of the outgoing vector closer to the orientation of its primary eigenvector. If the primary eigenvector in the new location is ambiguous, i.e. the diffusion tensor is shaped like a sphere, the moving direction stays the same, i.e. the outgoing vector has the same orientation as the incoming vector (right in Figure 8). [112]

The fundamental problem with deterministic tractography methods is that the results do not include any estimation of reliability. To produce this estimation, probabilistic tractography methods were developed. In these methods, the tracking algorithm is launched from each seed point several times. The number of launches is arbitrary, typically set high to, for example, 5000 repeats. In each consecutive data point, the next moving direction is drawn from the distribution of the possible orientations instead of setting it strictly parallel to the principle eigenvector. The distribution of the possible orientations can be produced with Bayesian methods [15], bootstrapping [113], or by devising a contingency between the uncertainty of the fibre orientation and the shape of the diffusion tensor using Monte Carlo random walk ([16], [114]). Since an ambiguous FA-value is not a problem when the moving direction is lifted from a distribution, probabilistic methods typically discard the FA-threshold. The angular threshold is often the only stopping criteria. Probabilistic tracking does not produce a singular tract, but instead a probability map in which the value in each point shows how many times the tracking algorithm went through it during the whole run of the algorithm, typically in percentages. Hence, the map shows the likelihood of a connection between given data point and the seed point.

Both tractography methods can faithfully construct the major anatomical fibre pathways (e.g. [18], [17] for deterministic methods, [19] for probabilistic methods). However, both can also create connections that are anatomically false by combining separate tracts. These false positives may be caused by insufficient data resolution or by a too large size of the smoothing window that is used to make the data continuous and remove noise. Tracking may also terminate prematurely and omit known parts of fibre pathways (false negatives), especially if those pathways are less pronounced or cross

other tracts. For example, several tractography studies of the cerebral penduncle or the internal capsule in the early 2000's could not find the connections with the lateral sensory-motor strip that are known to exist and reported only projections to the medial parts of the strip (see e.g.: [115]–[117]).

Such omissions in the construction of the tracts stem from the quality of the data as the noise and other data artefacts distort the diffusion tensor ([110], [111]). The problems might be reduced by increasing the imaging resolution. However, a mere change in the resolution cannot erase the problem of crossing pathways as the problem fundamentally stems from the limitations of the singular diffusion tensor. Several methods have aimed at tackling this problem by fitting more complex diffusion models in a voxel to estimate several fibre orientations (e.g. [118] for deterministic tractography, [119] for probabilistic tractography).

One of the most frequently used methods to account for multiple fibre-orientations within a voxel was developed by Behrens and colleagues [120] extending a previously published probabilistic tractography algorithm by the same authors [15]. The improved model constructs the same dominant pathways as "typical" probabilistic methods, but considerably improves tracking the non-dominant pathways of secondary fibre orientations.

In this method, the diffusion within a voxel is estimated with a partial volume model called "ball-and-stick" model. The diffusion-weighed signal is divided into two separate components: a single isotropic component accounting for the uncertainty (the ball) and an infinitely anisotropic component (the stick) showing the most prominent direction of diffusion. The model can include several "sticks" to show the prominent orientations of several fibre-populations. As tracking progresses, in each step the next moving direction is drawn from the modelled distribution constructed with Bayesian methods. The algorithm accounts for multiple fibre-orientations so that a sample is drawn separately from each fibre orientation distribution and the direction closest to the previous, incoming orientation, i.e. the direction most logically continuing the previously constructed streamline, is chosen. This allows the tracking of less prominent, non-dominant pathways: if just one sample would be drawn from the overall distribution that was weighted for the different fibre-populations, results would inevitably bias toward the most dominant fibre-orientation.

The strength of the ball-and-stick model is that multiple fibre-orientations, i.e. multiple "sticks", are used only when necessary. If adding a second orientation does not explain the diffusion within a voxel better than just one, only one fibre population is estimated. Fitting an unnecessarily complex model to data that is adequately explained with one fibre orientation would lead to a poor estimation of the true orientation as well as unnecessary mathematical complications. This is accomplished with the Bayesian method called automatic relevance determination (ARD). ARD initially fits a more complex model accounting for several fibre orientations to the data, but for each parameter it then forces the value to or near zero if the parameter in question does not contribute to a better explanation of the data. For full details, see: [120].

Despite improvements in finding the non-dominant pathways, this model is still vulnerable to the same data discrepancies as any other tractography method. The false positives that are found with the same method allowing only one fibre orientation (one "stick") are present also in tracts constructed when accounting for multiple fibre orientations (using several "sticks") [120]. Therefore, more complex modelling of the diffusion tensor cannot account for all the sources of uncertainty in the results.

4.3 Transcranial magnetic stimulation

Transcranial magnetic stimulation (TMS) is a method for non-invasively activating areas of the human brain with a brief magnetic field. It was introduced by Barker and colleagues in 1985 [121]. At first, the method was exclusively used for stimulating the motor cortex, but in the years since the first publication, the range of applications have increased rapidly. Currently, TMS is utilized widely in neuroscientific studies, neuropsychology and clinical therapy, for example in treating severe depression [122].

TMS is based on the principle of electromagnetic induction. The principle, discovered by Michael Faraday in 1838, states that a pulsing magnetic field induces an electromotive force across an electrical conductor. In TMS, a brief electrical current passes through a coil of wire, called a magnetic coil. The moving current creates a changing magnetic field that penetrates the skull and scalp when the coil is placed sufficiently close to the head. This field induces an electric field perpendicular to the magnetic field and parallel to the coil. The magnetic field also induces secondary ionic currents that predominantly cause the TMS effect. These currents depolarize the membrane of the nerve cells and therefore disrupt the natural activation of the neural cell potentials that carry information from one cell to another. Thus TMS can inhibit or excite brain activity.

The TMS pulse can be singular or rapidly repeated. When a pulse with the same characteristics is repeatedly applied to a single area, it is called repetitive TMS (rTMS). In general, a singular TMS pulse creates temporal, rapidly vanishing effects whereas the effects of repeated pulses can last longer, depending on the stimulation variables.

Characteristics of the electrical current created in the coil modulate the effects of the TMS. Most important are the intensity, duration, and, in the case of repeated stimulation, the frequency. The shape of the coil also impacts the effect of the pulse as it determines the extent of the stimulated area and the focus of stimulation.

TMS intensity determines the magnitude of the induced magnetic field which in turn determines the magnitudes of induced electric currents. The greater the magnitude, the greater the effect on the activity of the neurons. The intensity must exceed a certain threshold to have a notable effect. When targeting the motor cortex, such a threshold is called the motor threshold. The term refers to the lowest intensity that evokes a response, typically a twitch, in the target muscle. Similarly, in studies targeting the occipital lobe, an analogous phosphene threshold is established. It refers to the lowest intensity needed to produce a visual perception of a spot of light. The thresholds reflect the connectivity and condition of the motor and visual pathways, respectively. They naturally vary among individuals and depend heavily on the correct placement of the pulse inducing coil. However, a change of the threshold can also indicate an abnormal condition. The motor threshold is often higher for individuals with diseases affecting the corticospinal tracts, such as a spinal injury [123], or multiple sclerosis [124]. Similarly, there is evidence of a decreased phosphene threshold in individuals prone to migraine which reflects greater visual cortical excitability ([125], [126]). However, pulses with a full threshold intensity are often not used, especially in rTMS studies, as higher intensities create a greater possibility of side effects, such as unpleasant feeling through muscle stimulation and, in very rare cases, seizures. (For a review of the risks and the safety measures, see: [127]). Alternatively, the same effect of inhibition or excitability can be achieved by varying the repetition (the frequency) or the duration of the pulse.

The induced magnetic field lasts typically around 100 μs. The duration depends on the duration of the electrical current in the coil. Shorter pulses cause excitation with less energy since cell membrane does not insulate the current but acts as a leaky integrator. The duration and intensity of the pulse are deeply intervened as the duration of the

electric current required to stimulate a nerve cell depends on the intensity of the current. A brief, very intense pulse maximises the efficiency, but its application places high demands on the used apparatus as low capacitance and a high capacitor voltage are needed. [128]

Frequency is critical for predicting the effects of the pulse when using rTMS. Frequencies range from less than 1 Hz to 20 Hz. In motor cortex, lower frequencies tend to inhibit activity [129], whereas higher frequencies temporarily increase the cortical excitability [130]. In frontal lobes, rTMS with a low frequency have been successfully used to treat severe, drug-resistant depression ([131], [122]).

The shape of the coil determines where the focus of the magnetic field and therefore the largest direct effect of the pulse is located. The two most commonly used are a circular coil and a coil shaped as a figure of an eight. The circular coil has no singular area of the greatest focus as the current creates a uniformly strong field around the whole circumference of the coil. The field weakens gradually toward the centre. The affected area is large so circular coils are used especially when the exact location of the target area is uncertain. In contrast, the figure-of-eight-shaped coil, also known as the butterfly coil, provides an opportunity for highly targeted pulses. The coil typically consists of two circular coils mounted adjacent to each other. The currents in the two coils move in opposite directions so that they parallel at the intersection and the currents add up. This makes the intersection a focus point where the current and therefore the induced magnetic field are at their strongest. Due to the added focus and magnitude, the figure-of-eight-shaped coils are typically used when accuracy is required, for example in mapping studies. [132]

A TMS pulse activates most strongly the cortical area under the focus of the coil as the strength of the magnetic field decreases with distance. However, the activation can spread to the subcortical areas or to the other hemisphere through anatomical connections (First demonstrated in the motor and visual cortices with by Ilmoniemi and colleagues [133]). The effect and spreading of the activation can be detected with electroencephalography (EEG), fMRI or PET. For example, repeated TMS-pulse to the DLPFC stimulates dopamine release in the caudate nucleus, as detected by PET [24], and a repeated TMS pulse to the primary motor cortex activates dopamine release in the putamen [25].

5 Materials and methods

Subjects

Five healthy individuals participated in this study. None of the subjects had any history of neurological or psychiatric disorder.

Data acquisition

DTI- and T_1-images were acquired with a 3 T MAGNETOM Skyra whole-body scanner (Siemens Healthcare, Erlangen, Germany), using a standard 20-channel head-neck coil at AMI-centre in Aalto University, Otaniemi. Diffusion weighted images were acquired using an echo-planar imaging (EPI) sequence with the following parameters: slice thickness 2.0 mm, repetition time 9.7 s, echo time 81.0 ms, field of view 240 mm, number of slices 65, base resolution 120. Imaging was weighted in 64 independent directions with a b-value 1000 s/mm^2. Eight un-weighted reference images were also obtained. High-resolution anatomical T_1-weighted images were collected using an MPRAGE-sequence with following parameters: slice thickness 1.0 mm, repetition time 2.53 s, echo time 3.3 ms, flip angle 7 degrees, field of view 256 mm, base resolution 256.

Data pre-processing

All pre-processing and analysis was performed with FMRIB Software library (FSL 5.0, http://fsl.fmrib.ox.ac.uk/fsl, [134]–[136]). Pre-processing followed the typical DTI-data pipeline and was done with FMRIB's Diffusion Toolbox, FDT.

First, the data was corrected for motion artefacts, eddy-currents and susceptibility induced distortions ([135], [137], [138]). The brain matter was extracted from the surrounding, non-brain structures such as the skull and scalp using the Brain Extraction Tool, BET [139]. Diffusion tensors were reconstructed using DTIFIT, and the eigenvalues, eigenvectors and FA-values were calculated. Afterwards, a probabilistic model of the fibre orientations was fitted to voxels with BedpostX ([15], [120]) that estimated the diffusion parameters. To better account for the crossing fibre populations, the algorithm was run with two fibre orientations per voxel.

Determining the seed surfaces

FIRST, an integrated registration and segmentation tool of the FSL [140], was used to segment the caudate nucleus and the putamen. The structures were segmented from the T_1-images of each subject for both hemispheres. The volume of the segments varied to accommodate individual anatomical differences, but the resulting mesh-surfaces had the same number of vertex points whose locations corresponded among individuals. These vertex points were used as the seed points for tractography.

Determining the target areas

Six target areas were selected: the hand controlling area of the primary motor cortex (M1), the supplementary motor area (SMA), the pre-supplementary motor cortex (preSMA), the premotor cortex (PMC), the dorsolateral prefrontal cortex (DLPFC), and the ventrolateral prefrontal cortex (VLPFC). A ROI (a mask for the region of interest) for each area was hand-drawn separately to the T_1-weighted images of each subject for both hemispheres. Table 1 depicts the average sizes of the target ROIs. Locations of the ROIs are shown in Figure 9.

The motor cortex occupies the precentral gyrus immediately anterior to the central sulcus that separates the frontal and parietal lobes. The motor cortex ROI (the M1-ROI, orange in Figure 9) was restricted to the hand motor area that is also known as the hand knob. The hand knob is a protrusion of the precentral gyrus into the central sulcus. The

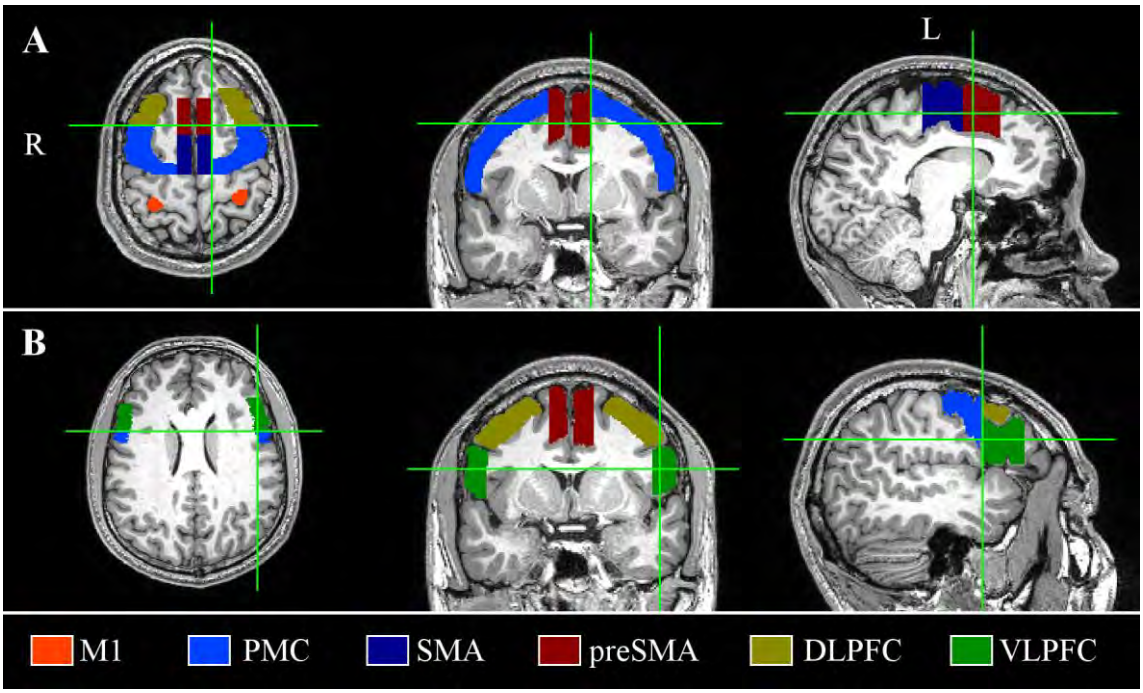

Figure 9: TargetROIs in the axial, coronal and left sagittal slices in the T_1-images of one subject (S4). Green crosshairs indicate the locations of the slices. DLPFC – ROI for the dorsolateral prefrontal cortex (yellow); M1 – ROI for the motor cortex (orange); PMC – ROI for the premotor cortex (light blue); SMA – ROI the for the supplementary motor area (dark blue); preSMA – ROI for the presupplementary motor area (dark red); VLPFC – ROI for the ventrolateral prefrontal cortex (green).

hand knob is highly consistent among individuals and therefore broadly used as an identifying landmark for the precentral gyrus. [141]

The supplementary motor area corresponds to the medial section of Brodmann's area 6. It is located anterior to the motor cortex and consists of three anatomically separable areas: the SMA, preSMA, and an oculomotor-related area, supplementary eye field (SEF) [142]. This study used ROIs for the SMA and preSMA as defined in an earlier study by Lehéricy and colleagues [21]. Both ROIs were superiorly confined by the brain vertex and inferiorly by the cingulate sulcus. The lateral end of the cingulate sulcus was used as the lateral limit from which the ROIs extended to the medial line that separates the hemispheres. The SMA-ROI (dark blue in Figure 9) reached in the posterior-anterior direction from the precentral sulcus to the VAC-line, an imaginary vertical line through the anterior commissure (AC) in the coronal plane. The preSMA-ROI (dark red in Figure 9) extended anteriorly from the aforementioned VAC-line to another imaginary vertical line that travels through the genu of the corpus callosum in the coronal plane.

The premotor cortex is situated anterior to the motor cortex and lateral to the SMA with which it occupies Brodmann's area 6. The ROI for the premotor cortex was defined as in a study by Cramer and colleagues [143]. The PMC-ROI (light blue in Figure 9) followed posteriorly the shape of the precentral sulcus extending laterally from the lateral edge of the cingulate sulcus, also defining the limit of the SMA-ROI, to the Sylvian fissure. Anteriorly the PMC-ROI ended at a "rostral limit" that is defined as the

Table 1: Mean sizes and their standard deviations of the target ROIs in voxels.

ROI	Mean size	SD of size
M1 - Left	641	55
M1 - Right	628	131
SMA - Left	7039	926
SMA - Right	7465	748
preSMA - Left	6910	1442
preSMA - Right	6540	869
PMC - Left	18587	1027
PMC - Right	16218	2196
DLPFC - Left	6806	1357
DLPFC - Right	6599	936
VLPFC - Left	6739	560
VLPFC - Right	6142	583

vertical halfway-point between the central sulcus and the most anterior point of the brain defined.

The DLPFC lies at the middle section of the superior and middle frontal gyri covering Brodmann's areas 9 and 46 [144]. The ROI for the DLPFC (yellow in Figure 9) consisted of the middle frontal gyrus confined by the superior and inferior frontal sulci. The posterior boundary was the aforementioned rostral limit that was used as the anterior end of the PMC-ROI to insure that the ROIs did not overlap. [145]

The VLPFC consists of Brodmann's areas 45 and 47 that occupy a large part of the pars triangularis in the inferior frontal gyrus and an area rostroventrally next to it, respectively [146]. The VLPFC-ROI (green in Figure 9) was superiorly limited by the inferior frontal sulcus and inferiorly by a horizontal line defined by the horizontal ramus of the Sylvian fissure. The ROI included the superior parts of the inferior frontal gyrus, the pars opercularis and the pars triangularis, but excluded the most rostral part, the pars orbitalis. The posterior boundary was the same as with the DLPFC-ROI. [145]

Tractography

Tractography was performed with the Probtrackx-function of FSL ([15], [120]). Number of launches per seed point (every vertex point in the seed surface) was 5000. The step length was 0.5 mm, the angular threshold 0.2 and the maximum number of steps 2000. Tracking was performed in the diffusion space and the results were then transformed to the structural space using 6 degrees of freedom and a correlation ratio.

Tracking was performed separately in both hemispheres for each subject. The algorithm was launched from the caudate nucleus seed area to the target areas in ipsilateral prefrontal cortex (the DLPFC-ROI and VLPFC-ROI) and from the putamen seed area to the target areas in the ipsilateral motor areas (the M1-ROI, PMC-ROI, SMA-ROI and preSMA-ROI). In all cases, only the tracts reaching or going through the targetROI were included in the results. The total number of tracts satisfying this criteria (the 'waytotal') was used to normalize the results in each case by dividing the tracts voxel-wise with the waytotal. After normalizing by the waytotal, the threshold was set to 0.001, corresponding to 0.1% of the waytotal, which removed the same proportion of the low probability data points and noise from all tracts.

Group analysis

For group analysis, the detected tracts were transformed to the standard space and summed to create a population map of each connection. The normalized and thresholded tracts acquired by the above explained methods were used for the group analysis. The trajectories were binarized to omit further probability information and registered to the MNI152 standard space using the transformation matrix generated by the registration tool in the FDT toolbox with 12 degrees of freedom. As registration to the standard space converts binary masks by assigning a probability value to each new voxel, the transformed tracts were again thresholded and binarized. The threshold was conservatively set to 0.5 to preserve the original volume of the masks. Combining the individual binary masks produced a group probability map with values ranging from zero to five as per number of subjects showing in how many subjects the tracts travelled through any given data point. The map was further thresholded to display only tracts that were present in at least two of the five subjects.

6 Results

6.1 Individual analysis

The constructed tracts between the seed surfaces and the target areas in individual level are shown in Figure 10 through Figure 18. Figure 10 and Figure 11 show the connections between the caudate nucleus and the DLPFC and VLPFC target areas, respectively. Figure 15 - Figure 18 depict connections between the putamen and the M1, PMC, SMA and preSMA target areas, respectively. Figure 12, Figure 14 and Figure 13 illustrate the tracts between the caudate nucleus and the prefrontal areas, the putamen and the M1 and the PMC, and the putamen and the SMA and preSMA, respectively, in one subject for reference.

In Figure 10, Figure 11 and Figure 15 through Figure 18, each row depicts the constructed tracts of an individual subject (S1-S5). Tracts in the left hemisphere are shown in red-yellow and the tracts in the right hemisphere in blue. Brighter colours indicate higher intensity, i.e. an increase in the number of tracts passing through a voxel. The intensity range runs from 0.1% of the total number of tracts traveling from the seed area (the caudate nucleus or the putamen) to the target area in question (the 'waytotal') as is indicated with dark red or dark blue, respectively, to 1% of the waytotal shown in bright yellow or light blue, respectively. The bright green crosshairs in the axial slices indicate the levels of the coronal and sagittal slices. For each individual, the slices showing the connections with the highest probability and consistency were selected. The source structures, the caudate nucleus (light blue) and the putamen (bright pink), are shown in for reference.

As visualizing three-dimensional tracts with two dimensional slices is occasionally misleading and unnecessarily hard to comprehend, the tracts of one subject (S4) are shown in Figure 12, Figure 13 and Figure 14 for reference without the probability values. Figure 12 shows the tracts between the caudate nucleus and the target areas in the DLPFC (orange) and the VLPFC (green). Figure 13 shows tracts between the putamen and the target areas in the M1 (blue) and the PMC (green). Figure 14 shows the tracts between the putamen and the target areas in the SMA (blue) and the preSMA (green).

In summary, the results demonstrate that in all subjects, each sought trajectory was found. The constructed tracts are consistent with the expected, previously known anatomical fibre pathways. They robustly hold their shape with the used threshold. The tract held generally the same shape in different hemispheres and subjects, but individual variability in the exact sites of the cortical connections and the pathway of the tracts was notable.

6.1.1 Tracts between the caudate nucleus and prefrontal cortex

Tracts between the caudate nucleus and the DLPFC are shown in Figure 10 for all subjects. The coronal and axial slices were chosen to show the most continuous tracts between the areas for each subject. The sagittal slices show the most lateral robust reach of the tracts.

Figure 11 illustrates connections between the caudate nucleus and the VLPFC. The axial slices were chosen to show the most continuous and consistent tracts within the plane. The coronal slice level was the same than was used to illustrate connections between the caudate nucleus and the DLPFC (Figure 10). The sagittal slices depict the site of the most lateral robust connection of the tracts. The VLPFC tracts occupy much of the same subcortical areas just superior to the caudate nucleus than the DLPFC tracts.

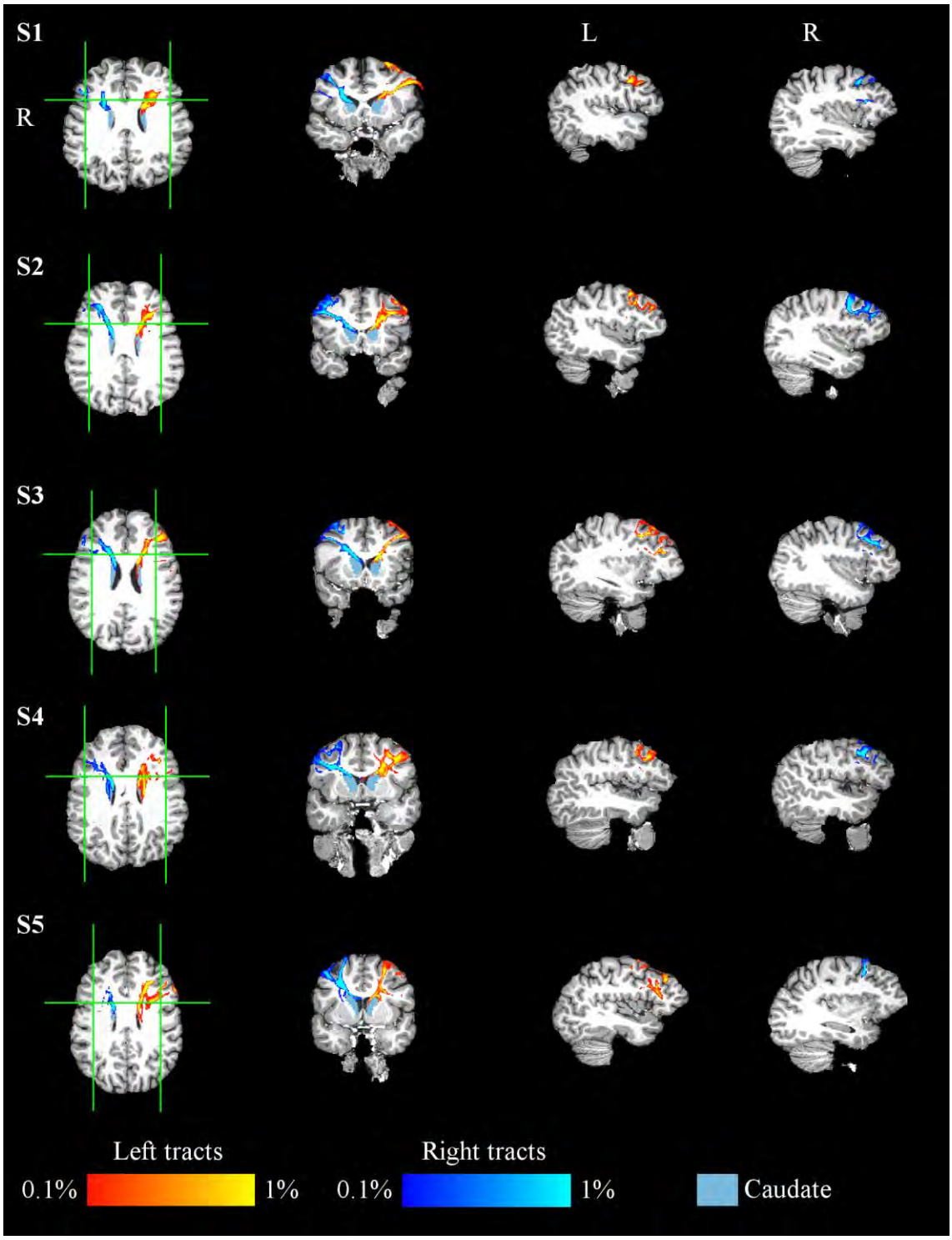

Figure 10: Constructed tracts between the caudate nucleus and the DLPFC target area in the axial, coronal and sagittal slices in the T_1-images of each subject (S1-S5). For tracts in both hemispheres, the intensity describes the number of tracts passing through a voxel, i.e. the likelihood of connection with the seed area, the caudate nucleus (light blue). The intensity scale ranges from 0.1% of the number of all tracts connecting the seed and target areas (red for the tracts in the left hemisphere, dark blue for the tracts in the right hemisphere) to 1% of same number (yellow for tracts in the left hemisphere, light blue for the tracts in the right hemisphere). Green crosshairs indicate the locations of the coronal and sagittal slices. DLPFC – dorsolateral prefrontal cortex.

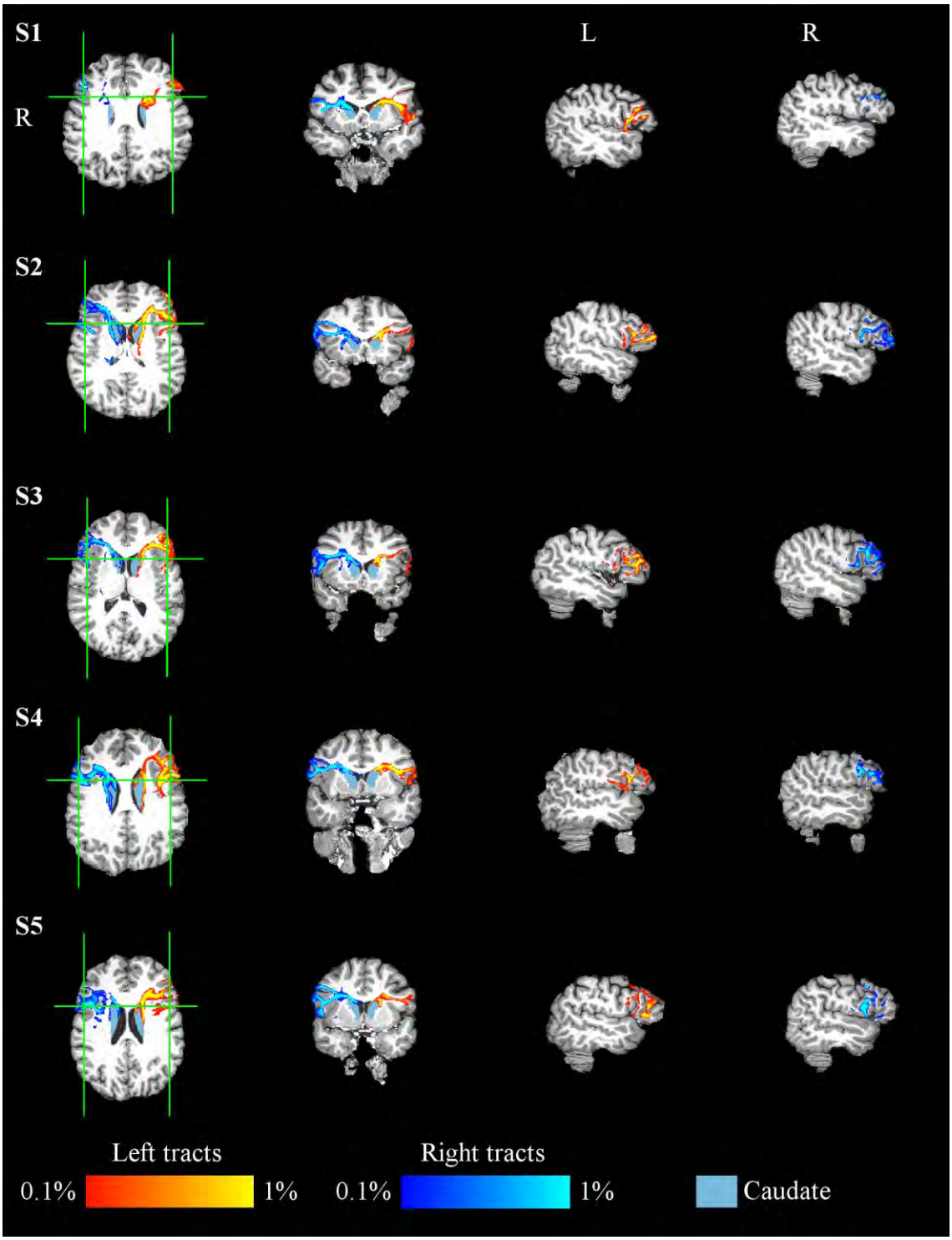

Figure 11: Constructed tracts between the caudate nucleus and the VLPFC target area in the axial, coronal and sagittal slices in the T_1-images of each subject (S1-S5). The other variables are as depicted in Figure 12. VLPFC – ventrolateral prefrontal cortex.

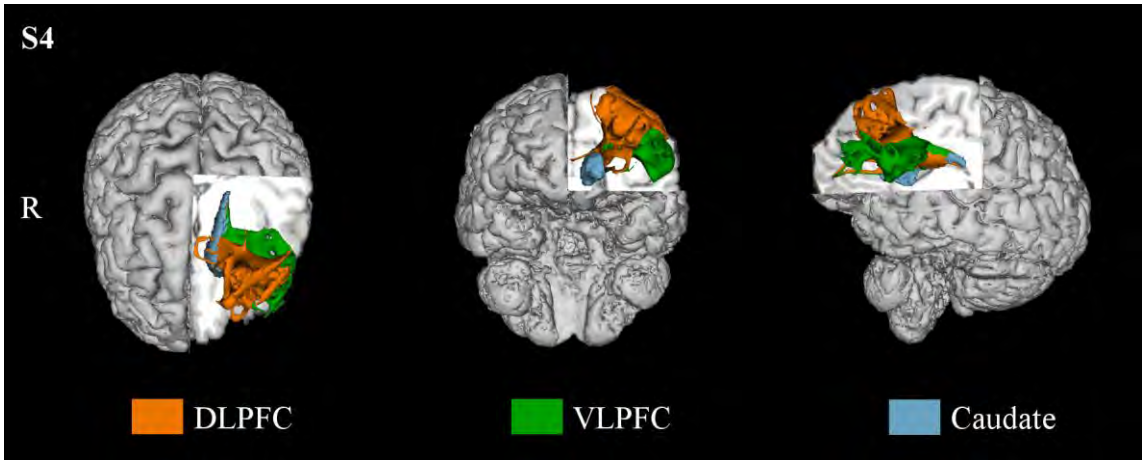

Figure 12: Tracts between the caudate nucleus and the target area in the DLPFC (orange), and between the caudate nucleus and the target area in the VLPFC (green) in the left hemisphere of one subject (S4). DLPFC- dorsolateral prefrontal cortex; VLPFC – ventrolateral prefrontal cortex.

The VLPFC tracts seem to connect with the caudate nucleus more posteriorly and ventrally than the DLPFC tracts. This is best illustrated in the Figure 12 that shows the tracts between the caudate nucleus and the DLPFC (orange) and the tracts between the caudate nucleus and the VLPFC (green) in three-dimensions without the probability information.

6.1.2 Tracts between the putamen and motor areas

Tracts between the putamen and the M1 (Figure 15) are highly consistent between subjects. The tracts consistently connect the posterior parts of the putamen with the M1. The axial slices were chosen to show the tracts at the horizontal level of the hand-knob area which was extracted as the target area. The coronal slices show the longest continuous tract reaching the cortex in the vertical plane between the putamen and the target area. The sagittal slices illustrate the most continuous within-slice connection between the cortical areas and the putamen.

The tracts between the putamen and the PMC (Figure 16) show especially poorly in two dimensional slices. The PMC tracts are tightly packed in areas immediately superior to the putamen. The tracts spread subcortically in a large area with several branches that have varying probability and robustness. Individual variability in the locations of the lateral branches is notable. The spreading of the tracts is best seen in the three-dimensional reference figure (Figure 13) illustrating the tracts between the putamen and the PMC (green) and M1 (blue). In the two dimensional slices (Figure 16), the axial slices were selected to illustrate the connection sites in the lateral areas in the horizontal plane. The coronal slice for each subject displays the most robust and continuous tracts observed reaching the lateral cortical areas. The sagittal slices were taken near the putamen to show tight packing of the tracts in the area since illustrating the lateral tendrils emphasized in the selection of the other slices proved difficult in the sagittal plane.

The tracts between the putamen and SMA are shown in Figure 17. These tracts were the only ones that showed connections with areas in the other hemisphere. The axial slices were chosen to illustrate how the constructed tracts locate in relation to the largest brain sulci and gyri. The coronal slice displays continuous and robust connections with the cortical areas within the slice. Such connections were evident in a large

number of the coronal slices, so the slices were also chosen to show the connections with the other hemisphere in subjects where such connections were found. The sagittal slices were from the level that shows the edges of the cingulate sulcus which served as the lateral boundary of the target mask for the SMA. The SMA trajectories connect with the lateral and medial parts of the putamen, and in many subjects reach fairly far in the anterior putamen.

Figure 18 displays the tracts connecting the putamen and preSMA. The coronal slices were chosen similarly than in Figure 10: to illustrate robust and continuous connections between the putamen and the cortical areas. The sagittal and axial slices were from the same level as the slices chosen for the SMA tracts to make comparing the two tracts easier. The preSMA tracts seem to connect to the more lateral, dorsal parts of the putamen than the SMA tracts.

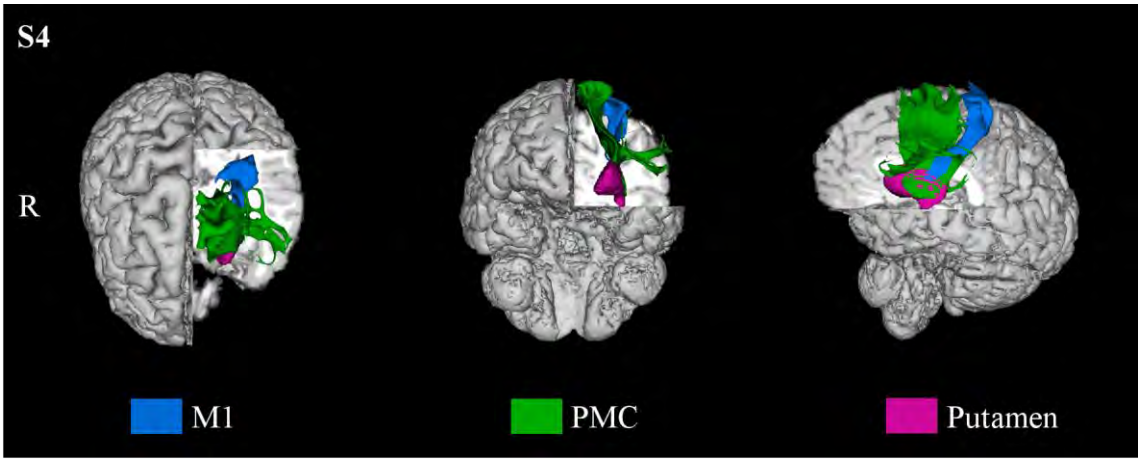

Figure 13: Tracts between the putamen and the target area in the M1 (blue), and between the putamen and the target area in the PMC (green) in the left hemisphere of one subject (S4). M1 – motor cortex; PMC – premotor cortex.

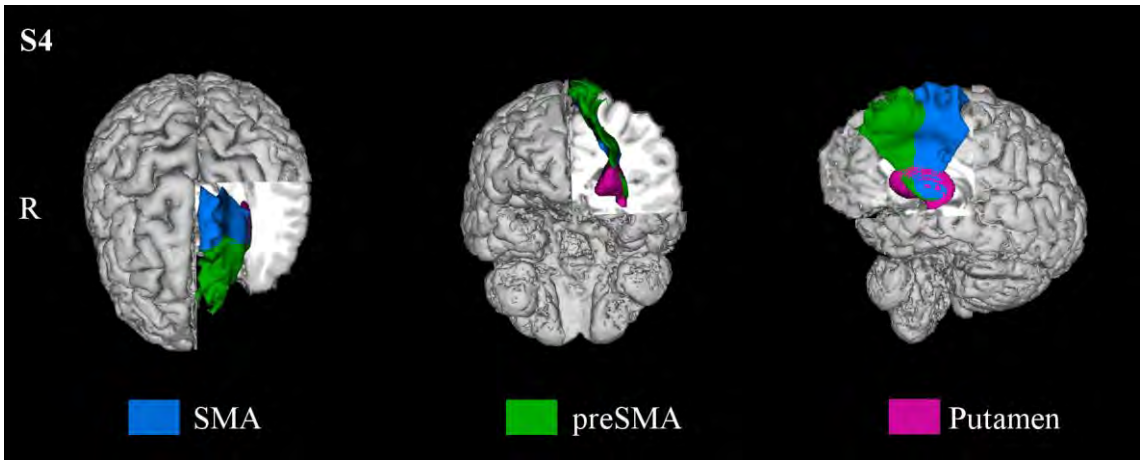

Figure 14: Tracts between the putamen and the target area in the SMA (blue), and between the putamen and the target area in the preSMA (green) in the left hemisphere of one subject (S4). SMA – supplementary motor area; preSMA – presupplementary motor area.

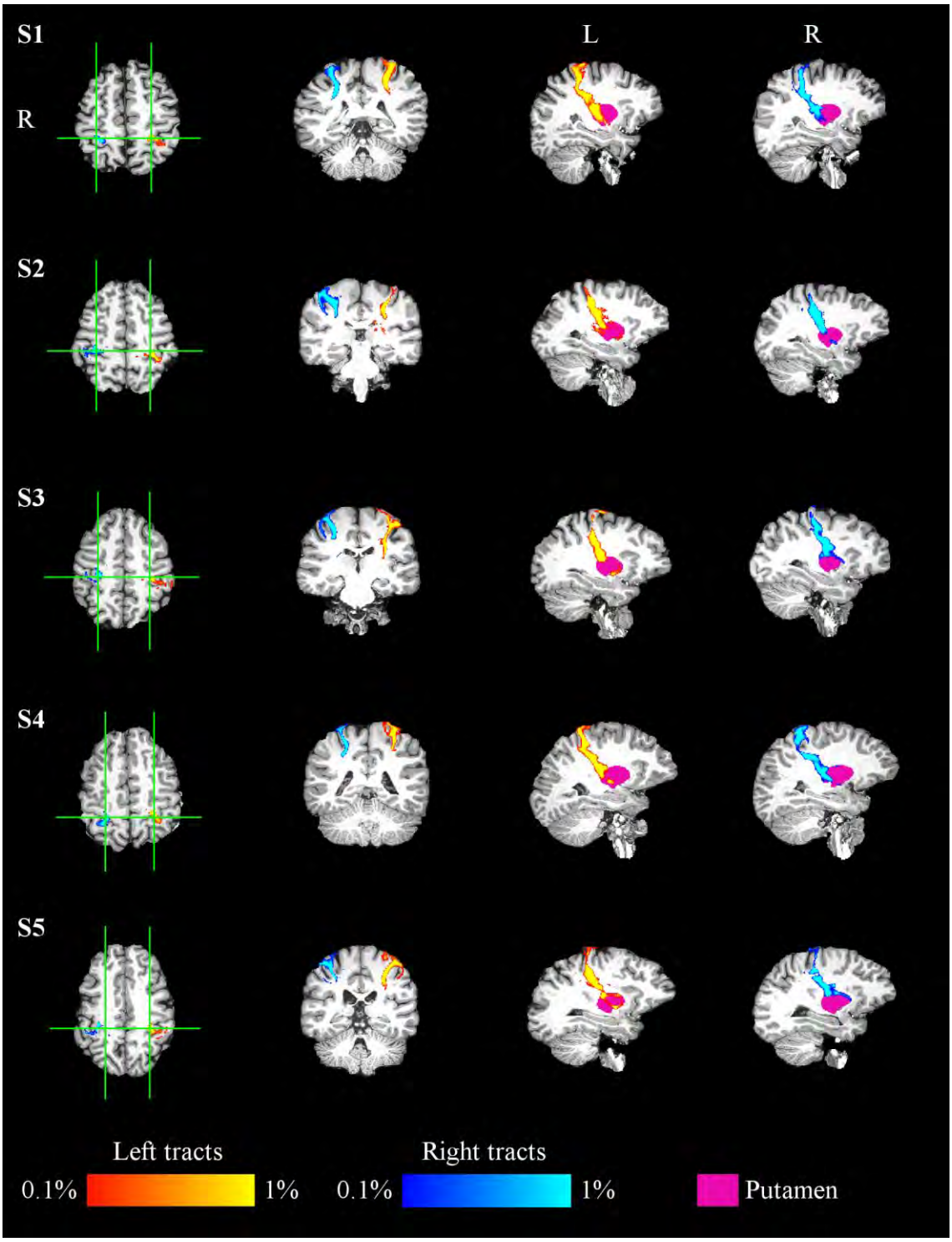

Figure 15: Constructed tracts between the putamen and the M1 target area in the axial, coronal and sagittal slices in the T_1-images of each subject (S1-S5). For the tracts in both hemispheres, the intensity describes the number of tracts passing through a voxel, i.e. the likelihood of connection with the seed area, i.e. the putamen (pink). The intensity scale ranges from 0.1% of the number of all tracts connecting the seed and target areas (red for the tracts in the left hemisphere, dark blue for the tracts in the right hemisphere) to 1% of same number (yellow for tracts in the left hemisphere, light blue for the tracts in the right hemisphere). Green crosshairs indicate the locations of the coronal and sagittal slices. M1 – motor cortex.

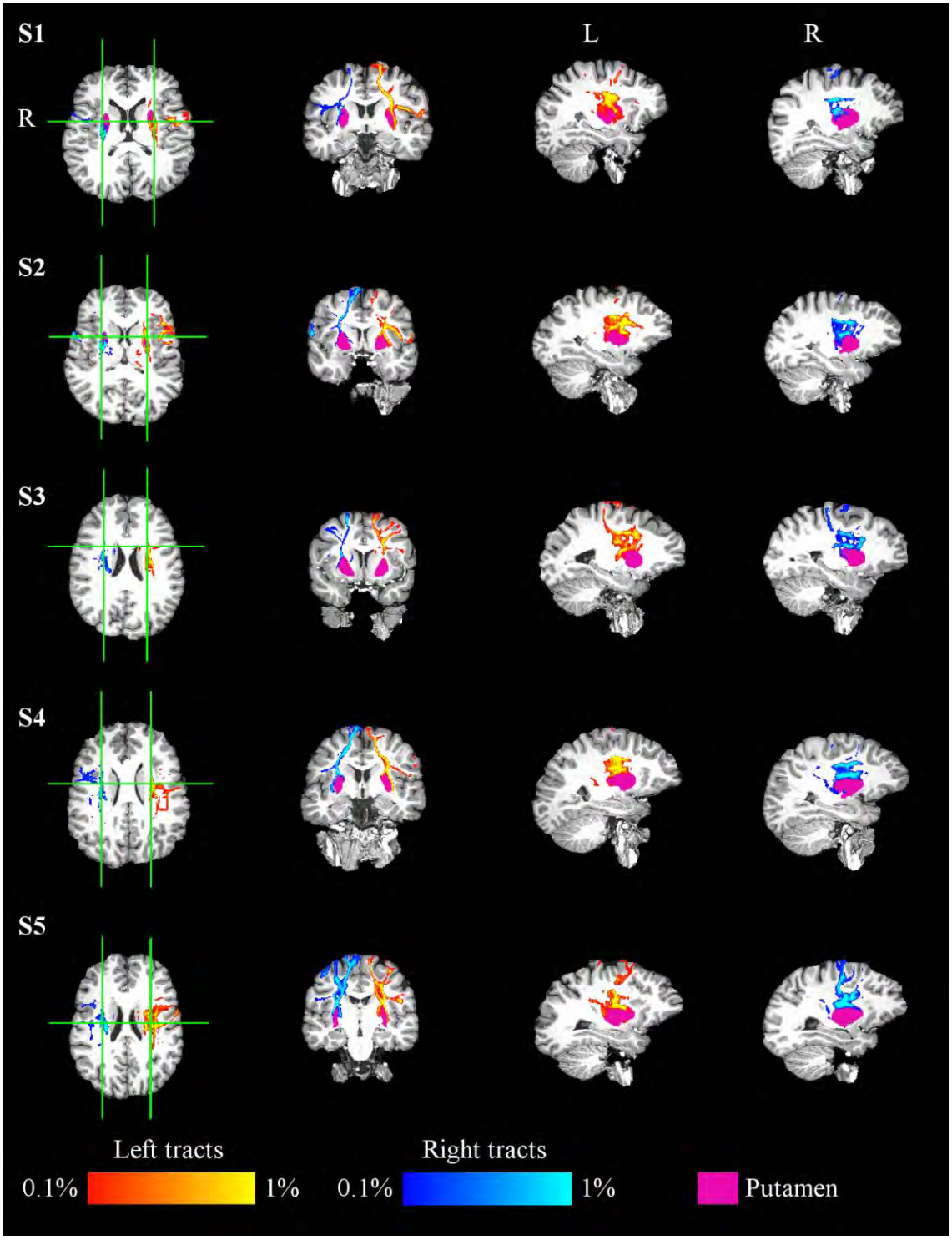

Figure 16: Constructed tracts between the putamen and the PMC target area in the axial, coronal and sagittal slices in the T_1-images of each subject (S1-S5). The other variables are as depicted in the Figure 15. PMC – premotor cortex.

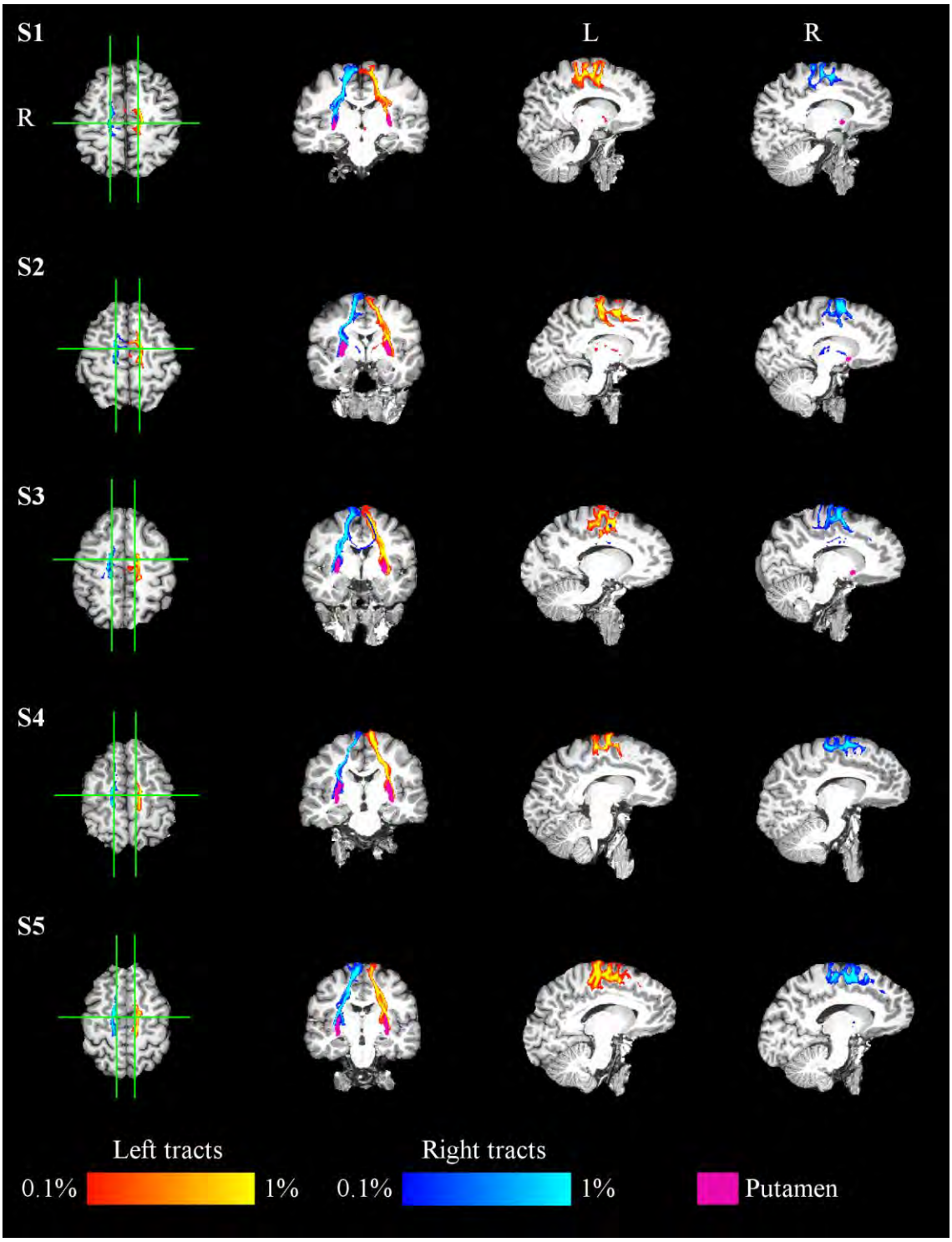

Figure 17: Constructed tracts between the putamen and the SMA target area in the axial, coronal and sagittal slices in the T_1-images of each subject (S1-S5). The other variables are as depicted in the Figure 15. SMA – supplementary motor area.

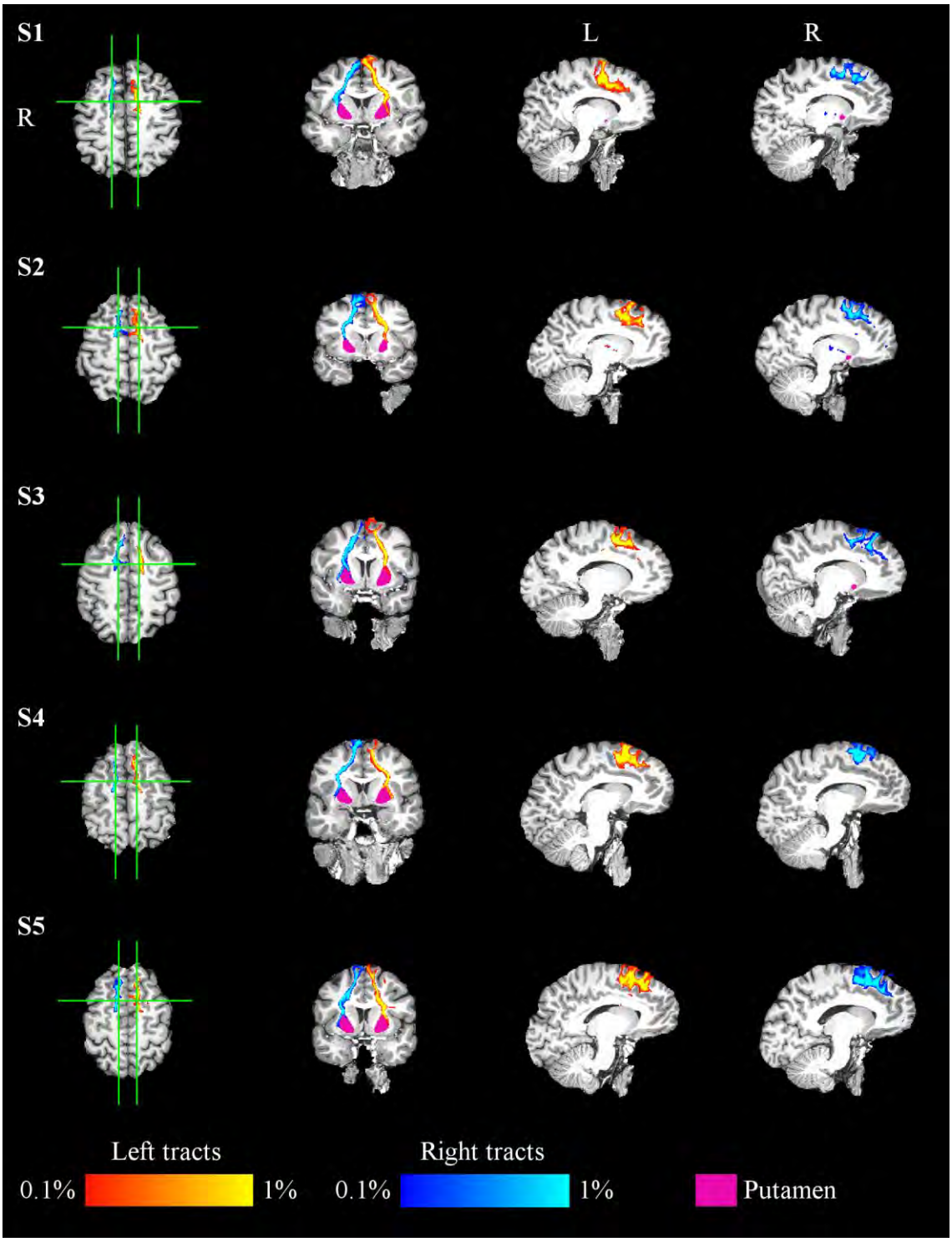

Figure 18: Constructed tracts between the putamen and the preSMA target area in the axial, coronal and sagittal slices in the T_1-images of each subject (S1-S5). The other variables are as depicted in the Figure 15. preSMA – presupplementary motor area.

6.2 Group analysis

The results at the group level are presented in Figure 19 and Figure 20 as population maps. Figure 19 illustrates the connections between the caudate nucleus and the target areas in the prefrontal cortex, the DLPFC and VLPFC. Figure 20 displays tracts between the putamen and the target areas in the M1, PMC, SMA and preSMA.

In both images, the tracts in the left hemisphere are shown in red-yellow and tracts in the right hemisphere in blue. Brighter colours indicate higher intensity that describes in how many subjects the constructed tracts travelled through the voxel in question. The values vary from two of the five subjects (dark red for tracts in the left the hemisphere and dark blue for the tracts in the right hemisphere) to four of the five subjects (bright yellow for tracts in the left hemisphere and light blue for the tracts in the right hemisphere). In both figures, the tracts are shown overlaid on the MNI152 standard brain. The seed structures, the caudate nucleus (light blue in Figure 19) and the putamen (pink in Figure 20) as depicted by the Harvard-Oxford sub-cortical atlas ([147]–[150]), are shown for reference. The green crosshairs on the axial slices indicate the locations of the coronal and sagittal slices.

The first row in Figure 19 displays the connections between the caudate nucleus and the DLPFC. The slices were selected similarly than the slices in the individual anal-

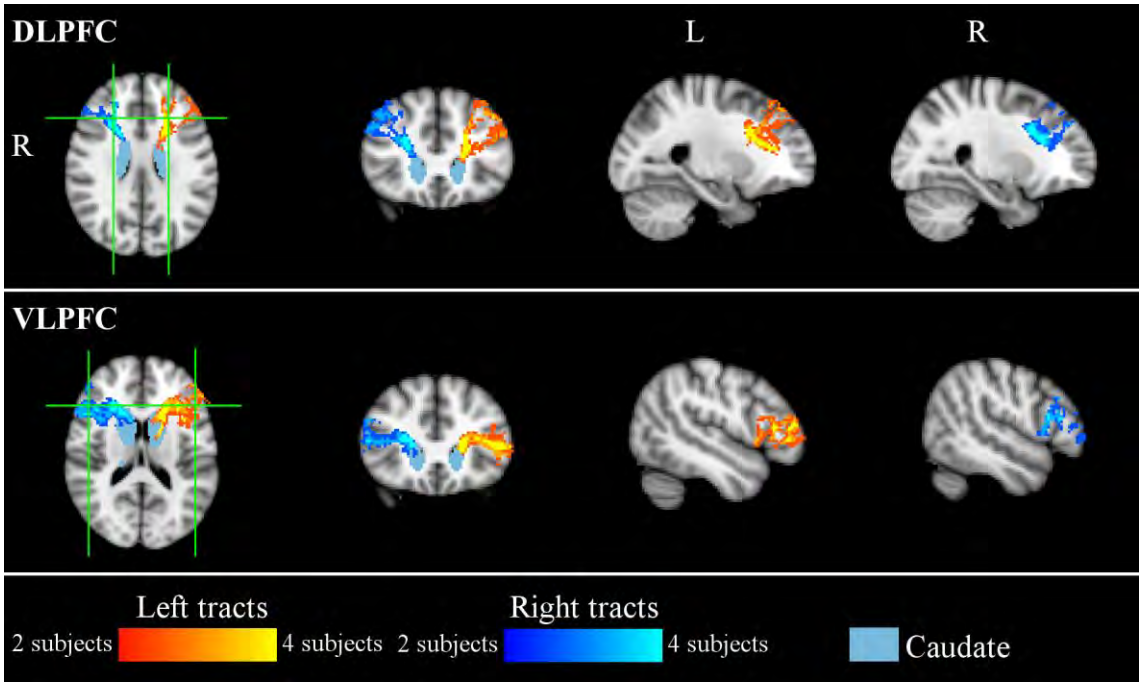

Figure 19: Reconstructed tracts connecting the caudate nucleus with the prefrontal cortex (the DLPFC and VLPFC) as population maps at the group level. For the tracts in both hemispheres, the intensity describes in how many subjects the found tracts pass through any given voxel i.e. the number of subjects in which the tracts exist in the given voxel. The intensity range varies from two of five subjects (dark red in the left hemisphere, dark blue in right hemisphere) to four of five subjects (yellow in the left hemisphere, light blue in the right hemisphere). Tracts are shown in MNI152 space with standard MNI152 brain. The caudate nucleus (light blue) is shown for reference as depicted by the Oxford-Harvard subcortical atlas ([147]–[150]). DLPFC – dorsolateral prefrontal cortex; VLPFC – ventrolateral prefrontal cortex.

ysis: The coronal and axial slices that best depict the in-slice continuous connection between the caudate nucleus and the cortex, and the sagittal slices that show laterally the furthest location with a high probability of connection.

The second row in the Figure 19 illustrates the connections between the caudate nucleus and the VLPFC. The locations of the coronal and sagittal slices were justified similarly as in the first row, i.e. to showcase the continuous connections between the caudate nucleus and the target area. The axial slice is from the same level than used to illustrate the connections between the caudate nucleus and the DLPFC in the first row.

In the Figure 20, the first row illustrates the population map that was constructed from the tracts between the putamen and the M1. Slice levels were chosen similarly than in the individual analysis: The axial slice highlights the location of the hand-knob, and the coronal and sagittal slices display the most continuous tracts between the putamen and the cortex. Unlike the other connections, the M1 tracts are notable different in different hemispheres. Tracts in the left hemisphere (red-yellow) have a high resemblance with the tracts seen at the individual level (Figure 15), but the tracts in the right hemisphere (blue) are significantly less robust than at the individual level and not consistently present in more than two subjects. As the tracts in both hemispheres are similarly robust in individuals (Figure 15), the loss of consistency exclusively in the right hemisphere in the group analysis suggests that there was variability in the locations of the target areas in different subjects in the right hemisphere.

The second row of Figure 20 displays the population map of connections between the putamen and the PMC. The slices were chosen similarly than at the individual level, i.e. the axial and coronal slices to display the lateral extensions of the tracts and the sagittal slices laterally near the putamen. The lateral extensions have mostly disappeared as only one branch reaching the left temporal lobe is visible (best seen on the coronal slice). This extension was present only in two of the five subjects. The finding that there were no other lateral extensions likely reflects considerable variance between individuals in the locations and robustness of the lateral branches of the tracts between the putamen and PMC as discussed previously in Chapter 6.1. As the placement and the probability of extensions vary between individuals, their locations are not consistent when warped to the standard space and therefore the extension are not seen in the population maps.

The third row in Figure 20 depicts the population map of the connections between the putamen and the SMA. Again, the locations of the slices corresponded to the levels used at the individual level: the axial slice displays the most robust and continuous connection between the cortex and putamen, the coronal slice illustrates the cortical probability of connection in relation to the sulci and gyri, and the sagittal slices show the tracts along the lateral edge of the cingulate sulcus. Notably, these tracts have a high resemblance with the tracts between the putamen and PMC. This likely reflects locational proximity of the defined target areas as the PMC-ROI and SMA-ROI are adjacent. The found tracts likely reflect more accurately connection between the putamen and SMA than the putamen and PMC as the above described absence of the lateral extensions of the PMC tracts that was suggested to be due to variability between subjects in the location of the target area leaves behind only the parts of the found tracts that connect to the medial parts of the PMC target area, i.e. areas close to the SMA target area.

The bottom row of Figure 20 displays the population map of the connections between the putamen and preSMA. The sagittal and coronal slices are from the same levels than the slices used to illustrate the tracts between the putamen and the SMA. The axial slice was chosen to display the most robust and continuous connection between the cortex and putamen.

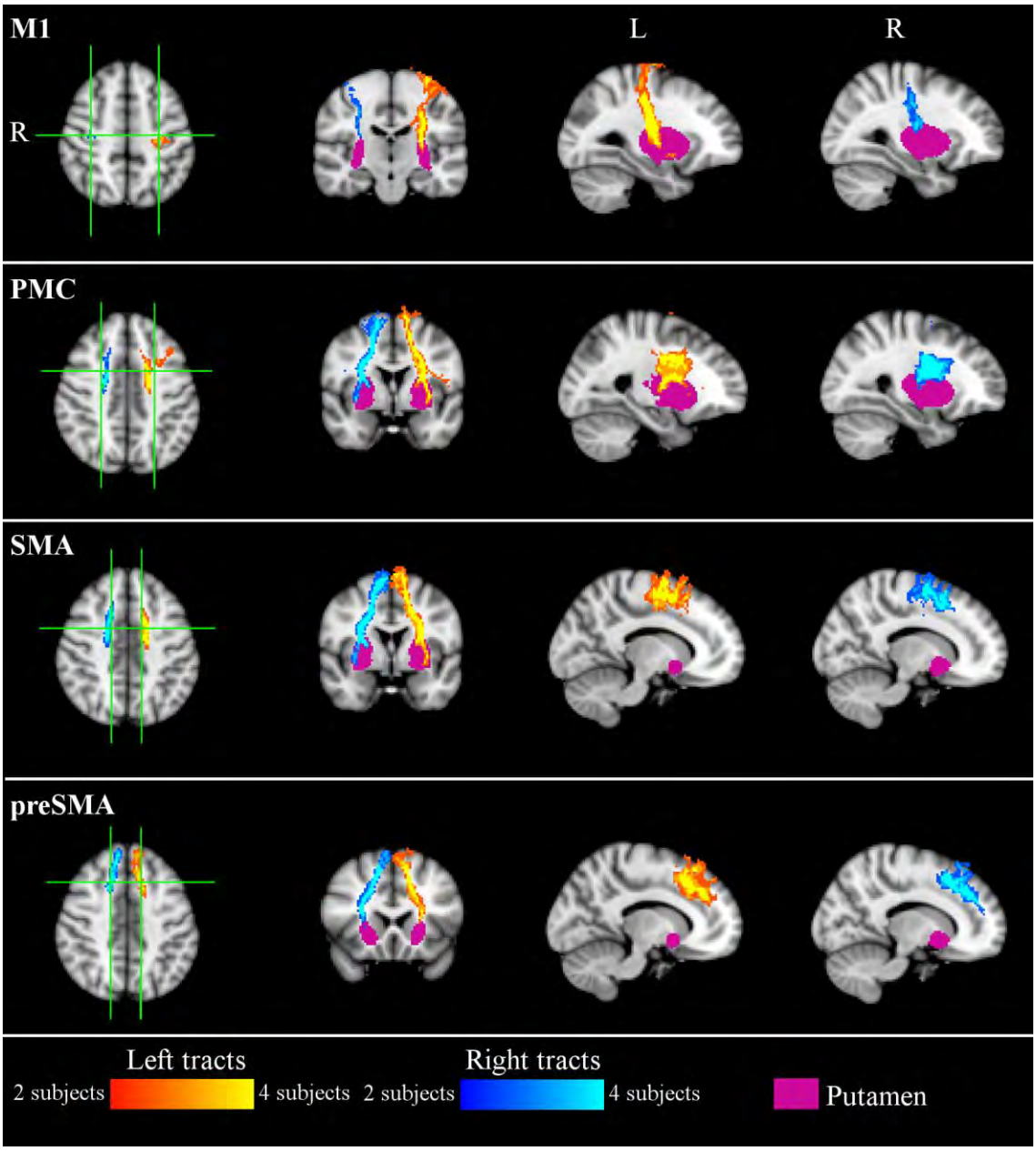

Figure 20: Reconstructed tracts connecting the putamen with the motor areas (M1, PMC, SMA and preSMA) as population maps at the group level. For both hemispheres the intensity describes in how many subjects the found tracts pass through any given voxel i.e. the number of subjects in which the tracts exist in the given voxel. The intensity range varies from two of five subjects (dark red in the left hemisphere, dark blue in right hemisphere) to four of five subjects (yellow in the left hemisphere, light blue in the right hemisphere). Tracts are shown in MNI152 space with standard MNI152 brain. The putamen (pink) is shown for reference as depicted by the Harvard-Oxford subcortical atlas ([147]–[150]). M1 – primary motor cortex; PMC – premotor cortex; SMA – supplementary motor cortex; preSMA – presupplementary motor cortex.

In summary, most tracts survived the conversion to the standard space and retained the general shape they had at the individual level, which indicates high consistency in the target areas between the subjects. An exception to this were the tracts between the putamen and the PMC in both hemispheres, and the tracts between the putamen and the M1 in the right hemisphere. In most cases, the tracts were highly similar in both hemispheres, with the exception of tracts between the putamen and M1 where the tracts in the right hemisphere were significantly less robust than in the left hemisphere.

7 Discussion

The results presented in the previous Chapter demonstrate that significant connections exist between the striatum and the frontal as well as motor cortices. Found tracts are consistent with previous studies examining the connections between the striatum and cortical areas ([20]–[22]). The caudate nucleus is robustly connected with the dorsal and ventral prefrontal cortices whereas the putamen is connected with the areas of the cortex that are associated with movement, such as the primary motor cortex, premotor cortex, supplementary motor area and presupplementary motor area.

In this chapter, I will evaluate some of the most consequential methodological choices that I made in this study and discuss how they need to be taken into account when interpreting the results. I will also suggest a few possible improvements that might add to the confidence of the results. In the last subchapter, I also look into the future and lay down a few possible avenues of future research.

7.1 Evaluation of the target area determination

All determined boundaries of the target areas in this study were based on previous studies and prior anatomical knowledge ([21], [141], [143], [145]). Nevertheless, however diligent the process, determining the absolute boundaries of different brain areas is not possible. Firstly, most brain areas have no exact anatomical boundaries. Secondly, locating the boundaries, when they do exist, from the T_1-images of individual subjects is difficult and time-consuming, and often impossible. Many classical divisions, such as Brodmann's areas, rely on differences at the level of cellular organization. That level of detail is not observable in T_1-images of any available resolution. Therefore, the determination of the target areas is unavoidably arbitrary.

The M1 target area in the left hemisphere was the most unambiguous to determine as the hand knob in the left hemisphere is an easily identifiable and highly consistent landmark in humans. This equivocality is reflected in the results of the group analysis as the population map for the tracts between the putamen and the M1 in the left hemisphere is robust and consistent with a high resemblance to the results at the individual level (Figure 20). However, results in the right hemisphere show significantly lower consistency in the connection, likely due to localization problems. These problems may stem from asymmetry of the brain sulci in the different hemispheres. The distinctive shape of the hand knob is not as distinct in the right hemisphere. The hand-knob area, true to its name, controls the fine motor movements of the contralateral hand. As the great majority of humans are right-handed, the area controlling hand movements is typically more pronounced in the left hemisphere. Interestingly, this problem does not show in the results at the individual level (Figure 15, on page 36): The tracts in the right hemisphere in individuals are as consistent as the tracts in the left hemisphere. However, in addition to the hand knob area also other areas of the primary motor cortex are connected with the putamen, so it is possible that similar results between the subjects were acquired even when the target areas compassed different parts of the primary motor cortex. Another possible explanation to the observed difference at the group level is that the corresponding cortical areas were correctly determined in individuals, and the weak connection probability in the right hemisphere at the group level resulted from faulty registration of the tracts. Registration is discussed more in-depth in Chapter 7.3.

Determination of the SMA and preSMA target areas relied on an earlier study by Lehéricy and colleagues [21]. The boundaries were based on the shape and location of the cingulate sulcus, but, nevertheless, ultimately arbitrary as the actual anatomical boundaries were not easily observable. Especially the distinction between the SMA and

preSMA target areas is debatable as it was based on an arbitrary line, the VAC-line (a vertical line through the anterior commissure). However, as the SMA and preSMA do not have an absolute, easily observable anatomical boundary, the VAC-line served the purpose.

The anterior limit, referred to as a rostral limit in the study used as a reference [143], of the PMC target area is the most explicitly arbitrary construction of the boundaries among the target areas used in this study. It was defined as a vertical line at the midpoint between the central sulcus and the most anterior part of the brain. Even though both of these are easily identifiable in T_1-images, the exact locations can be plausibly determined to a range of slices. A difference of a few slices at either end can move the determined rostral limit significantly. The central sulcus is not symmetrically located in the hemispheres and can be determined on several places on the axial plane, most obviously either on the top of the brain (brain vertex) or from the point where the sulcus contacts the Sylvian fissure. As there was no obviously optimal solution, I chose to value consistency and convenience. Therefore, I determined the location of the central sulcus from the dorsolateral part of the brain corresponding to the level of the cingulate sulcus to the most anterior coronal slice that still aligned with the central sulcus in both hemispheres. The most anterior point of the brain, the other variable in the calculation of the rostral limit to determine the anterior end of the PMC target area, was determined as the last coronal slice still containing voxels.

The other boundaries of the PMC target area were not as exactly defined, so for the sake of consistency and to avoid overlap with the other target areas, I used the same boundaries as defined for the SMA and preSMA target areas. Thus, the target area for the PMC extended laterally from the next sagittal slice adjacent to the SMA and preSMA target areas to the Sylvian fissure and slowly shrunk medially by following the shape of the precentral sulcus. Overall, the delineation of this target area was highly arbitrary. Most likely it still contained areas that anatomically belonged to the SMA or preSMA. It also seems likely that the edges drawn between the areas happened to be situated in the plane through which many tracts targeting the medial cortical areas travel, therefore obscuring the distinctions between the target areas. The SMA and preSMA might be laterally too narrow to accurately span over the whole anatomical area that they are meant to represent, thus allowing the PMC-ROI to cover overly medial areas. All this could result in that the tracts between the putamen and the PMC, especially at the group level, highly resemble the tracts between the putamen and the SMA. For these reasons, care is required when using the tracts between the putamen and the PMC in future analysis.

The DLPFC and VLPFC target areas as used in this study were adjacent to each other. Anatomically, the DLPFC is one of the areas that in humans have no detectable absolute boundaries. In this study, a distinction between the prefrontal areas was chosen to be easily detectable in the T_1-images, and thus the boundary between the areas was made to follow the shape of the middle frontal sulcus. The inferior frontal sulcus acted as the inferior boundary of the DLPFC and the superior boundary of the VLPFC. The VLPFC was anteriorly constricted by an arbitrary line at the level of the horizontal ramus of the Sylvian fissure. This distinction was strictly followed to avoid including areas in the temporal lobe to the ROI. It is, however, possible that this cut out inferior areas that anatomically belong in the VLPFC. The posterior limit was the same for the both prefrontal target areas, and it was set adjacent to the anterior end of the target area for the PMC to avoid overlap of the target areas. Anteriorly both the PFC target areas extended as far as the distinction between the middle frontal sulcus and the inferior frontal sulcus was easily detectable in the coronal plane, the target area for the DLPFC

reaching a few slices further than the ROI for the VLPFC. All in all, it is quite probable that both target areas contained some adjacent areas, especially in the anterior and orbitofrontal cortex as the set boundaries were arbitrary and chosen for with the ease of observation in mind. Especially the VLPFC-ROI might include slices of the anterior parts of the PMC as it covered areas directly adjacent to the target area for the PMC.

In conclusion, even though the determination of the target areas was in many places arbitrary, each had anatomically plausible boundaries that could be consistently determined in different individuals. Some ambiguity was inevitable as natural anatomical differences in the brains of individuals are vast. Certain limitations of the target areas, especially in the case of the PMC target area, need to be acknowledged when interpreting the acquired results, but there is no reason to believe that the target areas did not catch corresponding tracts in the different hemispheres and individuals.

7.2 Effect of the threshold

Another phenomenon that has a significant effect on the results is the threshold that was used to remove noise and connections with low probability. The threshold refers to the minimum number of times the tracking algorithm must travel through a data point for that point to be included in the results, i.e. the minimum allowed probability that the data point has a connection with the seed area. With probabilistic tractography, using a threshold is inevitable as the initial results include all data points the tracking algorithm travels through during all of the launches, therefore including the connections found through random happenstance and noise in the data (false positives). In addition, the thresholding is needed to make the found tracts comparable and combinable despite naturally occurring individual differences.

Thresholding tends to emphasize the distinctions created by the boundaries of the target areas. The tractography algorithm used in this study allowed tracking to continue onwards from the target areas instead of terminating immediately, thus spreading out of the designated target. However, these connections typically have lower probabilities as the distance from the seed area increases. Therefore, a strict threshold removes all but the most robust tracts and thus preserves the boundaries between areas. Some connections, such as few tracts crossing from one hemisphere to another in few constructions between the putamen and the SMA (Figure 17, on page 38) are robust enough to endure the threshold. Loosening the threshold affects immediately the number of tracts not strictly contained to the target area (phenomenon illustrated in Figure 21).

The threshold that was applied in this study was determined proportionally for each subject and tract by making it a percentage of the number of all tracts fulfilling the criteria, i.e. traveling from the seed area to the target mask (the “waytotal”) in each run of the algorithm. This removed the same proportion of low probability tracts for each subject and tract allowing direct comparisons between the tracts, hemispheres and subjects as the intensity markings indicate uniform likelihoods.

In the case of this study, the disadvantage of individually varying thresholding that could hide asymmetries between the hemispheres in individual subjects and size differences in the tracts in different subjects, is not critical as the interest is in the locations and the travel paths of the tracts, not in their size differences. Furthermore, the other normalizing options, dividing individual tracts by the total number of algorithm launches or using the same constant threshold for all subjects and tracts, were not sufficient as in this study each tract had the same number of seed points from which the tracking was initiated and the same number of launches, but the size of the target areas varied (Table 1, on page 29). The second option, dividing by the number of launches functions well when only the number of seed points varies between different tracts but it

cannot account for the size differences of the target areas and therefore, in the case of this study, would have only scaled the results. Furthermore, option three, using the same constant threshold, functions best when the sizes of both the seed and target areas stay constant in different subjects and tracts as is the case, for example, in the study by Leh and colleagues [22]. In the case of this study, however, the constant threshold would have only removed low probability tracts but not added to the comparability of different tracts or the tracts in different individuals.

In addition to making the results comparable, the proportional thresholding smoothed differences on "tractability" between different subjects and hemispheres. "Tractability" refers informally to the ease with which the tracts can be constructed from the data and is reflected in the size of the waytotal. The tractability varies wildly, in the range of tens of thousands, between individuals and even between different tracts within individuals without specific or consistent reasons. Some of the variability stems

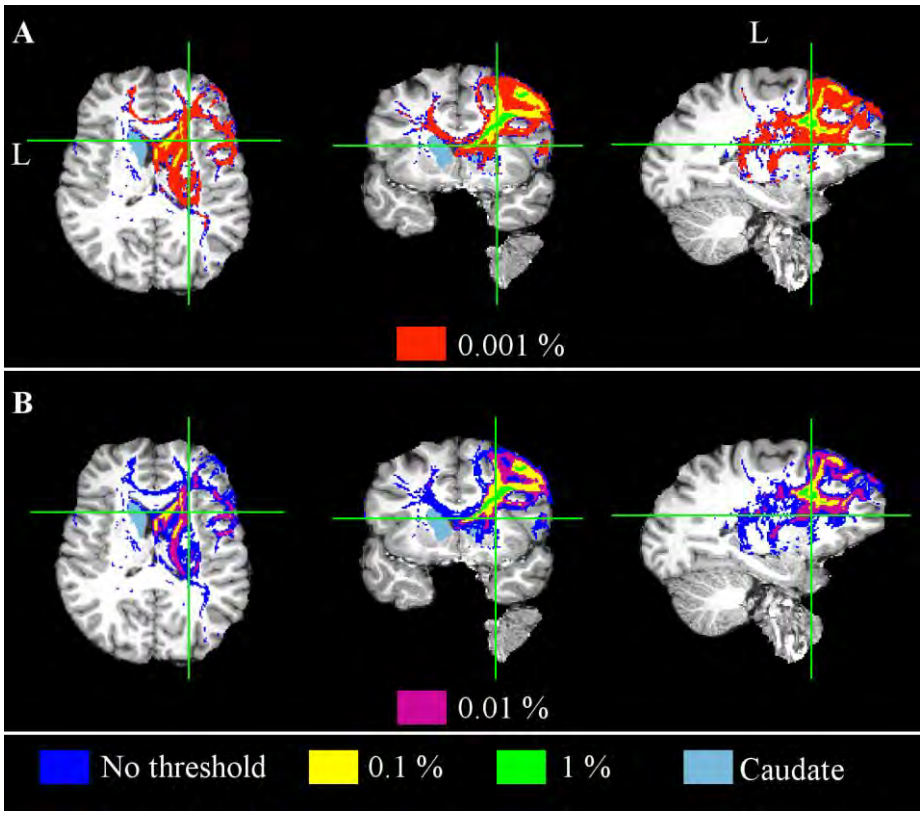

Figure 21: Effect of thresholding in the tracts connecting the caudate nucleus (light blue) and the target area in the DLPFC in the left hemisphere of one subject (S2). The percentages refer to corresponding percentages of the total number of tracts found connecting the caudate nucleus and the DLPFC (the waytotal) which in the case of this subject (S2) was 166095. Green crosshairs indicate locations of the slices. No threshold (blue) – all found tracts; 0.001% (red) – voxels through which the tracking algorithm travels at least 1.66 times during the whole run; 0.01% (violet) – voxels through which the algorithm travels at least 16.6 times during the whole run; 0.1% (yellow) - voxels through which the algorithm travels at least 166 times during the whole run, the threshold used in this study; 1% (green) - voxels through which the algorithm travels at least 1661 times during the whole run.

from the unavoidable data discrepancies, such as artefacts produced by noise in the imaging process ([110], [111]), but some indeterminable amount is due to natural anatomical differences between the individuals.

In this study, the threshold was set to 0.1% of the waytotal for all tracts. This may sound purposelessly small, but in reality corresponds to the numbers in a scale of few hundreds, depending on the subject and tract. This threshold removed large parts of the constructed tracts, as most of the found connections have a very low probability (Figure 21). However, this removal is justified, because in this study, the overall goal was to find the anatomical connections that one can assume are real so that this knowledge of the tracts and their cortical target locations can be used in future research. The possibility of losing real connection with lower probability through over-thresholding is preferable to having ambiguous locations of connection with the cortex with very low probability. The goal was to ensure high probability of the found connections being real. Moreover, a strict threshold makes comparisons between the different tracts in individual subjects and the same tracts in different subjects easier as the tracts are sleeker and likelihoods of actually existing connections are higher.

The threshold is especially crucial for the group analysis. In the production of a population map, the tracts of individual subjects with a probability exceeding the threshold were included when creating the individual binary mask. The binary mask did not discriminate between voxels with a high and low likelihood but treated all points equally in the further analysis so any deeper probability information of included data point was lost. The population maps resulting from summing the individual binary masks contained information only about the number of subjects in which the tracts travelled through any given data point. A strict threshold, as used in this study, ensured that the population maps did not contain unlikely connections or irrelevant noise, which was valued more than the possible downside of losing less robust connections that potentially could be observable in group level.

7.3 Limitations of registration

One fairly significant source of a possible problem in the results was registration, especially to the standard space. As it stands, the seed and target areas were defined in the native T_1-space for each subject and tractography was performed in the native DTI-space. The results were then converted to the T_1-space. For the group analysis, these tracts were directly converted from the T_1-space to the MNI152-standard space. Thus, it is possible that the starting and ending points of the tracking did not correspond to the same structures in the standard space. Due to time constraints, the registration to the standard space was optimized to neither subcortical nor cortical structures. Instead, automatic algorithms provided by FSL were used.

Registration, particularly of the DTI data, is difficult ([151], [152]). The data contains multiple dimensions and the diffusion tensors must retain their orientation in relation to the anatomical structures (For comparison and evaluation of several popular methods, see: [153]). Methods vary among studies, but registration to the standard space is often achieved by registering the FA-maps and using nonlinear transformation either alone or in concert with linear transformation (e.g. [154]–[157]). Registering the FA-maps is especially feasible when the object of the study is a comparison of the white matter areas instead of the construction of the anatomical tracts. Such methods might improve the automatic, linear registration used in this study as the probability value or information of the higher order orientations is not important in the binarized tracts that were transformed to the standards space from the native space of each subject. Additionally, a warp acquired with these methods could be used to transform the structural

images to the standard space and determining the seed and target areas in the standard space for tractography. This would ensure that the seed and target areas correspond to correct anatomical areas. However, this method would increase the time demands of the calculations as each tracking analysis should be performed twice, first in the structural space and then in the standard space.

Nonetheless, even as an automated process, registration used in this study produced reasonable results. The produced population maps correspond fairly well to the results at the individual level, with the glaring exception of the tracts between the putamen and the M1 in the right hemisphere as discussed above. In other cases, the constructed tracts held the same general shape and route than the tracts found in individual subjects, which suggest that registration made the right areas to correspond in different individuals and that at least parts of the corresponding anatomical areas in the individuals were identified.

7.4 About the subdivision of the striatum

Previous studies have indicated further anatomical and functional division in the projections connecting with the striatum (e.g. [21]). These studies indicate that the DLPFC preferably connects with the dorsal-posterior caudate nucleus, whereas the VLPFC links with the ventral parts of the caudate nucleus. On the other hand, it has been observed that the dorsal-posterior putamen links especially strongly with the SMA, whereas the premotor area is connected with the medial putamen and the primary motor area with the lateral putamen. Results in this study suggest, but cannot confirm, these further divisions.

The locations of connections are most clearly observable in the 3D model tracts of one subject (Figure 12 on page 34, Figure 13 and Figure 14 on page 35). The connections of the caudate nucleus with the cortical target areas that were obtained in the present study lend some support to the above-described division. It seems that tracts between the caudate nucleus and the VLPFC reach more ventral parts of the caudate than connections with the DLPFC. This is especially notable when comparing the tracts on the axial slices in Figure 10 (on page 32) and Figure 11 (on page 33). However, the overlap between these tracts makes it difficult to judge the exact locations of connections with respect to the caudate nucleus. Additionally, the connections between the putamen and the M1 are seemingly more posterior and lateral to the tracts between the putamen and the SMA which in turn are posterior to the tracts between the putamen and the preSMA. The PMC connections, however, again overlap with both the SMA and preSMA tracts making reliable judgements about their exact connections points in the putamen infeasible.

However, when judging the subdivision of the striatum based on these results, it is important to note that all the tracts, regardless of the target area, travel through very nearby subcortical areas near the striatum, overlapping and intervening especially in areas directly superior to the structure. Pathways through those voxels have high likelihood of connections with the striatum for each constructed tract. There are two main reasons for this. Firstly, the tractography algorithm tends to favour data points near the seed areas. This stems from the inevitable fact that the tracking algorithm travels through points near the seed area more times during its run than through the points farther away, thus creating a higher probability of connection to the nearby areas. Secondly, subcortical areas that are near the striatum have a large number of neural pathways traveling through them, among them the pathways tracked in this study, since the striatum, as discussed in Chapter 3, connects with numerous brain areas. These pathways naturally cross, branch and travel parallel to each other, and as they typically are

several times smaller than the voxel size, separating the pathways from each other in these areas is not possible with this level of image resolution. Thus, the results of the current study are not sufficient to draw conclusions about the connectional subdivision of the caudate nucleus and putamen.

To further explore the subdivision of the striatum, the seed areas could be divided into subparts, the caudate nucleus to the ventral and dorsal-posterior sections and the putamen to the dorsal-posterior, medial, and ventral sections. These subsections would then serve as the seed areas for the tractography algorithm. However, this would not remove the problem of overlapping tracts and might even amplify it as the tracking algorithm would travel through the same areas even more times in search of connections between the smaller areas. The significance of the overlap is hard to gauge without running the analysis. It might be countered purely by using an appropriate threshold as the thresholding tends to emphasize the distinctions between the areas as discussed in Chapter 7.2, or might not be relevant to the experiment in question as the tracts are naturally adjacent and intervened. Tractography as a method may not be sufficient to definitely determine whether the found connections are separate and discrete at the level of the striatum, or if they are different branches of the same pathway. Histological or cellular level studies may be needed to resolve the question of overlapping tracts. However, such judgements are for future researchers to make as in this study I concentrated on the structures of the caudate nucleus and the putamen as a whole.

7.5 Possible avenues for future research

A large avenue for future research, and in fact a driving authorization of this study, is TMS-research. The locations and robustness of the connections between the cortex and the striatum are invaluable information for placing the TMS-coil when the aim is to affect the striatum with the TMS via neural connections. With a more fit localization of the coil, the cortical activation induced by the TMS spreads along the a priori defined neural tracts and excites the wanted area more reliably. Moreover, more precise localization might allow pulses of smaller intensity or of fewer repetition to produce the same results as pulses of the stronger intensity since more of the energy reaches the target area. In an optimal case, individual tractography analysis could be performed before a TMS experiment to identify the cortical area with the most robust connection with the striatum (either the caudate nucleus or the putamen) and therefore the optimal location for the TMS-coil. Tractography guided TMS has the potential to provide more reliable and individually optimized results.

In addition to the neurological diseases, improving excitation or release of neurotransmitters in the striatum could open interesting study opportunities in other areas, such as working memory, habit forming, decision making, goal-directed action, and planning and executing motor functions, all processes to which the striatum contributes. There are indications that specific areas of the striatum mediate distinct functions. Therefore, determining the neural connection between the subareas of the striatum and the cortex could allow stimulating exclusively certain target areas (via the neural connections) with TMS and thus investigating the striatal function in more detail and even determining the degree of separation of the neural connections.

One alluring research possibility was shown by Strafella and colleagues who demonstrated that repetitive TMS to the motor or prefrontal cortex activates dopamine release in the striatum, selectively in either the putamen or caudate nucleus ([24], [25] respectively). These observations have longstanding implications as disruptions in dopamine release in the striatum are implicated in certain neurological disorders, such as Parkinson's disease and Huntington's disease. In the studies by Strafella and colleagues

([24], [25]), the TMS-coil was placed over the motor cortex or the DLPFC based on the anatomical MRI images of the subjects. Compared to these earlier studies, exciting the release of dopamine with repetitive TMS could plausibly be improved by determining the neural connections between the cortex and the striatum with DTI and tractography in individual subjects, and by placing the TMS-coil more exactly over the areas of the strongest connections.

In addition to yielding valuable information for improving the use of other experimental methods, DTI and tractography are important tools on themselves. DTI remains the only available non-invasive method for studying anatomical connections in the brain in vivo. The study of the white matter may reveal valuable information about the extent and width of white matter neural tracts and in clinical applications possibly function as an early diagnostic tool for diseases that are accompanied by degradation of white matter pathways to and from the striatum, such as Parkinson's disease and Huntington's disease. Tractography, on the other hand, is the best available method for parsing the discrete, voxel-wise distributed information about the white matter together to continuous streamlines representing the pathways of the neural fibres. DTI and tractography can be used to assess the connections found in animal studies in the human brain and to discover anatomical routes of neural pathways instead of just the locations of the ending and starting points.

8 Conclusions

This study provides further evidence of the existence of the cortico-striatal loops and demonstrates the anatomical connections between the caudate nucleus and prefrontal areas and between the putamen and the areas involved in motor functions. It also demonstrates the power of the DTI and tractography methods in studying neural connections in individuals as well as at the group level.

All expected connections were found, and the connection sites and the routes of the neural pathways were determined for all five subjects in this study. In individual analysis, the tracts held generally the same shape both in the two hemispheres and in different subjects, but exact sites of the connections with the cortex and the routes of the pathways varied, as could be expected based on previous anatomical knowledge ([26]). The variance was especially notable in the lateral extensions of the tracts between the putamen and the target area in the PMC. Furthermore, connections of these tracts with the more medial parts of cortex overlapped largely with the connections between the putamen and the target areas encompassing more of the medial cortex, namely the SMA. It is probable that the determined target area for the PMC captured also tracts belonging to the SMA connections and omitted some of the more lateral PMC projections.

In the group analysis, the general shape and robustness of the constructed connections corresponded fairly well with the connections found at the individual level. This suggests that corresponding target areas were successfully determined in different subjects. Exceptions to this resemblance were the tracts between the putamen and the PMC in both hemispheres and the tracts between the putamen and M1 in the right hemisphere. At the group level, the connections between the putamen and PMC lost all the lateral branches that were found at the individual level and the constructed tracts had a high resemblance to the tracts connecting the putamen and the SMA, most likely reflecting the adjacency of the target areas. In the case of the connections between the putamen and M1, the connections at the group level were significantly less robust in the right hemisphere than in the left hemisphere. This suggests that the determined target sites in the right hemisphere did not correspond well between different subjects since, at the individual level, the tracts were similar and equally robust in both hemispheres.

The methodology used in this study is transferable to other groups of subjects as no major problems were encountered while tracking the connections. However, it is advisable to use care in determination of the target area for the PMC as the similarity with the SMA tracts and variability between the locations of the lateral branches may be due to too lax determination of the target areas which also may have led to the poor correspondence of the target areas among the subjects. Similarly, the determination of the target area for the M1 in the right hemisphere should be done carefully as there seems to be a lot of variability of this area between individuals that led to significantly less robust connections in the right hemisphere at the group level. The hand-knob area, which was used for target area determination, is typically less pronounced in the right hemisphere as a majority of humans are right-handed. Therefore, identifying the corresponding area in the right hemispheres of individuals can be challenging and should be given special attention.

The information gathered in this study about the cortical connections sites and pathways of the anatomical connections can be applied in future studies where knowledge about the striatal connectivity and function is needed. This information is especially advantageous to TMS studies. It could be used to place the TMS coil to the location of the strongest connection with the striatum to ensure that the activation caused by the TMS pulse spreads optimally to the subcortical area one aims to stimulate. It is advisable to use the individual information of the tracts for this localization instead of

the results of the group analysis. The registration of the DTI-data is prone to distortions and there are notable individual differences in both the routes and locations of the connections. Use of individual DTI and tractography information will optimize the cortical localization of the TMS coil when targeting the caudate nucleus or putamen.

References

[1] E. Gerardin, J.-B. Pochon, J.-B. Poline, L. Tremblay, P.-F. Van de Moortele, R. Levy, B. Dubois, D. Le Bihan, and S. Lehéricy, "Distinct striatal regions support movement selection, preparation and execution.," *Neuroreport*, vol. 15, no. 15, pp. 2327–2331, 2004.

[2] F. Hoffstaedter, C. Grefkes, K. Zilles, and S. B. Eickhoff, "The 'what' and 'when' of self-initiated movements.," *Cereb. cortex*, vol. 23, no. 3, pp. 520–30, Mar. 2013.

[3] H. H. Yin and B. J. Knowlton, "The role of the basal ganglia in habit formation," *Nat. Rev. Neurosci.*, vol. 7, no. 6, pp. 464–476, Jun. 2006.

[4] O. Monchi, M. Petrides, A. P. Strafella, K. J. Worsley, and J. Doyon, "Functional role of the basal ganglia in the planning and execution of actions," *Ann. Neurol.*, vol. 59, no. 2, pp. 257–264, Feb. 2006.

[5] S. J. G. Lewis, A. Dove, T. W. Robbins, R. A. Barker, and A. M. Owen, "Striatal contributions to working memory: a functional magnetic resonance imaging study in humans," *Eur. J. Neurosci.*, vol. 19, no. 3, pp. 755–760, Feb. 2004.

[6] K. R. Chaudhuri, D. G. Healy, and A. H. Schapira, "Non-motor symptoms of Parkinson's disease: diagnosis and management," *Lancet Neurol.*, vol. 5, no. 3, pp. 235–245, Mar. 2006.

[7] A. Montoya, B. H. Price, M. Menear, and M. Lepage, "Examen critique Brain imaging and cognitive dysfunctions in Huntington ' s disease," *J. psychiatry Neurosci.*, vol. 31, pp. 21–29, 2006.

[8] S. N. Haber and B. Knutson, "The Reward Circuit: Linking Primate Anatomy and Human Imaging," *Neuropsychopharmacology*, vol. 35, no. 10, pp. 4–26, 2010.

[9] G. E. Alexander, M. R. DeLong, and P. L. Strick, "Parallel organization of functionally segregated circuits linking basal ganglia and cortex," *Ann. Rev. Neurosci*, vol. 9, pp. 357–81, 1986.

[10] S. N. Haber, "The primate basal ganglia: parallel and integrative networks," *J. Chem. Neuroanat.*, vol. 26, pp. 317–330, 2003.

[11] P. J. Basser, J. Mattiello, and D. LeBihan, "MR diffusion tensor spectroscopy and imaging," *Biophys. J.*, vol. 66, pp. 259–267, Jan. 1994.

[12] S. Mori, B. J. Crain, V. P. Chacko, and P. C. M. Van Zijl, "Three-dimensional tracking of axonal projections in the brain by magnetic resonance imaging," *Ann. Neurol.*, vol. 45, no. 2, pp. 265–269, Feb. 1999.

[13] T. E. Conturo, N. F. Lori, T. S. Cull, E. Akbudak, A. Z. Snyder, J. S. Shimony, R. C. Mckinstry, H. Burton, and M. E. Raichle, "Tracking neuronal fiber pathways in the living human brain," *Neurobiology*, vol. 96, pp. 10422–10427, 1999.

[14] P. J. Basser, S. Pajevic, C. Pierpaoli, J. Duda, and A. Aldroubi, "In vivo fiber tractography using DT-MRI data," *Magn. Reson. Med.*, vol. 44, pp. 625–632, Oct. 2000.

[15] T. E. J. Behrens, M. W. Woolrich, M. Jenkinson, H. Johansen-Berg, R. G. Nunes, S. Clare, P. M. Matthews, J. M. Brady, and S. M. Smith, "Characterization and propagation of uncertainty in diffusion-weighted MR imaging," *Magn. Reson. Med.*, vol. 50, no. 5, pp. 1077–1088, Nov. 2003.

[16] G. J. M. Parker, H. A. Haroon, and C. A. M. Wheeler-Kingshott, "A framework for a streamline-based probabilistic index of connectivity (PICo) using a structural interpretation of MRI diffusion measurements," *J. Magn. Reson. Imaging*, vol. 18, pp. 242–254, Aug. 2003.

[17] S. Mori, W. E. Kaufmann, C. Davatzikos, B. Stieltjes, L. Amodei, K. Fredericksen, G. D. Pearlson, E. R. Melhem, M. Solaiyappan, G. V. Raymond, H. W. Moser, and P. C. M. Van Zijl, "Imaging cortical association tracts in the human brain using

diffusion-tensor-based axonal tracking," *Magn. Reson. Med.*, vol. 47, pp. 215–223, 2002.

[18] M. Catani and M. Thiebaut de Schotten, "A diffusion tensor imaging tractography atlas for virtual in vivo dissections," *Cortex*, vol. 44, pp. 1105–1132, 2008.

[19] T. E. J. Behrens, H. Johansen-Berg, M. W. Woolrich, S. M. Smith, C. A. M. Wheeler-Kingshott, P. A. Boulby, G. J. Barker, E. L. Sillery, K. Sheehan, O. Ciccarelli, A. J. Thompson, J. M. Brady, and P. M. Matthews, "Non-invasive mapping of connections between human thalamus and cortex using diffusion imaging," *Nat. Neurosci.*, vol. 6, no. 7, pp. 750–757, Jul. 2003.

[20] S. Lehéricy, M. Ducros, P.-F. Van De Moortele, C. Francois, L. Thivard, C. Poupon, N. Swindale, K. Ugurbil, and D.-S. Kim, "Diffusion tensor fiber tracking shows distinct corticostriatal circuits in humans," *Ann. Neurol.*, vol. 55, pp. 522–529, Apr. 2004.

[21] S. Lehéricy, M. Ducros, A. Krainik, C. Francois, P. F. Van De Moortele, K. Ugurbil, and D. S. Kim, "3-D diffusion tensor axonal tracking shows distinct SMA and pre-SMA projections to the human striatum," *Cereb. Cortex*, vol. 14, no. 12, pp. 1302–1309, 2004.

[22] S. E. Leh, A. Ptito, M. M. Chakravarty, and A. P. Strafella, "Fronto-striatal connections in the human brain: A probabilistic diffusion tractography study," *Neurosci. Lett.*, vol. 419, no. 2, pp. 113–118, 2007.

[23] B. Draganski, F. Kherif, S. Klöppel, P. A. Cook, D. C. Alexander, G. J. M. Parker, R. Deichmann, J. Ashburner, and R. S. J. Frackowiak, "Evidence for Segregated and Integrative Connectivity Patterns in the Human Basal Ganglia," *J. Neurosci.*, vol. 28, no. 28, pp. 7143–7152, Jul. 2008.

[24] A. P. Strafella, T. Paus, J. Barrett, and A. Dagher, "Repetitive transcranial magnetic stimulation of the human prefrontal cortex induces dopamine release in the caudate nucleus," *J. Neurosci.*, vol. 21, pp. 1–4, 2001.

[25] A. P. Strafella, T. Paus, M. Fraraccio, and A. Dagher, "Striatal dopamine release induced by repetitive transcranial magnetic stimulation of the human motor cortex," *Brain*, vol. 126, no. 12, pp. 2609–2615, 2003.

[26] W. Penfield and E. Boldrey, "Somatic motor and sensory representation in the cerebral cortex of man as studied by electrical stimulation," *Brain*, vol. 60, pp. 389–443, 1937.

[27] J. A. Grahn, J. A. Parkinson, and A. M. Owen, "The cognitive functions of the caudate nucleus," *Prog. Neurobiol.*, vol. 86, no. 3, pp. 141–155, 2008.

[28] J. W. Mink, "The Basal Ganglia and Involuntary Movements," *Arch. Neurol.*, vol. 60, no. 10, p. 1365, Oct. 2003.

[29] A. M. Graybiel, "The basal ganglia: learning new tricks and loving it," *Curr. Opin. Neurobiol.*, vol. 15, no. 6, pp. 638–644, 2005.

[30] K. Doya, "Complementary roles of basal ganglia and cerebellum in learning and motor control," *Curr. Opin. Neurobiol.*, vol. 10, no. 6, pp. 732–739, 2000.

[31] R. C. O'Reilly and M. J. Frank, "Making Working Memory Work: A Computational Model of Learning in the Prefrontal Cortex and Basal Ganglia," *Neural Comput.*, vol. 18, no. 2, pp. 283–328, Feb. 2006.

[32] L. Schmidt, B. Forgeot, G. Lafargue, D. Galanaud, V. Czernecki, D. Grabli, M. Schu pbach, A. Hartmann, R. Le, B. Dubois, and M. Pessiglione, "Disconnecting force from money: effects of basal ganglia damage on incentive motivation," *Brain*, vol. 131, pp. 1303–1310, 2008.

[33] M. D. Pell and C. L. Leonard, "Processing emotional tone from speech in Parkinson's disease: A role for the basal ganglia," *Cogn. Affect. Behav. Neurosci.*,

vol. 3, no. 4, pp. 275–288, Dec. 2003.
[34] B. Knutson, C. M. Adams, G. W. Fong, and D. Hommer, “Anticipation of increasing monetary reward selectively recruits nucleus accumbens.,” *J. Neurosci.*, vol. 21, no. 16, p. RC159, 2001.
[35] J. Jensen, A. R. McIntosh, A. P. Crawley, D. J. Mikulis, G. Remington, and S. Kapur, “Direct Activation of the Ventral Striatum in Anticipation of Aversive Stimuli,” *Neuron*, vol. 40, no. 6, pp. 1251–1257, 2003.
[36] A. J. Calder, J. Keane, A. D. Lawrence, and F. Manes, “Impaired recognition of anger following damage to the ventral striatum.,” *Brain*, vol. 127, pp. 1958–69, Sep. 2004.
[37] A. Egerton, M. A. Mehta, A. J. Montgomery, J. M. Lappin, O. D. Howes, S. J. Reeves, V. J. Cunningham, and P. M. Grasby, “The dopaminergic basis of human behaviors: A review of molecular imaging studies,” *Neurosci. Biobehav. Rev.*, vol. 33, no. 7, pp. 1109–1132, 2009.
[38] S. M. Landau, R. Lal, J. P. O’Neil, S. Baker, and W. J. Jagust, “Striatal dopamine and working memory,” *Cereb. Cortex*, vol. 19, no. 2, pp. 445–454, 2009.
[39] H. H. Yin, B. J. Knowlton, and B. W. Balleine, “Blockade of NMDA receptors in the dorsomedial striatum prevents action-outcome learning in instrumental conditioning,” *Eur. J. Neurosci.*, vol. 22, no. 2, pp. 505–512, 2005.
[40] H. H. Yin, S. B. Ostlund, B. J. Knowlton, and B. W. Balleine, “The role of the dorsomedial striatum in instrumental conditioning,” *Eur. J. Neurosci.*, vol. 22, no. 2, pp. 513–523, 2005.
[41] Z. M. Williams and E. N. Eskandar, “Selective enhancement of associative learning by microstimulation of the anterior caudate,” *Nat. Neurosci.*, vol. 9, no. 4, pp. 562–568, Apr. 2006.
[42] C. A. Seger and C. M. Cincotta, “The Roles of the Caudate Nucleus in Human Classification Learning,” *J. Neurosci.*, vol. 25, no. 11, pp. 2941–2951, Mar. 2005.
[43] C. A. Seger and C. M. Cincotta, “Dynamics of frontal, striatal, and hippocampal systems during rule learning.,” *Cereb. Cortex*, vol. 16, no. 11, pp. 1546–55, Nov. 2006.
[44] M. E. Ragozzino, K. E. Ragozzino, S. J. Y. Mizumori, and R. P. Kesner, “Role of the dorsomedial striatum in behavioral flexibility for response and visual cue discrimination learning,” *Behav. Neurosci.*, vol. 116, no. 1, pp. 105–115, 2002.
[45] D. M. Eagle and T. W. Robbins, “Inhibitory Control in Rats Performing a Stop-Signal Reaction-Time Task: Effects of Lesions of the Medial Striatum and d-Amphetamine.,” *Behav. Neurosci.*, vol. 117, no. 6, pp. 1302–1317, 2003.
[46] D. . Eagle and T. . Robbins, “Lesions of the medial prefrontal cortex or nucleus accumbens core do not impair inhibitory control in rats performing a stop-signal reaction time task,” *Behav. Brain Res.*, vol. 146, pp. 131–144, 2003.
[47] H. H. Yin and B. J. Knowlton, “Contributions of Striatal Subregions to Place and Response Learning,” *Learn. Mem.*, vol. 11, no. 4, pp. 459–463, Jul. 2004.
[48] F. Simard, Y. Joanette, M. Petrides, T. Jubault, C. Madjar, and O. Monchi, “Fronto-striatal contribution to lexical set-shifting.,” *Cereb. Cortex*, vol. 21, no. 5, pp. 1084–93, May 2011.
[49] M. G. Lacourse, E. L. R. Orr, S. C. Cramer, and M. J. Cohen, “Brain activation during execution and motor imagery of novel and skilled sequential hand movements,” *Neuroimage*, vol. 27, pp. 505–519, 2005.
[50] E. M. Tricomi, M. R. Delgado, and J. A. Fiez, “Modulation of Caudate Activity by Action Contingency,” *Neuron*, vol. 41, no. 2, pp. 281–292, 2004.
[51] E. Tricomi, M. R. Delgado, B. D. Mccandliss, J. L. Mcclelland, and J. A. Fiez,

"Performance Feedback Drives Caudate Activation in a Phonological Learning Task," *J. Cogn. Neurosci.*, vol. 18, no. 6, pp. 1029–1043, 2006.

[52] J.-S. Provost, M. Petrides, and O. Monchi, "Dissociating the role of the caudate nucleus and dorsolateral prefrontal cortex in the monitoring of events within human working memory," *Eur. J. Neurosci.*, vol. 32, pp. 873–880, Sep. 2010.

[53] D. B. Willingham, "A neuropsychological theory of motor skill learning," *Psychol. Rev.*, vol. 105, no. 3, pp. 558–84, 1998.

[54] R. A. Poldrack and M. G. Packard, "Competition among multiple memory systems: converging evidence from animal and human brain studies," *Neuropsychologia*, vol. 41, pp. 245–251, 2003.

[55] K. P. Bhatia and C. D. Marsden, "The behavioural and motor consequences of focal lesions of the basal ganglia in man," *Brain A J. Neurol.*, vol. 117, no. 4, 1994.

[56] J. Jankowski, L. Scheef, C. Hüppe, and H. Boecker, "Distinct striatal regions for planning and executing novel and automated movement sequences," *Neuroimage*, vol. 44, pp. 1369–1379, 2009.

[57] S. Miyachi, O. Hikosaka, K. Miyashita, Z. Kárádi, and M. K. Rand, "Differential roles of monkey striatum in learning of sequential hand movement," *Exp. Brain Res.*, vol. 115, no. 1, pp. 1–5, 1997.

[58] R. E. Featherstone and R. J. McDonald, "Dorsal striatum and stimulus-response learning: lesions of the dorsolateral, but not dorsomedial, striatum impair acquisition of a stimulus-response-based instrumental discrimination task, while sparing conditioned place preference learning," *Neuroscience*, vol. 124, pp. 23–31, 2004.

[59] R. E. Featherstone and R. J. McDonald, "Lesions of the dorsolateral striatum impair the acquisition of a simplified stimulus-response dependent conditional discrimination task," *Neuroscience*, vol. 136, pp. 387–395, 2005.

[60] H. H. Yin, B. J. Knowlton, and B. W. Balleine, "Inactivation of dorsolateral striatum enhances sensitivity to changes in the action–outcome contingency in instrumental conditioning," *Behav. Brain Res.*, vol. 166, no. 2, pp. 189–196, 2006.

[61] B. Baier, H.-O. Karnath, M. Dieterich, F. Birklein, C. Heinze, and N. G. Muller, "Keeping Memory Clear and Stable--The Contribution of Human Basal Ganglia and Prefrontal Cortex to Working Memory," *J. Neurosci.*, vol. 30, no. 29, pp. 9788–9792, Jul. 2010.

[62] I. H. Jenkins, M. Jahanshahi, M. Jueptner, R. E. Passingham, and D. J. Brooks, "Self-initiated versus externally triggered movements II. The effect of movement predictability on regional cerebral blood flow," *Brain*, vol. 123, pp. 1216–1228, 2000.

[63] R. Cunnington, C. Windischberger, L. Deecke, and E. Moser, "The Preparation and Execution of Self-Initiated and Externally-Triggered Movement: A Study of Event-Related fMRI," *Neuroimage*, vol. 15, no. 2, pp. 373–385, 2002.

[64] S. Lehéricy, H. Benali, P.-F. Van de Moortele, M. Pélégrini-Issac, T. Waechter, K. Ugurbil, and J. Doyon, "Distinct basal ganglia territories are engaged in early and advanced motor sequence learning," *Proc. Natl. Acad. Sci. U. S. A.*, vol. 102, no. 35, pp. 12566–71, Aug. 2005.

[65] S. T. Grafton, E. Hazeltine, and R. Ivry, "Functional mapping of sequence learning in normal humans," *J. Cogn. Neurosci.*, vol. 7, no. 4, pp. 497–510, 1995.

[66] E. Hazeltine, S. T. Grafton, and R. Ivry, "Attention and sitimulus characteristics determine the locus of motor-sequence encoding A PET study," *Brain*, vol. 120, pp. 123–140, 1997.

[67] C. Exner, J. Koschack, and E. Irle, "The Differential Role of Premotor Frontal

Cortex and Basal Ganglia in Motor Sequence Learning: Evidence From Focal Basal Ganglia Lesions," *Learn. Mem.*, vol. 9, pp. 376–386, Nov. 2002.

[68] M. Emre, "Dementia associated with Parkinson's disease," *Lancet Neurol.*, vol. 2, pp. 229–37, 2003.

[69] N. Giladi, D. Mcmahon, S. Przedborski, E. Flaster, and S. Guillory, "Motor blocks in Parkinson' s disease," *Neurolo*, vol. 42, no. 2, pp. 333–339, 1992.

[70] S. L. Naismith, J. M. Shine, and S. J. G. Lewis, "The specific contributions of set-shifting to freezing of gait in Parkinson's disease," *Mov. Disord.*, vol. 25, no. 8, pp. 1000–1004, Jun. 2010.

[71] R. Cools, "Dopaminergic modulation of cognitive function-implications for l-DOPA treatment in Parkinson's disease," *Neurosci. Biobehav. Rev.*, vol. 30, no. 1, pp. 1–23, 2006.

[72] A. M. Owen, A. C. Roberts, J. R. Hodges, B. A. Summers, C. E. Polkey, and T. W. Robbins, "Contrasting mechanisms of impaired attentional set-shifting in patients with frontal lobe damage or Parkinson's disease," *Brain*, vol. 116, pp. 1159–1175, 1993.

[73] T. Shallice, "Specific impairments of planning," *Philos. Trans. R. Soc. Lond. B. Biol. Sci.*, vol. 298, pp. 199–209, 1982.

[74] A. M. Owen, M. James, P. N. Leigh, B. A. Summers, C. D. Marsden, N. P. Quinn, K. W. Lange, and T. W. Robbins, "Fronto-striatal cognitive deficits at different stages of Parkinson's disease," *Brain*, vol. 115, pp. 1727–1751, 1992.

[75] G. Douaud, V. Gaura, M. J. Ribeiro, F. Lethimonnier, R. Maroy, C. Verny, P. Krystkowiak, P. Damier, A. C. Bachoud-Levi, P. Hantraye, and P. Remy, "Distribution of grey matter atrophy in Huntington's disease patients: A combined ROI-based and voxel-based morphometric study," *Neuroimage*, vol. 32, no. 4, pp. 1562–1575, 2006.

[76] J. S. Paulsen, N. Butters, J. R. Sadek, S. A. Johnson, D. P. Salmon, N. R. Swerdlow, and M. R. Swenson, "Distinct cognitive profiles of cortical and subcortical dementia in advanced illness," *Neurology*, vol. 45, no. 5, pp. 951–956, 1995.

[77] K. W. Lange, B. J. Sahakian, N. P. Quinn, C. D. Marsden, and T. W. Robbins, "Comparison of executive and visuospatial memory function in Huntington's disease and dementia of Alzheimer type matched for degree of dementia.," *J. Neurol. Neurosurg. Psychiatry*, vol. 58, no. 5, pp. 598–606, 1995.

[78] G. Vallar and D. Perani, "The anatomy of unilateral neglect after right-hemisphere stroke lesions. A clinical/CT-scan correlation study in man," *Neuropsychologia*, vol. 24, pp. 609–622, 1986.

[79] G. Vallar and D. Perani, "The Anatomy of Spatial Neglect in Humans," *Adv. Psychol.*, vol. 45, pp. 235–258, 1987.

[80] J. M. Ferro, A. Kertesz, and S. E. Black, "Subcortical neglect: Quantitation, anatomy, and recovery," *Neurology*, vol. 37, no. 9, pp. 1487–1487, Sep. 1987.

[81] E. B. Healton, C. Navarro, S. Bressman, and J. C. M. Brust, "Subcortical neglect," *Neurology*, vol. 32, no. 7, pp. 776–776, Jul. 1982.

[82] D. Karussis, R. . Leker, and O. Abramsky, "Cognitive dysfunction following thalamic stroke: a study of 16 cases and review of the literature," *J. Neurol. Sci.*, vol. 172, no. 1, pp. 25–29, 2000.

[83] H.-O. Karnath, M. Himmelbach, and C. Rorden, "The subcortical anatomy of human spatial neglect: putamen, caudate nucleus and pulvinar," *Brain*, vol. 125, pp. 350–360, 2002.

[84] B. B. Averbeck, J. Lehman, M. Jacobson, and S. N. Haber, "Estimates of projection overlap and zones of convergence within frontal-striatal circuits.," *J.*

Neurosci., vol. 34, no. 29, pp. 9497–505, Jul. 2014.
[85] L. D. Selemon and P. S. Goldman-Rakic, "Longitudinal topography and interdigitation of corticostriatal projections in the rhesus monkey.," *J. Neurosci.*, vol. 5, no. 3, pp. 776–794, 1985.
[86] A. Parent and L.-N. Hazrati, "Functional anatomy of the basal ganglia. I. The cortico-basal ganglia-thalamo-cortical loop," *Brain Res. Rev.*, vol. 20, no. 1, pp. 91–127, 1995.
[87] K. Nakano, T. Kayahara, T. Tsutsumi, and H. Ushiro, "Neural circuits and functional organization of the striatum," *J. Neurol.*, vol. 247, no. S5, pp. V1–V15, Oct. 2000.
[88] J. A. Saint-Cyr, "Frontal-striatal circuit functions: Context, sequence, and consequence," *J. Int. Neuropsychol. Soc.*, vol. 9, pp. 103–127, 2003.
[89] P. S. Goldman and W. J. H. Nauta, "An intricately patterned prefronto-caudate projection in the rhesus monkey," *J. Comp. Neurol.*, vol. 171, no. 3, pp. 369–385, Feb. 1977.
[90] T. Zheng and C. J. Wilson, "Corticostriatal combinatorics: the implications of corticostriatal axonal arborizations," *J. Neurophysiol.*, vol. 87, pp. 1007–17, Feb. 2002.
[91] A. E. Kincaid, T. Zheng, and C. J. Wilson, "Connectivity and convergence of single corticostriatal axons.," *J. Neurosci.*, vol. 18, no. 12, pp. 4722–31, Jun. 1998.
[92] A. Nambu, K. Kaneda, H. Tokuno, and M. Takada, "Organization of corticostriatal motor inputs in monkey putamen.," *J. Neurophysiol.*, vol. 88, no. 4, pp. 1830–42, Oct. 2002.
[93] M. Takada, H. Tokuno, A. Nambu, and M. Inase, "Corticostriatal projections from the somatic motor areas of the frontal cortex in the macaque monkey: segregation versus overlap of input zones from the primary motor cortex, the supplementary motor area, and the premotor cortex," *Exp Brain Res*, vol. 120, pp. 114–128, 1998.
[94] M. Takada, H. Tokuno, A. Nambu, and M. Inase, "Corticostriatal input zones from the supplementary motor area overlap those from the contra- rather than ipsilateral primary motor cortex," *Brain Res.*, vol. 791, pp. 335–340, 1998.
[95] A. T. Ferry, D. Öngür, X. An, and J. L. Price, "Prefrontal cortical projections to the striatum in macaque monkeys: Evidence for an organization related to prefrontal networks," *J. Comp. Neurol.*, vol. 425, no. 3, pp. 447–470, 2000.
[96] K. Jarbo and T. D. Verstynen, "Converging Structural and Functional Connectivity of Orbitofrontal, Dorsolateral Prefrontal, and Posterior Parietal Cortex in the Human Striatum," *J. Neurosci.*, vol. 35, no. 9, pp. 3865–3878, 2015.
[97] A. Kamali, L. A. Kramer, and K. M. Hasan, "Feasibility of prefronto-caudate pathway tractography using high resolution diffusion tensor tractography data at 3T," *J. Neurosci. Methods*, vol. 191, no. 2, pp. 249–254, 2010.
[98] R. B. Postuma and A. Dagher, "Basal ganglia functional connectivity based on a meta-analysis of 126 positron emission tomography and functional magnetic resonance imaging publications.," *Cereb. cortex*, vol. 16, no. 10, pp. 1508–21, Oct. 2006.
[99] E. Y. Choi, B. T. T. Yeo, and R. L. Buckner, "The organization of the human striatum estimated by intrinsic functional connectivity.," *J. Neurophysiol.*, vol. 108, no. 8, pp. 2242–63, Oct. 2012.
[100] S. Bestmann, J. Baudewig, H. R. Siebner, J. C. Rothwell, and J. Frahm, "Functional MRI of the immediate impact of transcranial magnetic stimulation on cortical and subcortical motor circuits," *Eur. J. Neurosci.*, vol. 19, no. 7, pp. 1950–1962, Apr. 2004.

[101] D. Knoch, V. Treyer, M. Regard, R. M. Müri, A. Buck, and B. Weber, "Lateralized and frequency-dependent effects of prefrontal rTMS on regional cerebral blood flow," *Neuroimage*, vol. 31, pp. 641–648, 2006.
[102] C. Beaulieu, "The basis of anisotropic water diffusion in the nervous system - a technical review," *NMR Biomed.*, vol. 15, pp. 435–455, Nov. 2002.
[103] E. O. Stejskal and J. E. Tanner, "Spin Diffusion Measurements: Spin Echoes in the Presence of a Time-Dependent Field Gradient," *J. Chem. Phys.*, vol. 42, no. 288, pp. 288–292, 1965.
[104] M. E. Moseley, Y. Cohen, J. Kucharczyk, J. Mintorovitch, H. S. Asgari, M. F. Wendland, J. Tsuruda, and D. Norman, "Diffusion-weighted MR imaging of anisotropic water diffusion in cat central nervous system.," *Radiology*, vol. 176, no. 2, pp. 439–445, Aug. 1990.
[105] M. Doran, J. V. Hajnal, N. Van Bruggen, M. D. King, I. R. Young, and G. M. Bydder, "Normal and Abnormal White Matter Tracts Shown by MR Imaging using Directional Diffusion Weighted Sequences.," *J. Comput. Assist. Tomogr.*, vol. 14, pp. 865–873, 1990.
[106] T. L. Chenevert, J. A. Brunberg, and J. G. Pipe, "Anisotropic diffusion in human white matter: demonstration with MR techniques in vivo.," *Radiology*, vol. 177, pp. 401–405, Nov. 1990.
[107] C. Beaulieu and P. S. Allen, "Determinants of anisotropic water diffusion in nerves," *Magn. Reson. Med.*, vol. 31, no. 4, pp. 394–400, Apr. 1994.
[108] P. J. Basser and C. Pierpaoli, "Microstructural and physiological features of tissues elucidated by quantitative-diffusion-tensor MRI," *J. Magn. Reson.*, vol. B 111, pp. 209–219, 1996.
[109] K. Penttinen, "Diffuusiotensorikuvien traktografian optimointi kynnysarvojen ja kohdennuksen näkökulmasta," Aalto University, 2010.
[110] P. J. Basser and S. Pajevic, "Statistical artifacts in diffusion tensor MRI (DT-MRI) caused by background noise," *Magn. Reson. Med.*, vol. 44, no. 1, pp. 41–50, Jul. 2000.
[111] P. J. Basser and D. K. Jones, "Diffusion-tensor MRI: theory, experimental design and data analysis - a technical review," *NMR Biomed.*, vol. 15, pp. 456–467, 2002.
[112] D. Weinstein, G. Kindlmann, and E. Lundberg, "Tensorlines: Advection-Diffusion based Propagation through Diffusion Tensor Fields," in *IEEE Visualization*, 1999, pp. 249–253.
[113] D. K. Jones and C. Pierpaoli, "Confidence mapping in diffusion tensor magnetic resonance imaging tractography using a bootstrap approach," *Magn. Reson. Med.*, vol. 53, no. 5, pp. 1143–1149, May 2005.
[114] M. Koch, V. Glauche, J. Finsterbusch, U. Nolte, J. Frahm, and C. Büchel, "Estimation of anatomical connectivity from diffusion tensor data," *Neuroimage*, vol. 13, no. 6, 2001.
[115] M. Catani, R. J. Howard, S. Pajevic, and D. K. Jones, "Virtual in Vivo Interactive Dissection of White Matter Fasciculi in the Human Brain," *Neuroimage*, vol. 17, pp. 77–94, 2002.
[116] M. Lazar and A. L. Alexander, "Bootstrap white matter tractography (BOOT-TRAC)," *Neuroimage*, vol. 24, pp. 524–532, 2005.
[117] P. L. Croxson, "Quantitative Investigation of Connections of the Prefrontal Cortex in the Human and Macaque using Probabilistic Diffusion Tractography," *J. Neurosci.*, vol. 25, no. 39, pp. 8854–8866, 2005.
[118] P. Hagmann, T. G. Reese, W.-Y. I. Tseng, R. Meuli, J.-P. Thiran, and V. J. Wedeen, "Diffusion Spectrum Imaging tractography in complex cerebral white

matter: an investigation of the centrum semiovale," in *International Society for Magnetic Resonance in Medicine*, 2004, p. 623.

[119] T. Hosey, G. Williams, and R. Ansorge, "Inference of multiple fiber orientations in high angular resolution diffusion imaging," *Magn. Reson. Med.*, vol. 54, pp. 1480–1489, Dec. 2005.

[120] T. E. J. Behrens, H. Johansen-Berg, S. Jbabdi, M. F. S. Rushworth, and M. W. Woolrich, "Probabilistic diffusion tractography with multiple fibre orientations: What can we gain?," *Neuroimage*, vol. 34, pp. 144–155, 2007.

[121] A. T. Barker, R. Jalinous, and I. L. Freeston, "Non-invasive magnetic stimulation of human motor cortex," *Lancet*, vol. 325, no. 8437, pp. 1106–1107, May 1985.

[122] L. L. Carpenter, P. G. Janicak, S. T. Aaronson, T. Boyadjis, D. G. Brock, I. A. Cook, D. L. Dunner, K. Lanocha, H. B. Solvason, and M. A. Demitrack, "Transcranial magnetic stimulation (TMS) for major depression: A multisite, naturalistic, observational study of acute treatment outcomes in clinical practice," *Depress. Anxiety*, vol. 29, no. 7, pp. 587–596, Jul. 2012.

[123] N. J. Davey, H. C. Smith, E. Wells, D. W. Maskill, G. Savic, P. H. Ellaway, and H. L. Frankel, "Responses of thenar muscles to transcranial magnetic stimulation of the motor cortex in patients with incomplete spinal cord injury," *J. Neurol. Neurosurg. Psychiatry*, vol. 65, pp. 80–87, Jul. 1998.

[124] S. J. Boniface, K. R. Mills, and M. Schubert, "Responses of single spinal motoneurons to magnetic brain stimulation in healthy subjects and patients with multiple sclerosis.," *Brain*, vol. 114, pp. 643–62, 1991.

[125] S. K. Aurora, B. K. Ahmad, K. M. A. Welch, P. Bhardhwaj, and N. M. Ramadan, "Transcranial magnetic stimulation confirms hyperexcitability of occipital cortex in migraine," *Neurology*, vol. 50, no. 4, pp. 1111–1114, Apr. 1998.

[126] W. M. Mulleners, E. P. Chronicle, J. E. Palmer, P. J. Koehler, and J.-W. Vredeveld, "Visual Cortex Excitability in Migraine With and Without Aura," *Headache J. Head Face Pain*, vol. 41, pp. 565–572, Jun. 2001.

[127] E. M. Wassermann, "Risk and safety of repetitive transcranial magnetic stimulation: report and suggested guidelines from the International Workshop on the Safety of Repetitive Transcranial Magnetic Stimulation, June 5–7, 1996," *Electroencephalogr. Clin. Neurophysiol.*, vol. 108, pp. 1–16, 1998.

[128] J. Ruohonen, "Transcranial Magnetic Stimulation: Modelling and New Techniques," Helsinki University of Technology, 1998.

[129] R. Chen, J. Classen, C. Gerloff, P. Celnik, E. M. Wassermann, M. Hallett, and L. G. Cohen, "Depression of motor cortex excitability by low-frequency transcranial magnetic stimulation," *Neurology*, vol. 48, no. 5, pp. 1398–1403, May 1997.

[130] A. Pascual-Leone, J. M. Tormos, J. Keenan, F. Tarazona, C. Cañete, and M. D. Catalá, "Study and Modulation of Human Cortical Excitability With Transcranial Magnetic Stimulation," *J. Clin. Neurophysiol.*, vol. 15, no. 4, pp. 333–343, 1998.

[131] M. S. George, Z. Nahas, M. Molloy, A. M. Speer, N. C. Oliver, X.-B. Li, G. W. Arana, and S. C. Risch, "A controlled trial of daily left prefrontal cortex TMS for treating depression," *Biol. Psychiatry*, vol. 48, no. 10, pp. 962–970, Nov. 2000.

[132] M. S. George and R. H. Belmaker, *Transcranial Magnetic Stimulation in Clinical Psychiatry*. Amerivan Psychiatric Pub, 2007.

[133] R. J. Ilmoniemi, J. Virtanen, J. Ruohonen, J. Karhu, H. J. Aronen, R. Näätänen, and T. Katila, "Neuronal responses to magnetic stimulation reveal cortical reactivity and connectivity," *Neuroreport*, vol. 8, pp. 3537–3540, 1997.

[134] M. W. Woolrich, S. Jbabdi, B. Patenaude, M. Chappell, S. Makni, T. Behrens, C. Beckmann, M. Jenkinson, and S. M. Smith, "Bayesian analysis of neuroimaging

data in FSL," *Neuroimage*, vol. 45, no. 1, pp. S173–S186, 2009.
[135] S. M. Smith, M. Jenkinson, M. W. Woolrich, C. F. Beckmann, T. E. J. Behrens, H. Johansen-Berg, P. R. Bannister, M. De Luca, I. Drobnjak, D. E. Flitney, R. K. Niazy, J. Saunders, J. Vickers, Y. Zhang, N. De Stefano, J. M. Brady, and P. M. Matthews, "Advances in functional and structural MR image analysis and implementation as FSL," *Neuroimage*, vol. 23, pp. S208–S219, 2004.
[136] M. Jenkinson, C. F. Beckmann, T. E. J. Behrens, M. W. Woolrich, and S. M. Smith, "FSL," *Neuroimage*, vol. 62, no. 2, pp. 782–790, 2012.
[137] J. L. R. Andersson, M. S. Graham, E. Zsoldos, and S. N. Sotiropoulos, "Incorporating outlier detection and replacement into a non-parametric framework for movement and distortion correction of diffusion MR images," *Neuroimage*, vol. 141, pp. 556–572, Nov. 2016.
[138] J. L. R. Andersson, S. Skare, and J. Ashburner, "How to correct susceptibility distortions in spin-echo echo-planar images: application to diffusion tensor imaging.," *Neuroimage*, vol. 20, no. 2, pp. 870–88, Oct. 2003.
[139] S. M. Smith, "Fast robust automated brain extraction," *Hum. Brain Mapp.*, vol. 17, no. 3, pp. 143–155, Nov. 2002.
[140] B. Patenaude, S. M. Smith, D. N. Kennedy, and M. Jenkinson, "A Bayesian model of shape and appearance for subcortical brain segmentation," *Neuroimage*, vol. 56, pp. 907–922, 2011.
[141] T. Yousry, U. D. Schmid, H. Alkadhi, D. Schmidt, A. Peraud, A. Buettner, and P. Winkler, "Localization of the motor hand area to a knob on the precentral gyrus. A new landmark," *Brain*, vol. 120, no. 1, pp. 141–157, 1997.
[142] J. Tanji, "New concepts of the supplementary motor area," *Curr. Opin. Neurobiol.*, vol. 6, pp. 782–787, 1996.
[143] S. C. Cramer, G. Nelles, R. R. Benson, J. D. Kaplan, R. A. Parker, K. K. Kwong, D. N. Kennedy, S. P. Finklestein, and B. R. Rosen, "A Functional MRI Study of Subjects Recovered From Hemiparetic Stroke," *Stroke*, vol. 28, no. 12, pp. 2518–2527, Dec. 1997.
[144] M. Petrides and D. N. Pandya, "Dorsolateral prefrontal cortex: comparative cytoarchitectonic analysis in the human and the macaque brain and corticocortical connection patterns," *Eur. J. Neurosci.*, vol. 11, pp. 1011–1036, Mar. 1999.
[145] J. C. Klein, M. F. S. Rushworth, T. E. J. Behrens, C. E. Mackay, A. J. de Crespigny, H. D'Arceuil, and H. Johansen-Berg, "Topography of connections between human prefrontal cortex and mediodorsal thalamus studied with diffusion tractography," *Neuroimage*, vol. 51, no. 2, pp. 555–564, 2010.
[146] M. Petrides and D. N. Pandya, "Comparative cytoarchitectonic analysis of the human and the macaque ventrolateral prefrontal cortex and corticocortical connection patterns in the monkey," *Eur. J. Neurosci.*, vol. 16, pp. 291–310, Jul. 2001.
[147] N. Makris, J. M. Goldstein, D. Kennedy, S. M. Hodge, V. S. Caviness, S. V Faraone, M. T. Tsuang, and L. J. Seidman, "Decreased volume of left and total anterior insular lobule in schizophrenia.," *Schizophr. Res.*, vol. 83, no. 2–3, pp. 155–71, Apr. 2006.
[148] J. A. Frazier, S. Chiu, J. L. Breeze, N. Makris, N. Lange, D. N. Kennedy, M. R. Herbert, E. K. Bent, V. K. Koneru, M. E. Dieterich, S. M. Hodge, S. L. Rauch, P. E. Grant, B. M. Cohen, L. J. Seidman, V. S. Caviness, and J. Biederman, "Structural Brain Magnetic Resonance Imaging of Limbic and Thalamic Volumes in Pediatric Bipolar Disorder," *Am. J. Psychiatry*, vol. 162, no. 7, pp. 1256–1265, Jul. 2005.

[149] R. S. Desikan, F. Ségonne, B. Fischl, B. T. Quinn, B. C. Dickerson, D. Blacker, R. L. Buckner, A. M. Dale, R. P. Maguire, B. T. Hyman, M. S. Albert, and R. J. Killiany, "An automated labeling system for subdividing the human cerebral cortex on MRI scans into gyral based regions of interest," *Neuroimage*, vol. 31, no. 3, pp. 968–980, 2006.

[150] J. M. Goldstein, L. J. Seidman, N. Makris, T. Ahern, L. M. O'Brien, V. S. Caviness, D. N. Kennedy, S. V. Faraone, and M. T. Tsuang, "Hypothalamic Abnormalities in Schizophrenia: Sex Effects and Genetic Vulnerability," *Biol. Psychiatry*, vol. 61, no. 8, pp. 935–945, 2007.

[151] D. C. Alexander, C. Pierpaoli, P. J. Basser, and J. C. Gee, "Spatial transformations of diffusion tensor magnetic resonance images," *IEEE Trans. Med. Imaging*, vol. 20, no. 11, pp. 1131–1139, 2001.

[152] J. C. Gee and D. C. Alexander, "Diffusion-tensor image registration," in *Visualization and Processing of Tensor Fields*, J. Weickert and H. Hagen, Eds. Berlin, Heidelberg: Springer Berlin Heidelberg, 2006, pp. 327–342.

[153] Y. Wang, A. Gupta, Z. Liu, H. Zhang, M. L. Escolar, J. H. Gilmore, S. Gouttard, P. Fillard, E. Maltbie, G. Gerig, and M. Styner, "DTI registration in atlas based fiber analysis of infantile Krabbe disease," *Neuroimage*, vol. 55, pp. 1577–1586, 2011.

[154] M. F. Glasser and J. K. Rilling, "DTI Tractography of the Human Brain's Language Pathways," *Cereb. Cortex*, vol. 18, pp. 2471–2482, Nov. 2008.

[155] C. G. Schwarz, R. I. Reid, J. L. Gunter, M. L. Senjem, S. A. Przybelski, S. M. Zuk, J. L. Whitwell, P. Vemuri, K. A. Josephs, K. Kantarci, P. M. Thompson, R. C. Petersen, and C. R. Jack, "Improved DTI registration allows voxel-based analysis that outperforms Tract-Based Spatial Statistics," *Neuroimage*, vol. 94, pp. 65–78, 2014.

[156] I. Bohanna, N. Georgiou-Karistianis, and G. F. Egan, "Connectivity-based segmentation of the striatum in Huntington's disease: Vulnerability of motor pathways," *Neurobiol. Dis.*, vol. 42, no. 3, pp. 475–481, 2011.

[157] J. Pacheco, C. G. Beevers, C. Benavides, J. McGeary, E. Stice, and D. M. Schnyer, "Frontal-Limbic White Matter Pathway Associations with the Serotonin Transporter Gene Promoter Region (5-HTTLPR) Polymorphism," *J. Neurosci.*, vol. 29, no. 19, pp. 6229–6233, May 2009.

[158] P. Mukherjee, J. I. Berman, S. W. Chung, C. P. Hess, and R. G. Henry, "Diffusion Tensor MR Imaging and Fiber Tractography: Theoretic Underpinnings," *Am. J. Neuroradiol.*, vol. 29, no. 4, pp. 632–641, Apr. 2008.

[159] S. Mori, *Introduction to diffusion tensor imaging*. Elsevier, 2007.

[160] M. Björnemo and A. Brun, "White Matter Fiber Tracking Using Diffusion Tensor MRI," Linköping University, 2002.

[161] S. Mori and P. C. M. van Zijl, "Fiber tracking: principles and strategies - a technical review," *NMR Biomed.*, vol. 15, pp. 468–480, Nov. 2002.